

Mathematical World

---

---

# Intuitive Topology

V. V. Prasolov

Translated from the Russian by  
A. Sossinsky



Universities Press

**Universities Press (India) Limited**

*Registered Office*

3-5-819, Hyderguda, Hyderabad 500 029 A.P., INDIA

*Distributed by*

**Orient Longman Limited**

*Registered Office*

3-6-272, Himayatnagar, Hyderabad 500 029 A.P., INDIA

*Other Offices*

Bangalore/Bhopal/Bhubaneshwar/Calcutta/Chennai

Ernakulam/Guwahati/Hyderabad/Jaipur

Lucknow/Mumbai/New Delhi/Patna

© 1995 by the author

First published in India by

Universities Press (India) Limited 1998

ISBN 81 7371 118 6

This edition has been authorized by the American Mathematical Society for sale in India, Bangladesh, Bhutan, Nepal, Sri Lanka and the Maldives only, and not for export therefrom.

*Printed in India at*

Isvarya Graphics, Hyderabad 500 004

*Published by*

Universities Press (India) Limited

3-5-819, Hyderguda, Hyderabad 500 029

---

---

# Table of Contents

---

---

|  |            |
|--|------------|
| <b>Foreword</b>  | <b>vii</b> |
| <b>Chapter 1. Deformations</b>                                 | <b>1</b>   |
| <b>Chapter 2. Knots and Links</b>                              | <b>7</b>   |
| <b>Chapter 3. Spans of Knots and Links</b>                     | <b>15</b>  |
| <b>Chapter 4. A Knot Invariant</b>                             | <b>29</b>  |
| <b>Chapter 5. Homeomorphisms</b>                               | <b>33</b>  |
| <b>Chapter 6. Vector Fields on the Plane</b>                   | <b>45</b>  |
| <b>Chapter 7. Vector Fields on Two-Dimensional Surfaces</b>    | <b>63</b>  |
| <b>Chapter 8. Fixed Point Free and Periodic Homeomorphisms</b> | <b>71</b>  |
| <b>Chapter 9. Two-Dimensional Surfaces</b>                     | <b>81</b>  |
| <b>References</b>  | <b>93</b>  |
| <b>Index</b>   | <b>95</b>  |

---

---

# Foreword

---

---

Topology studies the properties of geometrical objects that remain unchanged under transformations called homeomorphisms and deformations. The initial acquaintance with this field is hindered by the fact that rigorous definitions of even the simplest notions of topology are rather abstract or very technical. For this reason the first really meaningful (and in fact readily understandable) topological theorems appear only after tedious preliminaries have been overcome. This preliminary work is mostly devoted to the detailed and accurate proofs of intuitively obvious statements: admittedly not a very exciting activity.

This book is an introductory course in topology of rather untraditional structure. We begin by defining the main notions in a tangible and perceptible way, on an everyday level, and as we go along we progressively make them more precise and rigorous, reaching the level of fairly sophisticated proofs. This allows us to tackle meaningful problems from the very outset with some success.

Another unusual trait of this book is that it deals mainly with constructions and maps (of surfaces, knots, and links in space), rather than with proofs of general theorems implying that certain maps and constructions don't exist. Such proofs, usually based on complicated invariants (e.g., so-called homotopy and homology functors), are in fact a more traditional activity for topologists, but are not the main subject matter of this book. We do consider some invariants, but only simple and effective ones.

The (numerous) illustrations are essential. In many parts of the book they are more important than the text, which is then little more than a commentary to the pictures.

In the study of mathematics, problem solving plays a crucial role. Reading ready-made proofs of theorems is a poor substitute for trying to prove them on your own. Many statements that the reader can profitably think about himself appear in the form of problems. These problems are an inherent part of our exposition, and therefore their solutions are presented at the end of each section.

A bibliography, mainly consisting of books that we recommend for the

further study of topology, appears at the end of the book. Among the books and articles that had the greatest influence on this book, I would like to name the book by Rolphsen [3] and the article by Viro [5].

As is usually done in mathematical books and papers, the symbol  $\square$  marks the end of the proof of a proposition or a theorem.

It should be mentioned that the present text is based on a series of lectures given by the author in the academic year 1990–1991 to students of High School no. 57 in Moscow.

I am grateful to N. M. Fleischer for useful discussions of the manuscript.

---

---

# 1

---

---

## Deformations

Our first look at topology will involve some problems about the deformation of elastic bodies and surfaces. We shall assume that the objects considered are made from a very elastic material: their shape may be changed at will, you can bend, distort, stretch, and compress them as much as you like, but of course you may not tear them or glue parts of them together.

The deformations that you will be asked to find will seem impossible at first glance. But actually they are not difficult to visualize, as you can verify by reading their description in the solution section. However, we emphatically suggest that you try to find the solution on your own before looking at our answers.

*Problem 1.1.* Show that the elastic body represented in Figure 1.1 (a) can be deformed so as to become the one shown in Figure 1.1 (b). In other words, were the human body elastic enough, after making linked rings with your index fingers and thumbs, you could move your hands apart without separating the joined fingertips.

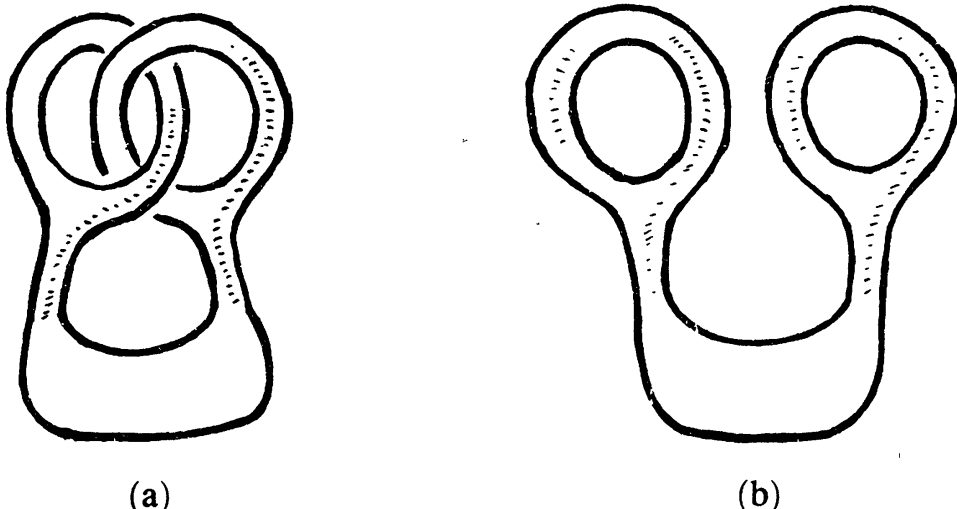


FIGURE 1.1

## 1. DEFORMATIONS

*Problem 1.2.* A pretzel has two holes that “hold” a doughnut (see Figure 1.2 (a)). Show that the pretzel can be deformed in such a way that one of its “handles” will unlink itself from the doughnut (Figure 1.2 (b)).

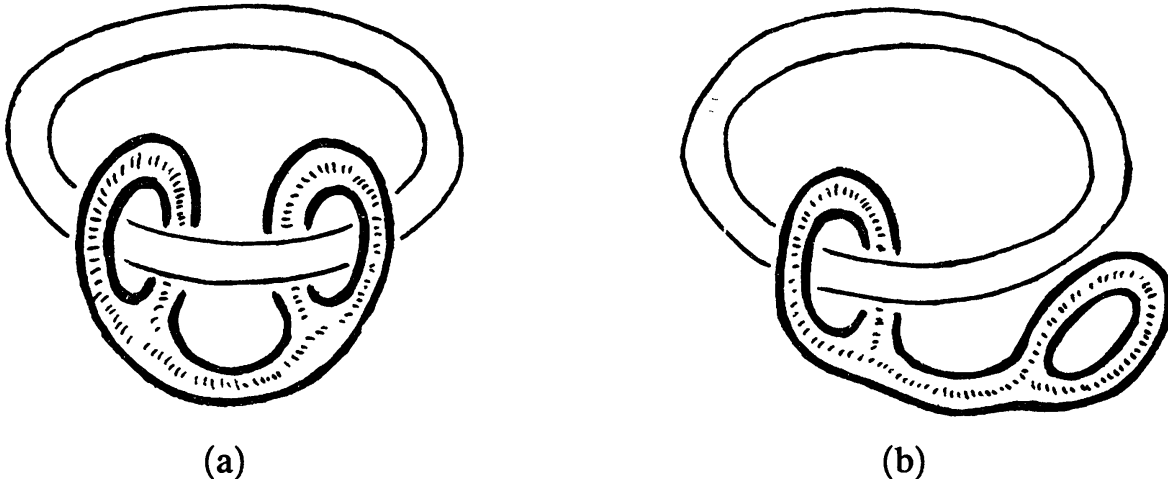


FIGURE 1.2

*Problem 1.3.* A circle is drawn on a pretzel with two holes (Figure 1.3 (a)). Show that it is possible to deform the pretzel so that the circle will be in the position represented in Figure 1.3 (b).

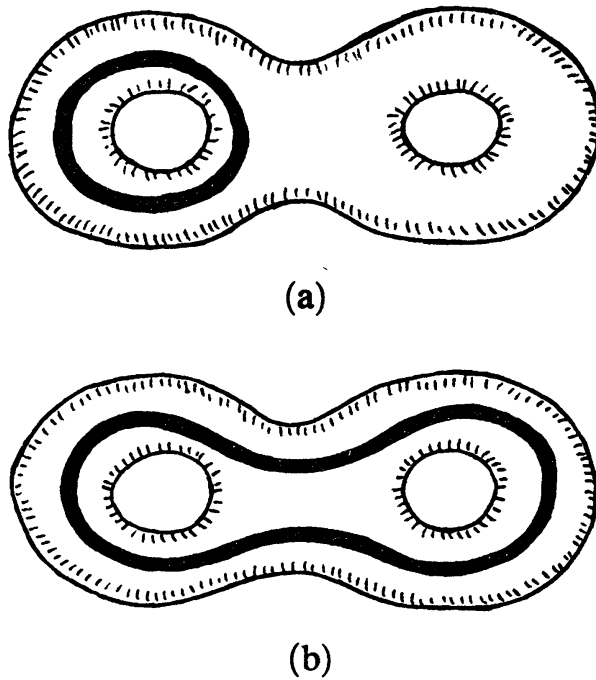


FIGURE 1.3

*Problem 1.4.* Show that a punctured tube from a bicycle tire can be turned inside out. (More precisely, this would be possible if the rubber from which the tube is made were elastic enough. In real life it is impossible to turn a punctured tube inside out.)

*Problem 1.5.* Show that the fancy pretzel represented in Figure 1.4 (a) can be deformed into the ordinary pretzel with two holes (Figure 1.4 (b)).

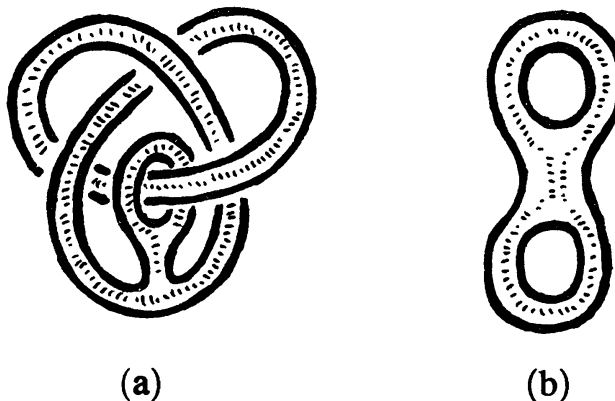


FIGURE 1.4

### Solutions.

We present most of the solutions to the problems in this book by means of pictures, which, as a rule, are self-explanatory. We sometimes indicate by arrows on the pictures the direction of motion or of deformation.

1.1. See Figure 1.5. We shall return to this deformation in §4.

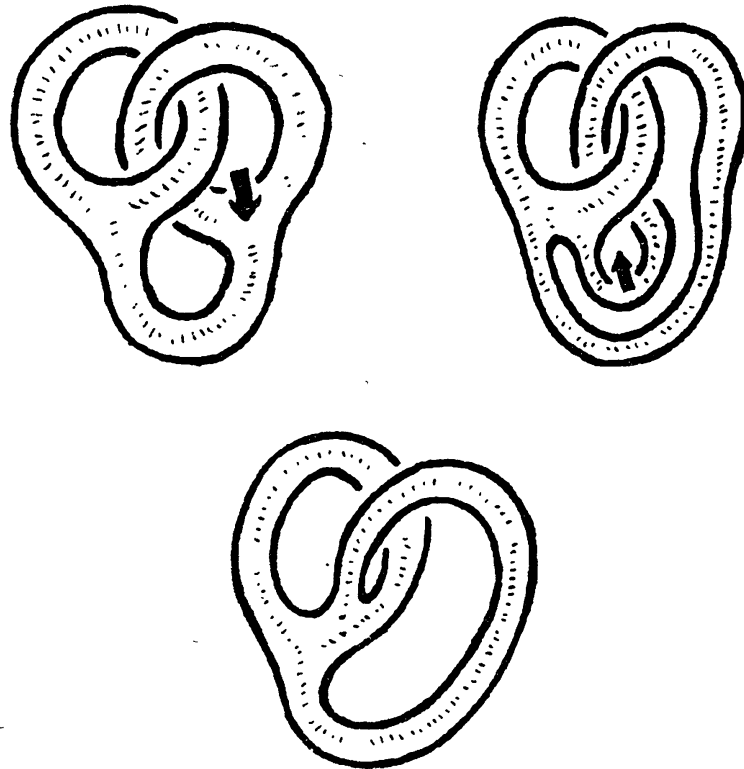


FIGURE 1.5

## 1. DEFORMATIONS

1.2. See Figure 1.6.

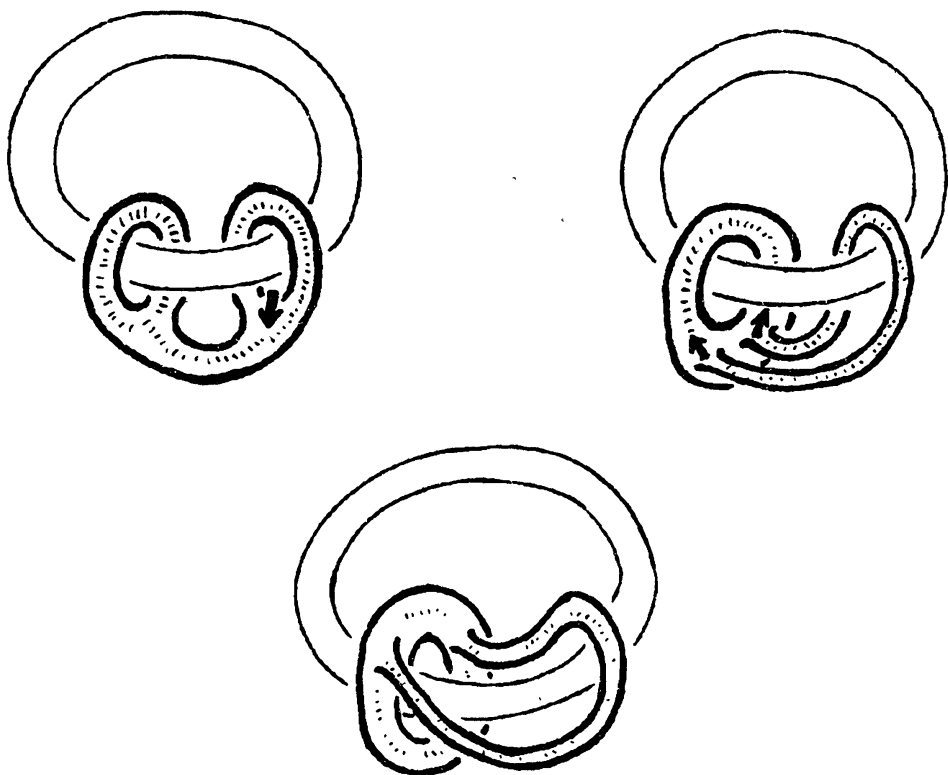


FIGURE 1.6

1.3. See Figure 1.7.

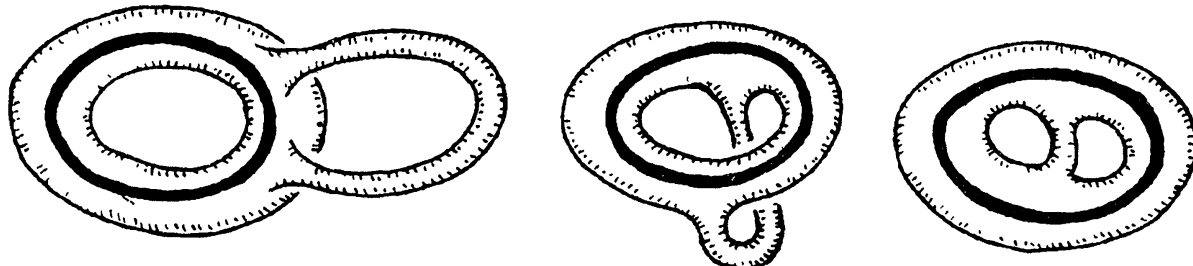


FIGURE 1.7

1.4. First we perform the deformations shown in Figure 1.8.

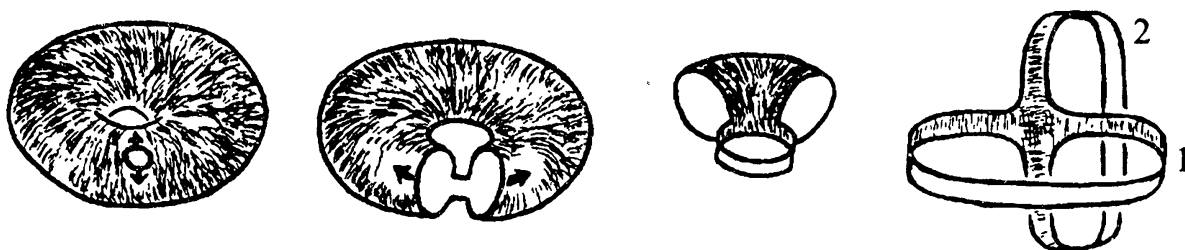


FIGURE 1.8

Then we can change the position of the obtained figure so that its “inside” (shown in white) becomes its “outside” (the shaded side of the surface) and vice-versa, simply by moving it as a rigid body in space until the hoop 1 occupies the position of the hoop 2. Once this is done, the previous deformations performed in reverse order result in the tube being turned inside out as required.

Note that this procedure interchanges the “parallel” and the “meridian” of the tube (see Figure 1.9).

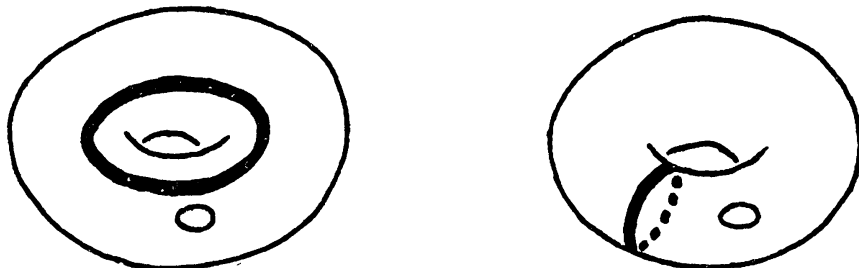


FIGURE 1.9

1.5. First we perform the deformation shown in Figure 1.10. The solid thus obtained (provided it is elastic) can clearly be deformed into the one shown in Figure 1.1 (a). It now remains to apply the solution of Problem 1.1.

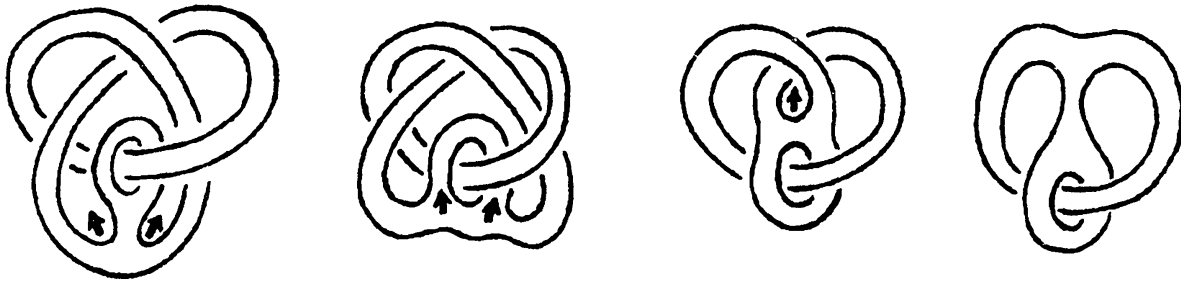


FIGURE 1.10



---

---

# 2

---

---

## Knots and Links

Knots are an important object of study in topology. You can imagine a *knot* as a thin elastic string whose extremities have been glued together. One of the simplest knots is shown in Figure 2.1 (a). It is known as the *trefoil*, or more precisely as the *right trefoil*. There is also a *left trefoil*, represented in Figure 2.1 (b). It can be proved that the left and right trefoils are different knots, i.e., one cannot be deformed into the other. By a *deformation* of a knot we understand its deformation in space as a thin elastic string.

Knots are usually represented by their plane projections (often called *knot diagrams*), but it should be kept in mind that the projections of the same knot on different planes can look quite dissimilar.

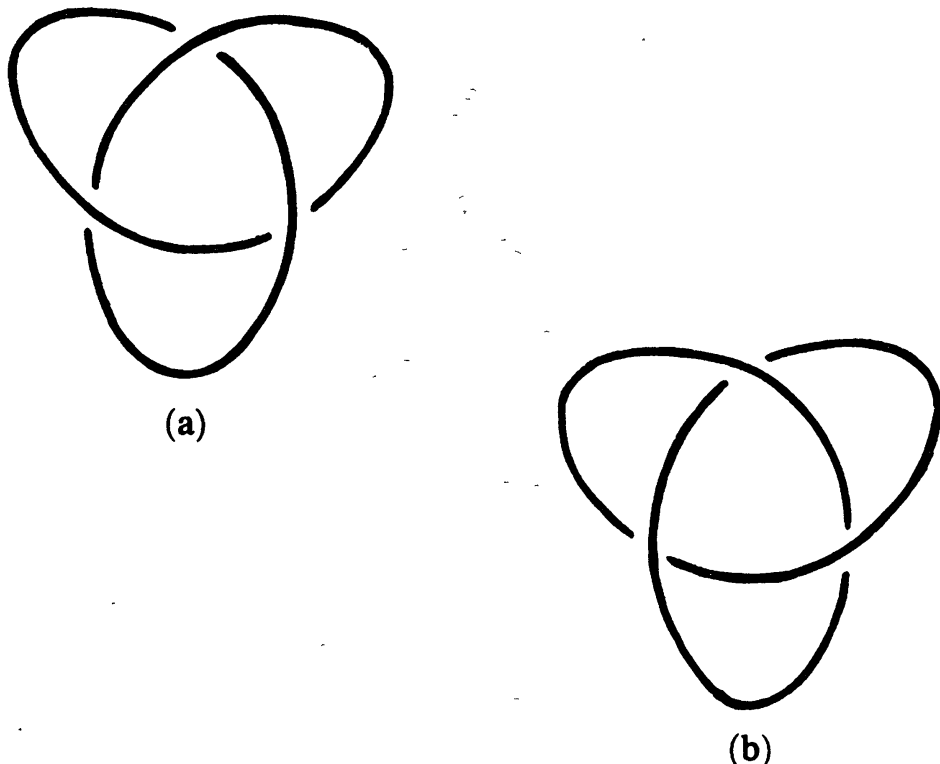


FIGURE 2.1

**Problem 2.1.** Draw the projections on the  $xy$ -plane and the  $xz$ -plane of the trefoil shown in Figure 2.2.

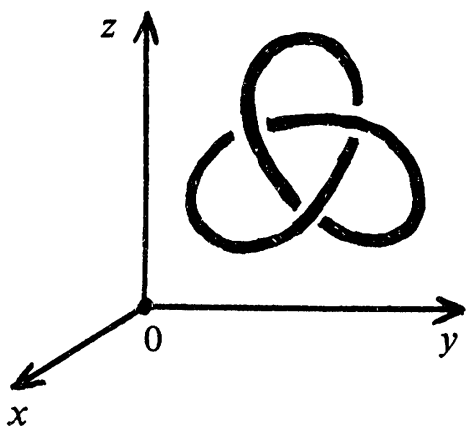


FIGURE 2.2

**Problem 2.2.** Show that the curve given in the  $x$ ,  $y$ ,  $z$  coordinates by the parametric equations

$$x = \cos t(3 \cos t + 2), \quad y = 5 \cos t \sin t, \quad z = \sin t(25 \cos^2 t - 1)$$

is the trefoil by representing its projection on one of the coordinate planes.

The next knot after the trefoil in order of complexity is the *figure eight* knot, whose shape does indeed recall that of the digit 8 (Figure 2.3).

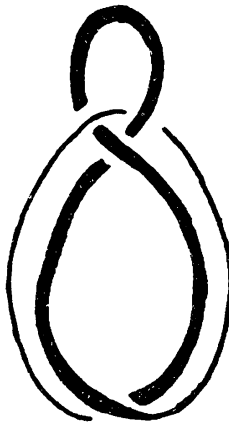


FIGURE 2.3

By deforming a knot, one can make it look very tangled. And even a fairly simple knot such as the trefoil or the eight, after it has been slightly tangled up by someone, may not be too easy to recognize. For example, it is not immediately obvious that all the knots shown on the top row of Figure 2.4 are in fact different representations of the same trefoil knot, while the ones on the second row are all figure eights. Moreover, several representations of the trefoil closely resemble some of the pictures of the figure eight knot. We have placed such matching knots one under the other.

- Problem 2.3.* a) Show that all the knots represented on the top row of Figure 2.4 can be deformed into each other.  
 b) Prove a similar statement for the bottom row.

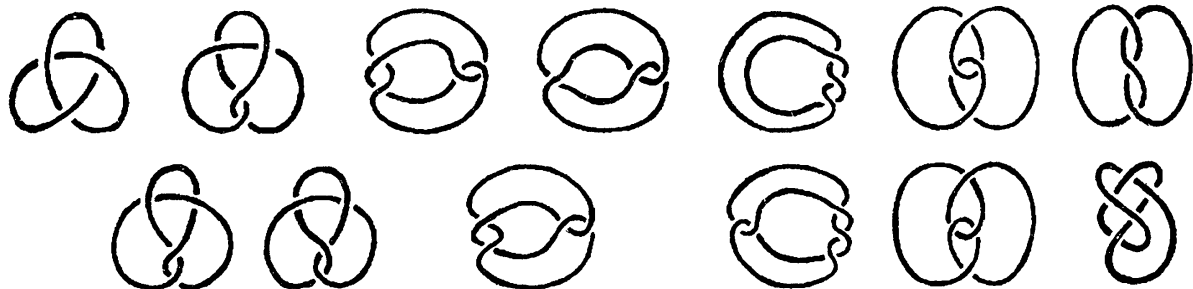


FIGURE 2.4

The left trefoil can be obtained from the right one by a mirror symmetry (i.e., a symmetry with respect to a plane). As we have already mentioned, these two knots cannot be deformed into each other. The figure eight knot, however, behaves differently under mirror symmetry: it becomes a knot that can be transformed into the original one. Indeed, it is easily seen that the first two knots from the left in the second row are mirror symmetric.

If, instead of one string, we take several and glue together the extremities of each, we obtain a *link*. Two examples are shown in Figure 2.5. The first is known as the *Hopf link*, the second is the *Whitehead link*.

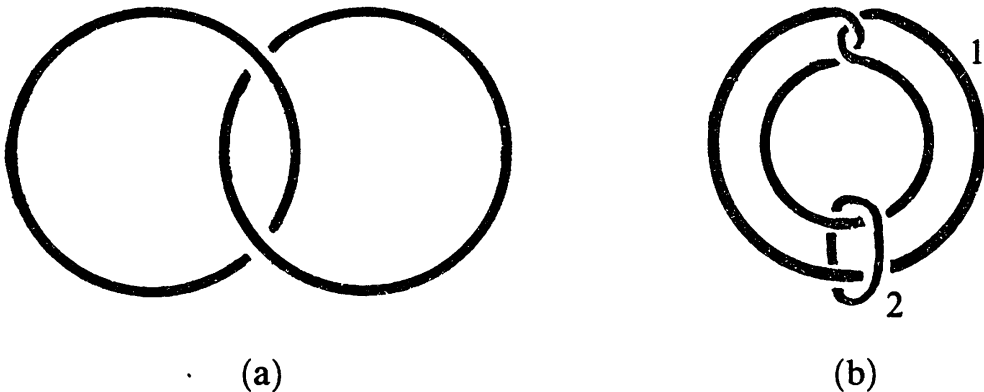


FIGURE 2.5

For the Hopf link from Figure 2.5, there is a symmetry with respect to a (vertical) line that interchanges the two strings (the *components* of the link, as a topologist would say). Here the word “vertical” can be understood in either of two possible ways: perpendicular to the plane of the picture or lying in that plane parallel to the long side of the page. So actually there are two such symmetries. A symmetry in a line is the same as the rotation about the line by an angle of  $180^\circ$ . Hence there exists a deformation that switches the components of the Hopf link. It seems at first glance that no such deformation can exist for the Whitehead link. Indeed, if you cut string 1 near the top of the picture in one place, slip the other part of this string through the cut just once, and glue back the cut ends, you will then have no trouble unlinking the two strings from each other. This is quite obvious for

string 1. It seems just as obvious that this cannot be done with string 2. But in fact it can.

*Problem 2.4.* a) Deform the Whitehead link so that its components become symmetric with respect to some straight line.

b) For string 2 perform the cut-and-paste operation described above for string 1.

The link shown in Figure 2.6 has several unusual properties. It is known as the *Borromean rings* because it appears on the coat of arms of the Borromeo clan, a famous and prosperous family from the ancient Italian nobility.<sup>1</sup> A more interesting property of this link is that the three circles in it are pairwise unlinked: if any one of the rings is removed, the two remaining rings can be unlinked. An even stranger property is that if you link two of the rings in the simplest way (so that they form a Hopf link), then the third ring can be slipped off these two (Figure 2.7).

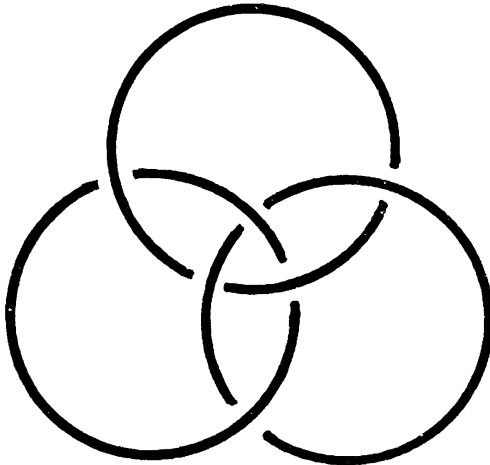


FIGURE 2.6

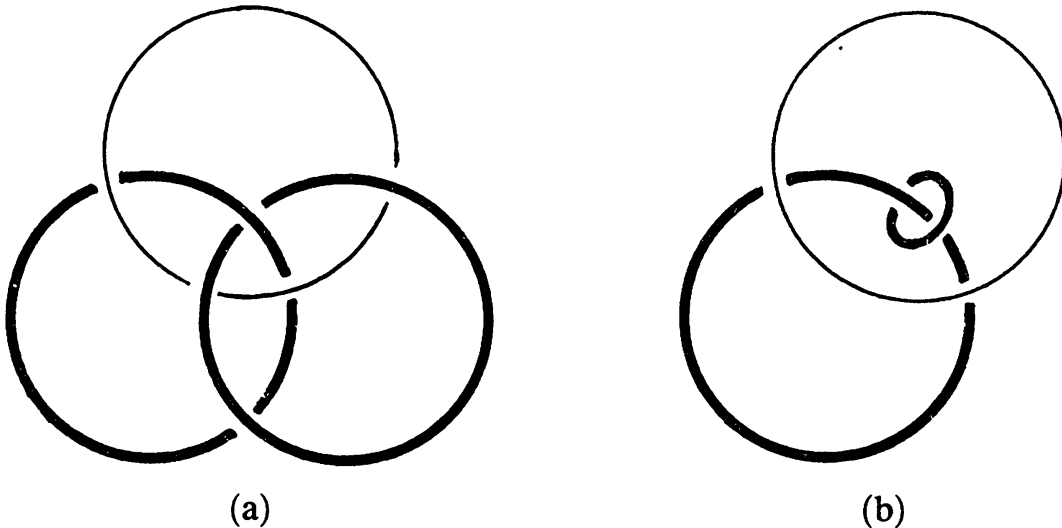


FIGURE 2.7

---

<sup>1</sup>In America it is more familiar as the logo of a brand of beer (*Translator's Note*).

This property of the Borromean rings can be restated so that it sounds like the description of a magician's trick. Since the Borromean rings are pairwise unlinked, two of them (thought of as being rigid hoops) can be pulled far apart from each other; then the third (which we can imagine as an elastic string or rope) will wind itself around the two hoops. How will this look? First let us find out what happens to a rope passing between two rods if these rods switch places, the rod marked 1 passing under the one marked 2 (see Figure 2.8 (a)). The result is shown in Figure 2.8 (b).

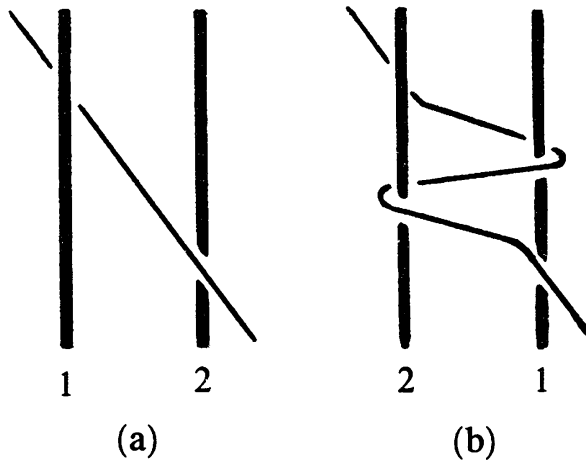


FIGURE 2.8

Now it is easy to see what happens to our third Borromean ring when the first two are pulled away from each other (Figure 2.9).

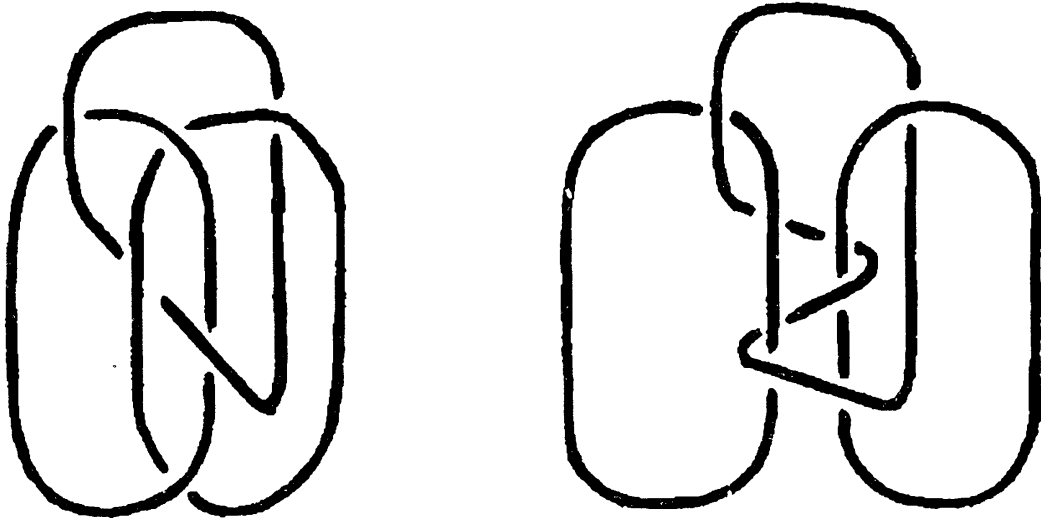


FIGURE 2.9

Suppose that the two rigid Borromean rings are supplied with gadgets that allow us to link and unlink them at will. Then the rope is held fast by the

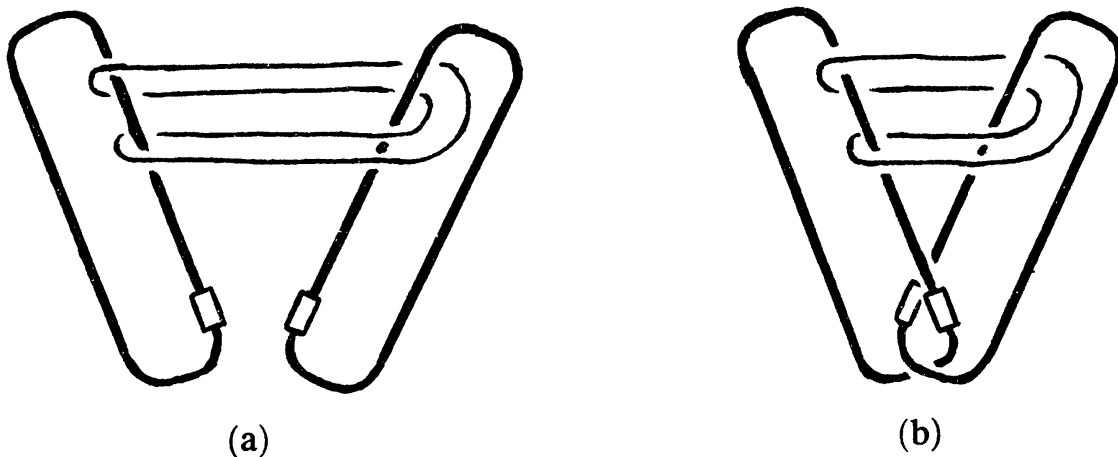


FIGURE 2.10

rings. But now if we link the rings together (Figure 2.10 (b)), presto, the rope is free! Indeed, Figure 2.10 (b) shows the same link as Figure 2.7.

This example should serve as a warning to mountain climbers. They often use locking-unlocking rings, called carabiners in alpinist slang, to fasten their ropes; these rings play the role of the rigid Borromean rings described above. They are constructed so that they are easy to link together but will not unlink of their own accord. However, we have seen that a rope may cease to be secure not only when we unlink, but also when we link together the two carabiners holding it. The ignorance of the possible outcome of this seemingly safe action can lead to tragic consequences.

### Solutions.

2.1. Of course, this problem as stated is somewhat ambiguous: the projection of a knot on one coordinate plane does not determine its projections on the other ones. Nevertheless, given one projection, since there are many constraints on the other projections, the first “solutions” that come to mind may turn out to be contradictory. A possible correct solution is shown in Figure 2.11.

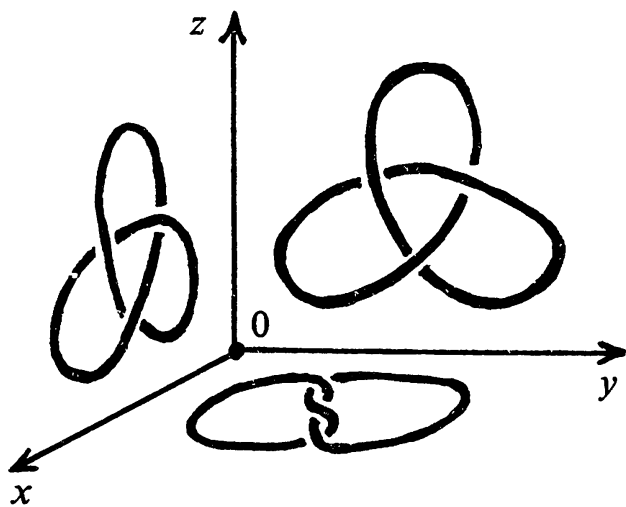


FIGURE 2.11

2.2. It is most convenient to project the curve on the  $xy$ -plane (Figure 2.12). Then the  $z$ -coordinate is used to determine which branch of the projection at the crossing points is the overpass.

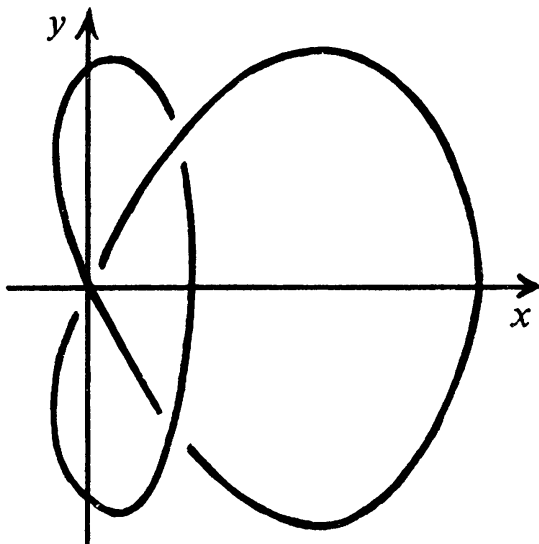


FIGURE 2.12

2.3. Probably the best way of solving this problem is to make a model of the trefoil and the figure eight knot by using a shoelace and then move it around from one position to the other. Figure 2.13 gives some hints concerning transformations of the figure eight knot.

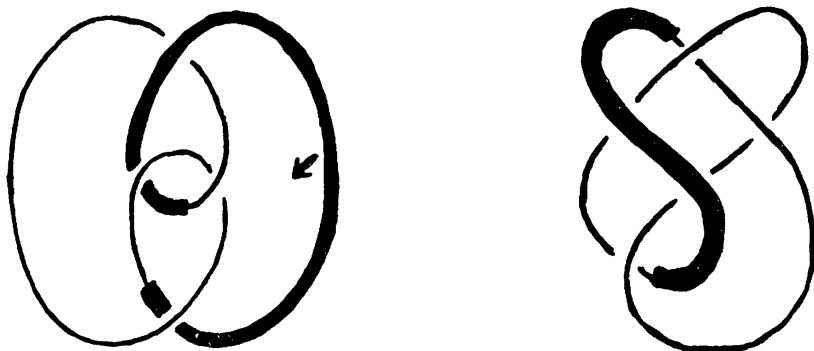


FIGURE 2.13

2.4. a) See Figure 2.14.

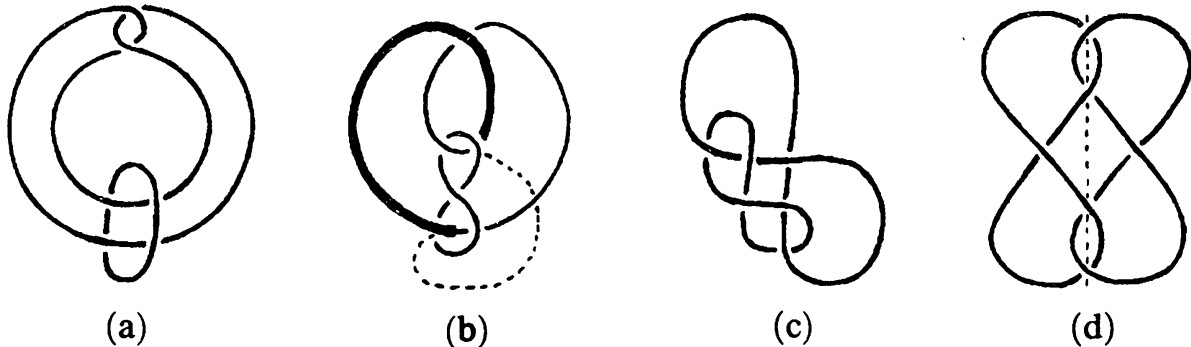


FIGURE 2.14

b) First give the lower component a twist by moving it through a cut on its left side and gluing back the ends (the result is shown in Figure 2.15 (a)). Then the sequence of moves (b)–(f) shown in the picture unlinks the two components.

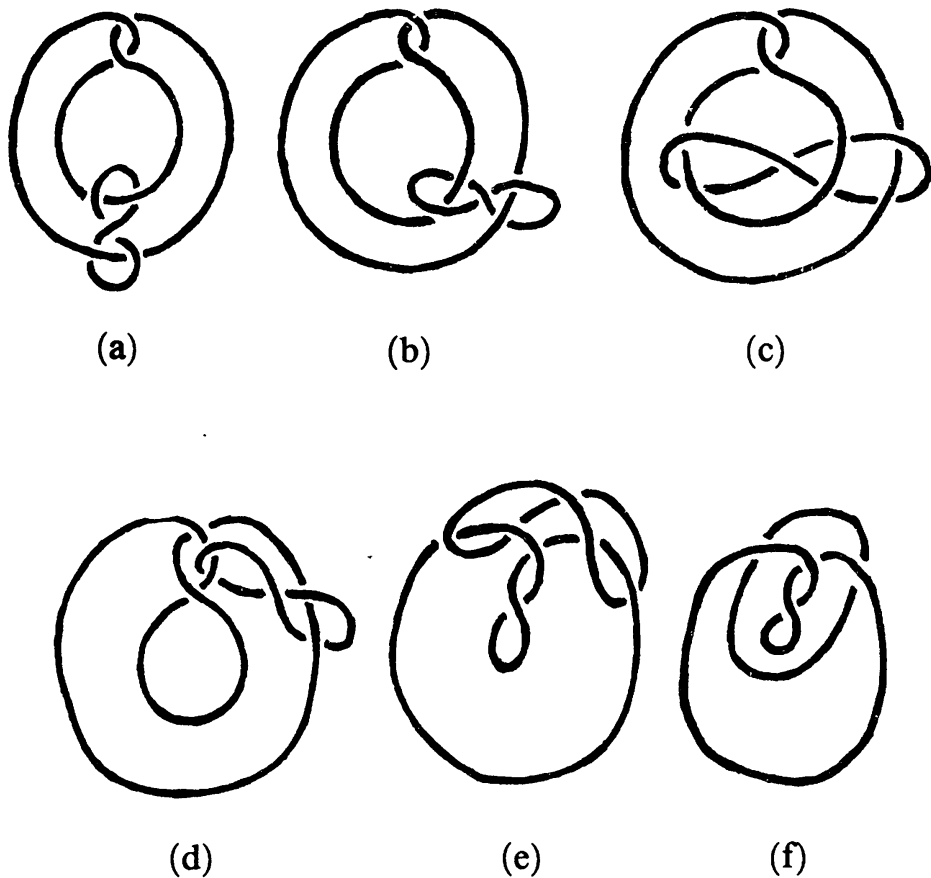


FIGURE 2.15

# 3

## Spans of Knots and Links

Let a knot be given. Imagine that we have positioned a thin flexible film in space so that its contour fits neatly around the given knot. Such a film is called a *spanning surface* or *spanning film* or simply *span* of the knot. Two examples of spanning films are shown in Figure 3.1. There is an essential difference between these two spans: the film (b) is orientable while the film (a) is not. What does this mean? Suppose that the film is transparent and a frame of perpendicular vectors (a short vector and a longer one) moves along the film, remaining tangent to its surface. Then if we move the frame along the path  $1 \rightarrow 2 \rightarrow 3 \rightarrow 4 \rightarrow 1$ , we get a frame that cannot be made to coincide with the initial frame by a rotation: if the short vectors are superimposed, then the long ones point in opposite directions. (Actually, if we do this on a physical model instead of using our imagination, we shall observe that the two frames 1 and 4 will be located on opposite sides of the surface.) Now for the film (b) no such path exists: moving along any closed path on the film that does not intersect its boundary (the knot), our frame will return to a position that can be made to coincide with the original one.

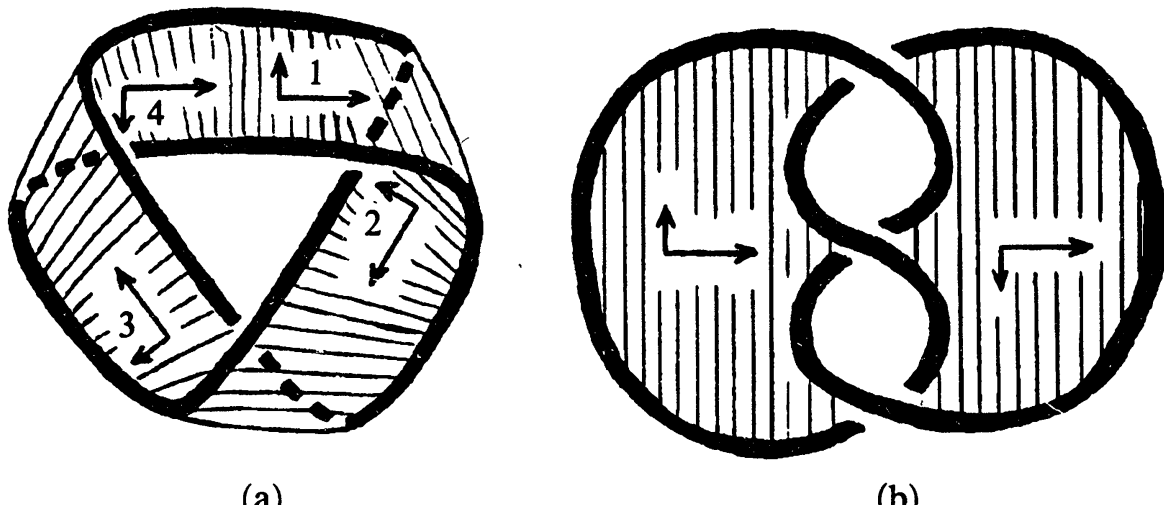


FIGURE 3.1

by rotation. Spans of type (a) are called *nonorientable*, while spans of type (b) are *orientable*.

The flat film spanning a circle can easily be transformed into a nonorientable span with the same boundary (see Figure 3.2 (a)). The following drawings (b), (c) show how this span can be deformed into a Klein bottle from which a disk has been removed. But here we have skipped ahead of our exposition: what a Klein bottle is will not be explained until §9.

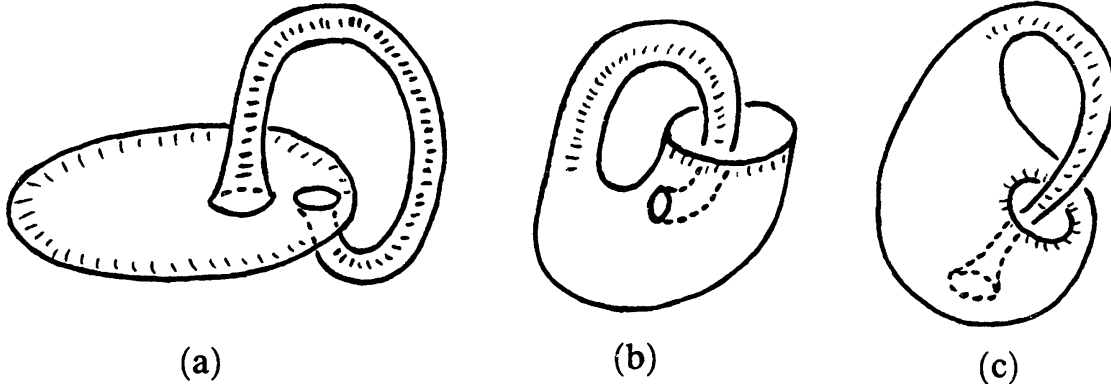


FIGURE 3.2

*Problem 3.1.* Show that the circle can also be spanned by a Möbius band (Figure 3.3), i.e., the Möbius band can be deformed so that its boundary becomes a circle lying in some plane.

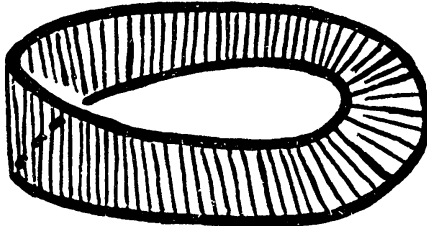


FIGURE 3.3

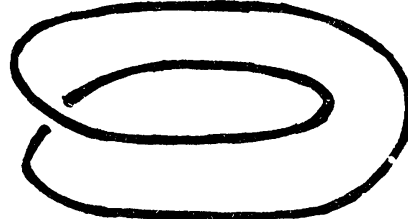


FIGURE 3.4

In Figure 3.3, you can see that the curve shown in Figure 3.4 can be spanned by a Möbius band. This same curve can be spanned by a Klein bottle with a disk removed. How this can be done is shown in Figures 3.5 (a)–(c); notice that the curve represented in Figure 3.5 (a) differs from the one in Figure 3.4 by a rotation (as a rigid object).

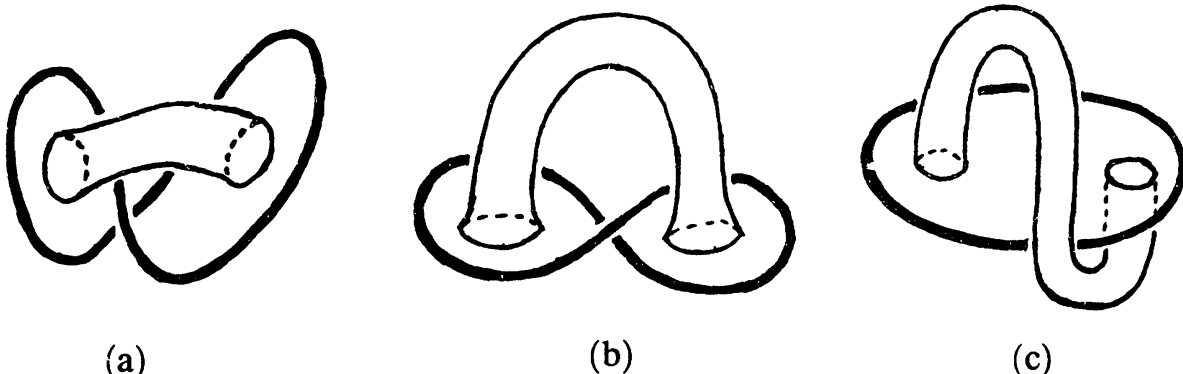


FIGURE 3.5

- Problem 3.2.* a) Show that the curve appearing in Figure 3.4 can also be spanned by an orientable surface, namely a disk (deformed, of course).  
 b) Show that the curve in Figure 3.6 can also be spanned by a disk.

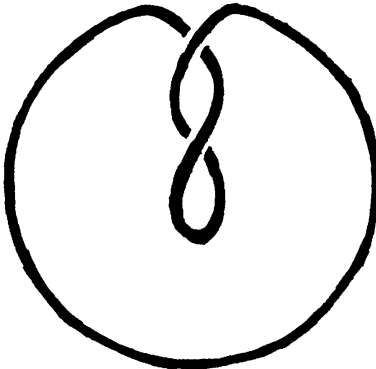


FIGURE 3.6

In 1930 F. Frankl and L. Pontryagin published a paper in which they proved that any knot or link can be spanned by an oriented film. Four years later Seifert published a paper with his proof of the same fact. Since then orientable surfaces spanning knots or links are called *Seifert surfaces*.

We shall prove this theorem following Seifert's method. But first let us present one more problem, which shows that the theorem is far from obvious.

*Problem 3.3.* Show that the figure eight knot can be spanned by an oriented surface.

Now let us pass to a description of the *Seifert algorithm*. We shall assume that the knot is located near its projection, i.e., it lies almost entirely in the horizontal projection plane, only at the crossings one branch is positioned slightly above the plane, the other branch slightly below it. Fix one of the two directions for going around the knot. Let us move along the knot in that direction, jumping to the other branch at each crossing point and continuing to move in the chosen direction until we return to our starting point. The closed curve thus obtained is said to be a *Seifert circle*. It may happen that we return to the starting point without having visited the entire circumference of the knot. Then we start moving from some previously unvisited point, creating more Seifert circles until the whole curve is covered by them. Figure 3.7 on the next page shows the Seifert circles for the trefoil.

Let us construct spanning disks for all these circles, positioning them, say, at different levels just above the plane so that they don't intersect each other. Then near each crossing point the appropriate spanning disks may be joined by little twisted strips (with two opposite sides attached to parts of the knot not on Seifert circles) as shown on Figure 3.7 (b).

A similar construction works for any knot. Indeed, there are no problems in constructing spanning disks for all the Seifert circles: one should begin with an innermost circle (i.e., one that does not enclose another one) and work outwards, attaching spanning disks to Seifert circles that do not enclose

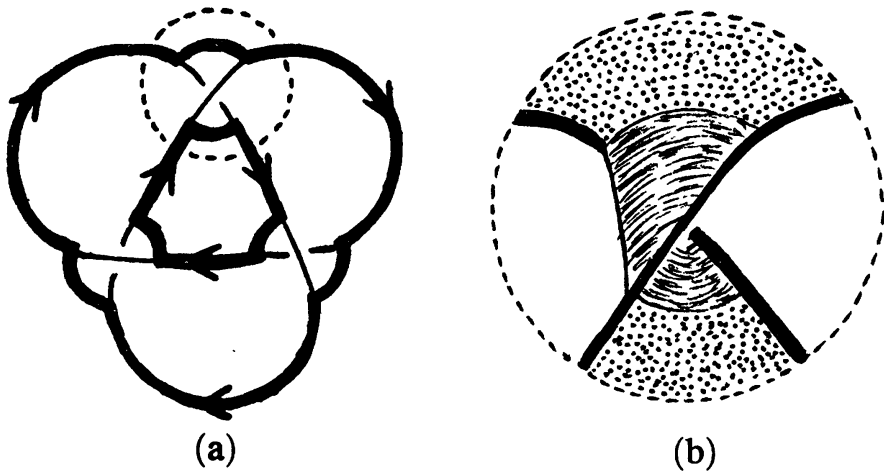


FIGURE 3.7

any unspanned circles. Each subsequent spanning disk can then be placed slightly above the previous ones. And no difficulties arise when we attach the twisted strips, the configuration being the same at all crossing points.

Only one question remains, but an important one: why does this construction yield an *orientable* surface? To answer it, we need a new definition of orientability. This is because the definition given above is rather inconvenient for proving that a surface is orientable: it requires considering all possible closed paths, and there are too many of them.

First let us prove that the plane is orientable. Suppose that a frame of vectors moves in the plane and returns to its initial point. We must show that the direction of rotation from the first vector to the second one is the same for the two frames. In the plane any closed path can be pulled to a point by taking its decreasing similar images (Figure 3.8). We can supply any point of such an image with the frame obtained by parallel translation from the one at the corresponding point of the given path as shown in Figure 3.8. Then the motion of the frame along the path pulled to a point reduces to rotations of the frame about this point. Clearly this means that the direction of rotation from the first vector of the frame to the second one will not change. Hence the plane is orientable.

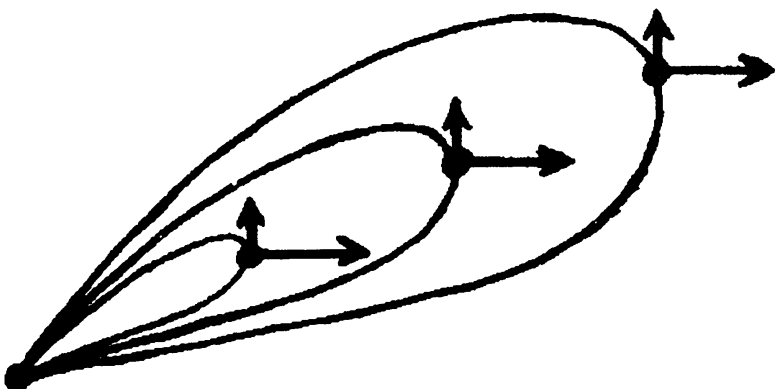


FIGURE 3.8

It is easy to prove that on any surface the direction of rotation from the first vector to the second one does not change when the frame goes around a closed path that can be pulled to a point. This is because two frames whose first vectors differ little from each other, as well as their second vectors, determine the same direction of rotation. Hence if two closed paths differ very little, then the directions of rotation corresponding to these two paths will be the same. Hence in the process of pulling the path to a point, the corresponding directions cannot change. Let us also note that the direction of rotation depends only on the path, and not on the way the frame moves along the path.

Thus the direction of rotation from the first vector to the second one can change only if the frame goes around a closed path that cannot be pulled to a point. When the frame is taken around the Möbius band along the path shown in Figure 3.9 (a), the direction of rotation is reversed. Hence this path cannot be pulled to a point.

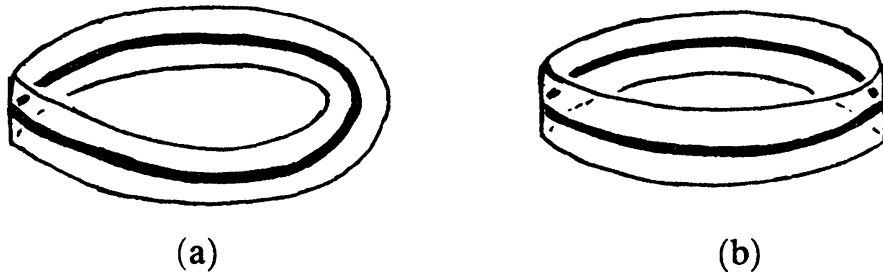


FIGURE 3.9

Let us note that if a path cannot be pulled to a point, this does not necessarily mean that the direction of rotation will change when we go around it. For example, the trip around the cylinder (see Figure 3.9 (b)) does not change the direction of rotation, although this path cannot be pulled to a point on the cylinder.

Two paths  $\gamma_1$  and  $\gamma_2$  joining the points  $A$  and  $B$  give rise to a closed path  $\gamma$  starting and ending at  $A$  (Figure 3.10). This is the path obtained if we move from  $A$  to  $B$  along  $\gamma_1$  and then return to  $A$  by moving along  $\gamma_2$  in the opposite direction. It is easy to verify that the two following conditions are equivalent:

1. The direction of rotation is unchanged when we go around the path  $\gamma$ .
2. The direction of rotation transported from  $A$  to  $B$  along  $\gamma_1$  is the same as the one transported along  $\gamma_2$ .

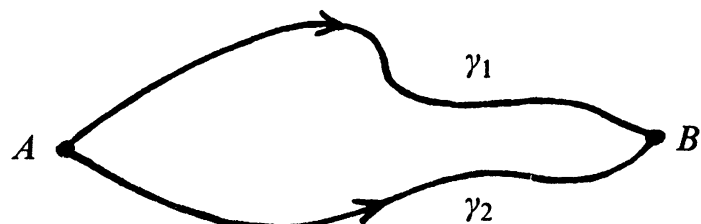


FIGURE 3.10

Now the definition of orientability can be restated in a form more convenient for proofs. We shall say that an *orientation* is given on a surface if a direction of rotation is fixed at each of its points so that the transport along any path takes the direction of rotation at the initial point to the one at the terminal point. In this definition we can restrict ourselves to very short paths (because any long path is composed of several short ones). A surface possessing an orientation is called *orientable*. This definition is equivalent to our original one.

An even more convenient definition of orientability may be obtained by indicating the orientation in explicit form. Let us cut the surface apart into curvilinear polygons. In order to fix the orientation on a polygon, it suffices to choose a direction for going around its boundary. For neighboring polygons, the orientations must agree as shown in Figure 3.11. The surface will be orientable if it is possible to choose orientations that agree with each other on all the polygons.

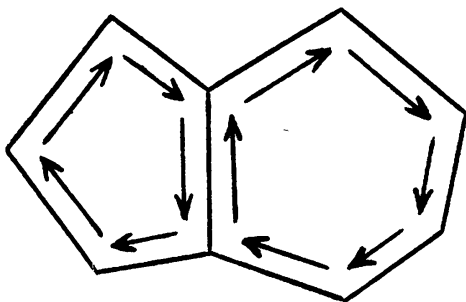


FIGURE 3.11

Using this definition of orientability, it is easy to prove that any surface obtained by the Seifert algorithm is orientable. Indeed, a surface constructed in that way is naturally cut up into curvilinear polygons, and their orientations may be chosen from that of the knot (see Figure 3.12). It is easy to see that the directions going around the polygons thus obtained agree with each other. If we reflect the spanning disks of the Seifert circles in the horizontal plane, we see that the new spanning disks can also be attached to each other by twisted rectangular strips, using an obvious modification of Figure 3.7 (b).

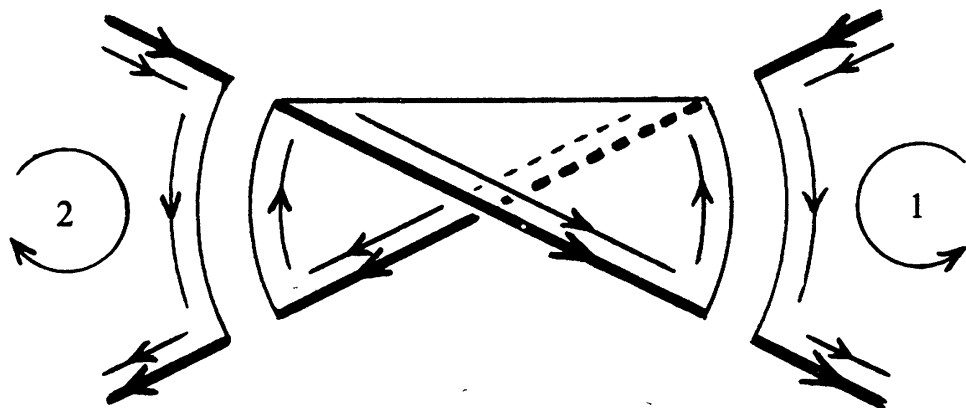


FIGURE 3.12

Indeed, the attaching strip can be regarded as a piece of the lateral surface of a cylinder. The new disks may be glued together by means of the remaining part of the lateral surface of the cylinder (see Figure 3.13). As the result, our knot will lie on a certain orientable surface without boundary, cutting this surface apart into two pieces.

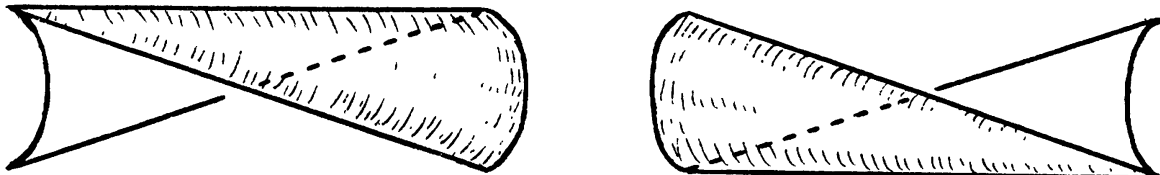


FIGURE 3.13

*Problem 3.4.* Prove that any knot can be placed on a certain oriented surface without boundary so that it does not cut this surface into disjoint pieces.

The Seifert algorithm can be used not only for constructing spanning surfaces for knots, but for links as well. In that case the orientation of each component of the link may be chosen independently. Figure 3.14 shows two different choices of orientations on the same link. If we glue together the corresponding pairs of spanning surfaces, we get two different oriented surfaces without boundary (Figure 3.15).

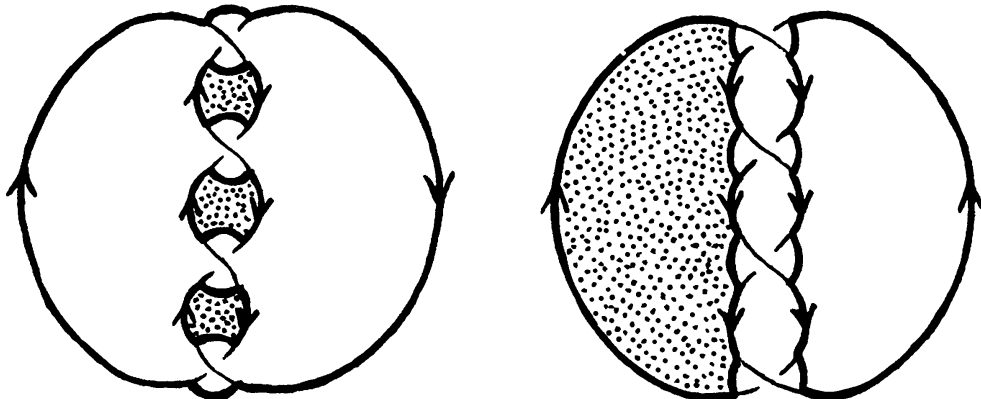


FIGURE 3.14

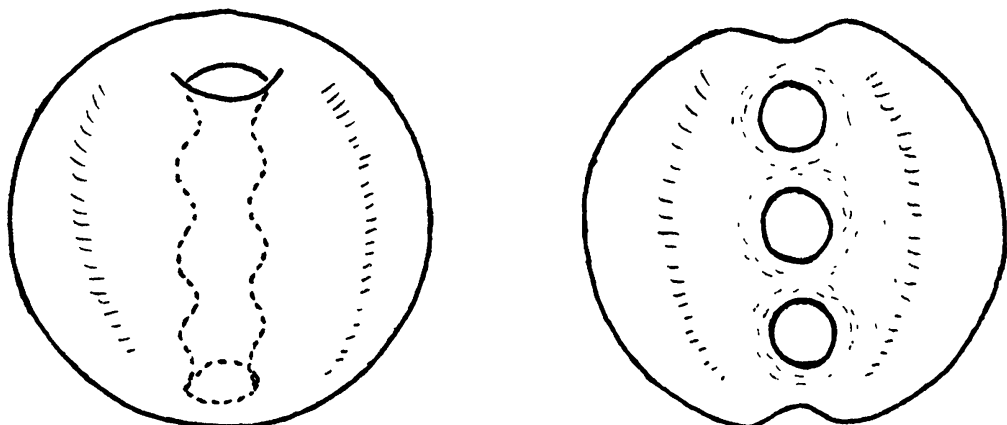


FIGURE 3.15

The Seifert algorithm does not always give a *connected* surface (i.e., a surface consisting of one piece). For example, if the link consists of two nonintersecting circles in the plane, then this algorithm gives two nonintersecting disks. But from several oriented disjoint surfaces it is always possible to obtain a connected surface by attaching the pieces to each other by means of tubes. By a Seifert surface we shall always understand a connected oriented surface whose boundary is the given link.

To construct a Seifert surface of a link it would suffice to span each component of the link by its own spanning surface so that these surfaces don't intersect each other (and then connect them by tubes). However, this is not always possible. For example, the Hopf link cannot be spanned in this way. Moreover, it is even impossible to construct a span of one of the Hopf circles that does not intersect the other one. We shall not prove this.

**Problem 3.5.** Show that curve 1 in Figure 3.16 can be spanned by a surface that does not intersect curve 2.

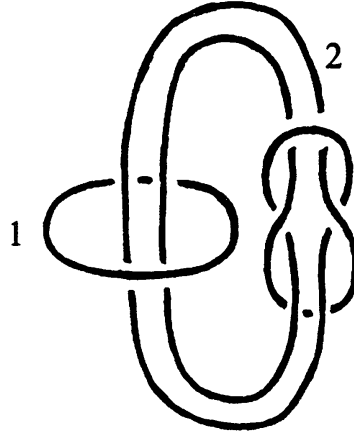


FIGURE 3.16

**Problem 3.6.** Show that the three curves in Figure 3.17 may be spanned by three pairwise nonintersecting oriented surfaces.

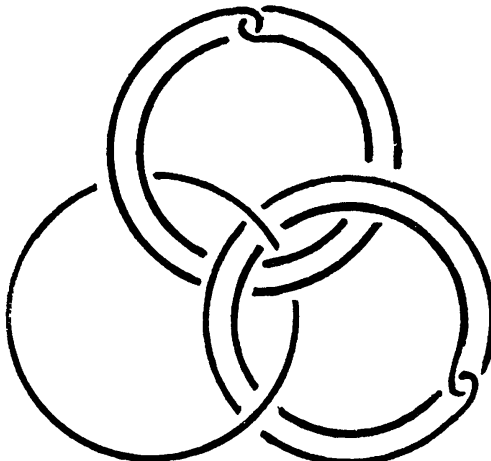


FIGURE 3.17

*Problem 3.7.* Show that curve 1 in Figure 3.18 may be spanned by a Möbius band that does not intersect curve 2.

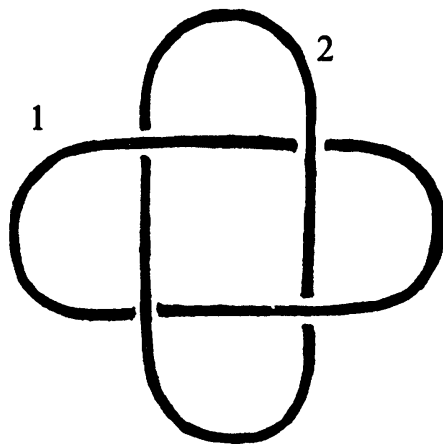


FIGURE 3.18

### Solutions.

3.1. On the one hand, this problem is obvious: it is easy to deform the boundary of the Möbius band so that it becomes a round circle. In the process, the band itself will be deformed in some way. The corresponding deformation of the carcass of the Möbius band is shown in Figure 3.19. Unfortunately, this figure is not easy to visualize.

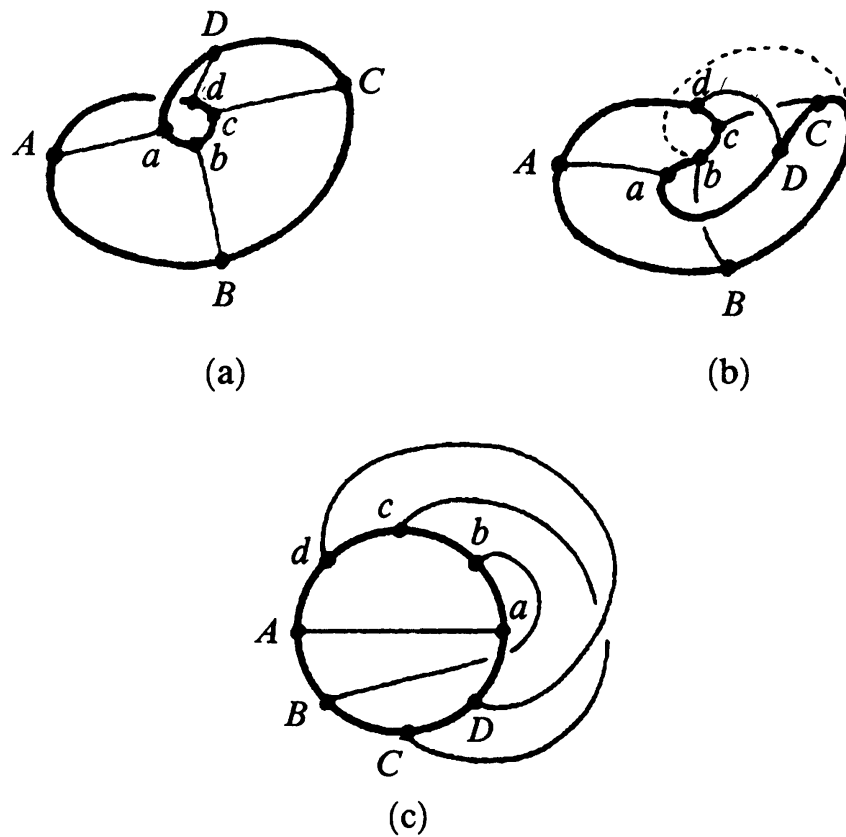


FIGURE 3.19

One can present the solution in a much more tangible way, namely by imagining that the required surface is pasted together from the thin cardboard cutout shown in Figure 3.20. To do that, one must glue the cutout into the shape of an octahedron by means of the identifications ( $A = A$ ,  $B = B$ , etc.) shown in the figure. Then one obtains the surface of an octahedron with two triangles removed ( $ADE$  and  $DCF$ , see Figure 3.21 (a)) together with the surface shown separately in Figure 3.21 (b) but actually located inside the octahedron. The boundary of the entire surface obtained will be triangle  $ACD$ .

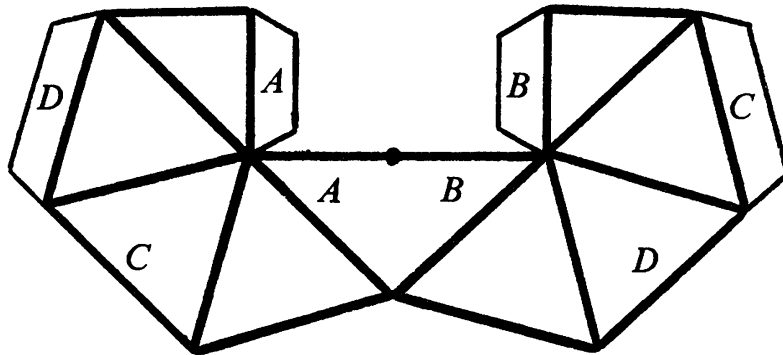


FIGURE 3.20

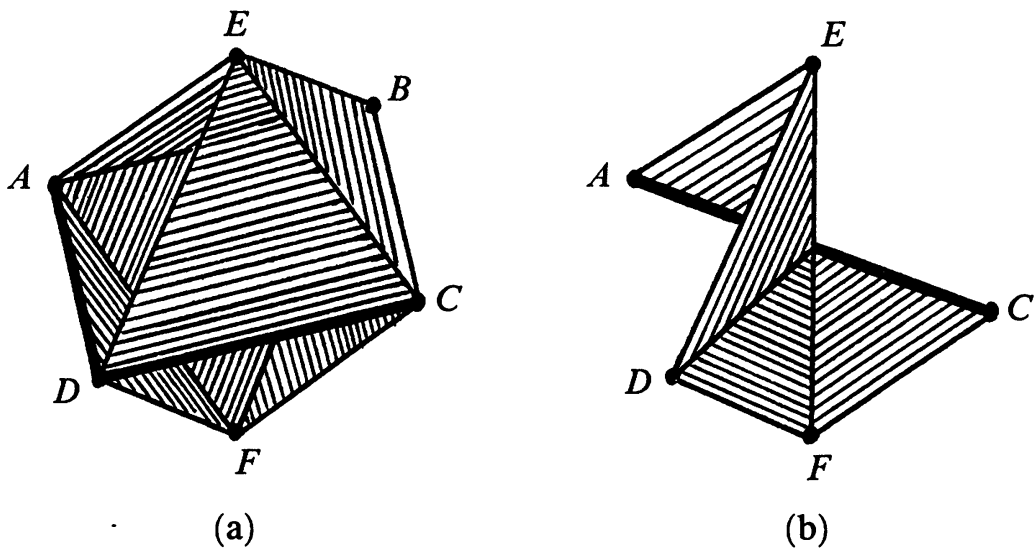


FIGURE 3.21

Another very tangible representation of the Möbius band with flat boundary may be obtained in the following way. Take a square rubber strip  $ABCD$ . In order to get a Möbius band from it, we must glue together the arrows  $AB$  and  $CD$  (Figure 3.22 (a)). But let's not hurry to do that. First let us blow the strip into a bubble as if it were a slab of bubble gum, obtaining a sphere with a hole  $ABCD$  (Figure 3.22 (b)). Now deform the sphere, bringing closer

together the arcs  $AB$ ,  $BC$  and the arcs  $AD$ ,  $DC$  (Figure 3.22 (c)). Now it is easy to imagine what will happen when the arcs  $AB$  and  $CD$  are glued together (Figure 3.22 (d)).

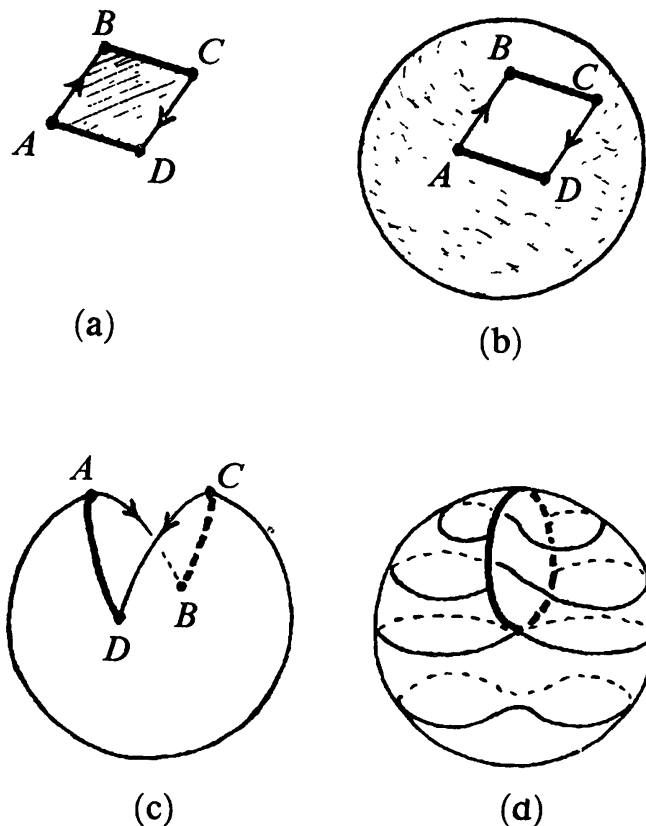


FIGURE 3.22

3.2. Cut the sphere in half along a meridian and depress downwards a part of the upper half of one of the hemispheres (Figure 3.23 (a)). Give the indented part of the hemisphere a  $180^\circ$  twist (Figure 3.23 (b)), and then another one (Figure 3.23 (c)).

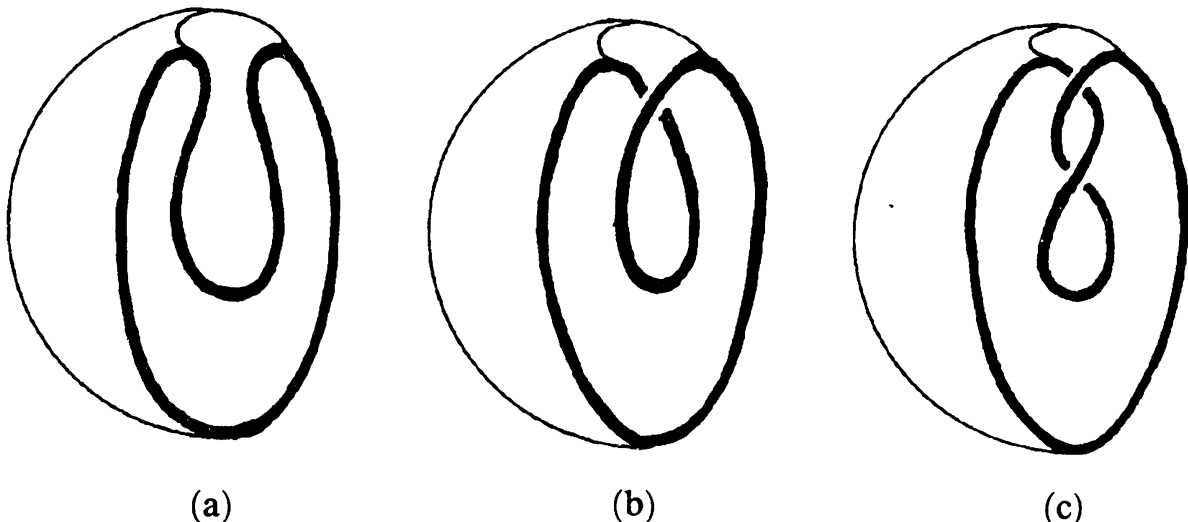


FIGURE 3.23

3.3. The easiest way is to use the diagram of the figure eight knot shown in the right side of Figure 2.4. The spanning surface is shown in Figure 3.24.

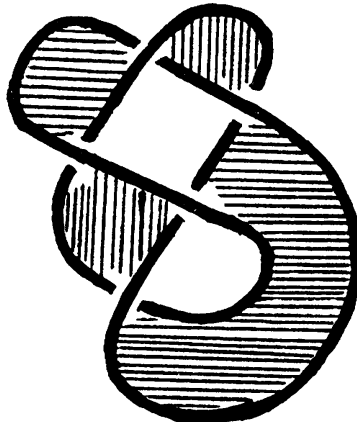


FIGURE 3.24

For the other diagrams of the figure eight knot shown in Figure 2.4, the spanning surface obtained in the same way will not be orientable. As to orientable spanning surfaces obtained for these diagrams by the Seifert algorithm, they will have several levels; it is hard to represent them in an easy-to-visualize way.

3.4. We give a proof in the specific case of the trefoil (the general case is quite similar). Consider the neighborhood of the given knot shown in Figure 3.25 (a). Its boundary is the knotted torus, on which the knot may be assumed to lie. Now squeeze together the parts of this torus at the places where they cross, obtaining an unknotted surface that looks like a fancy pretzel with four holes (Figure 3.25 (b)).

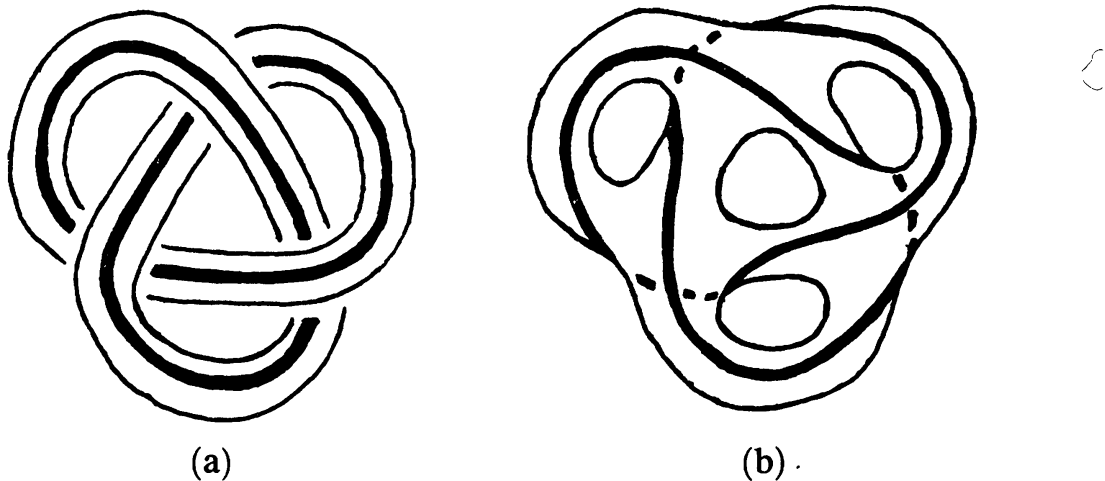


FIGURE 3.25

3.5. The required surface is shown in Figure 3.26.

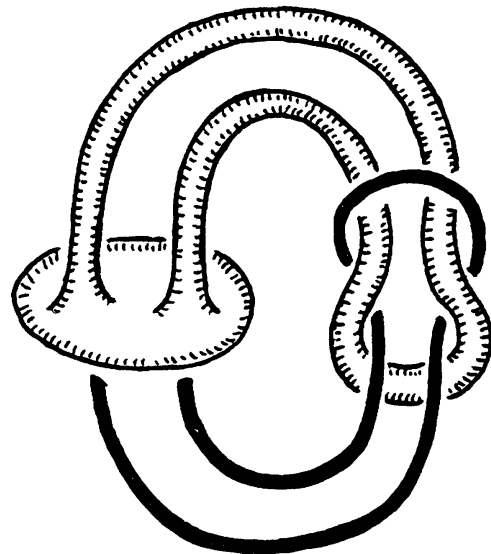


FIGURE 3.26

3.6. First let us construct spans of the two twisted circles. For each one, take the spanning film (with two extra circular boundary components  $C_1$  and  $C_2$ ) shown in Figure 3.27 (a) and attach the annulus shown in Figure 3.27 (b) to this film along  $C_1$  and  $C_2$ . We can assume that the two spanning surfaces thus obtained lie near the circles 2 and 3 from Figure 3.28 (a) on the next page. It remains to construct an oriented spanning surface for the circle 1 with a “tunnel” that lets it avoid the circles 2 and 3 (Figure 3.28 (b)).

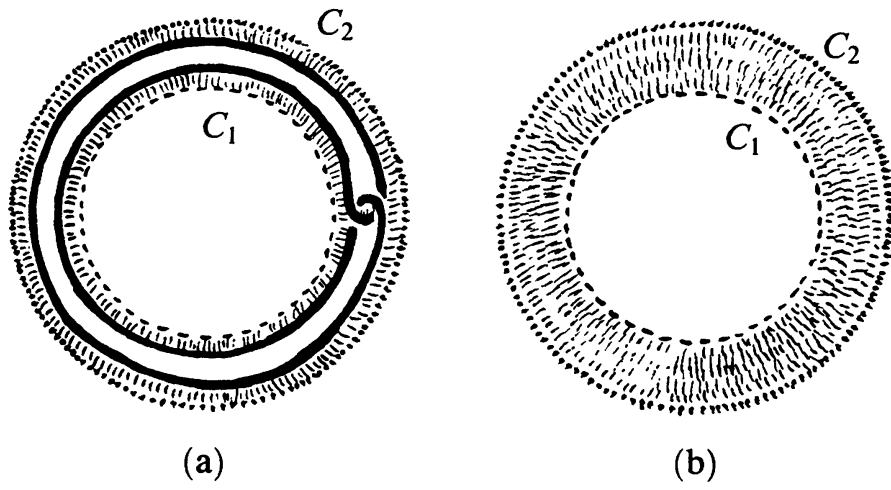


FIGURE 3.27

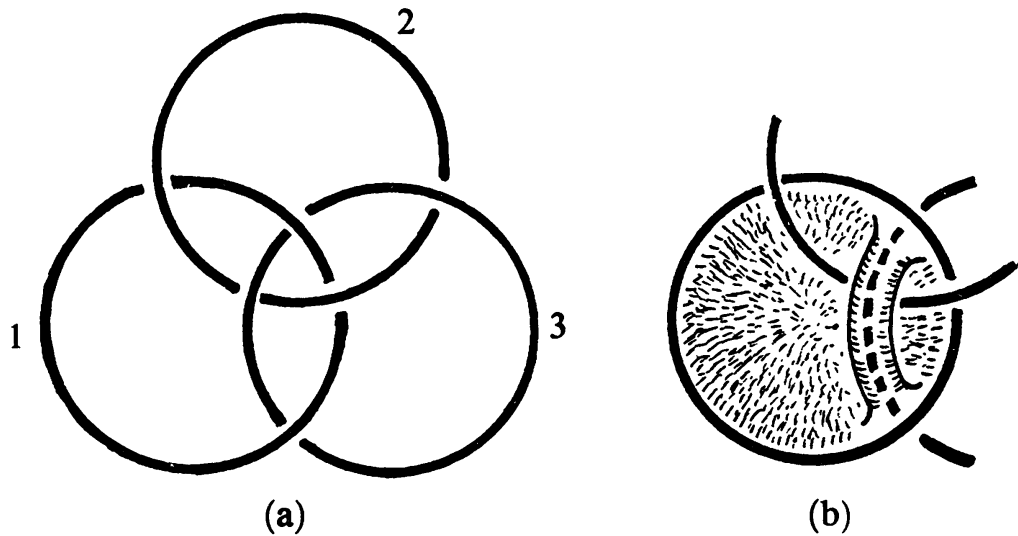


FIGURE 3.28

3.7. Let us use the Möbius band with flat boundary shown in Figure 3.21. It is easy to verify that the circle 2 represented in Figure 3.29 does not intersect this Möbius band.

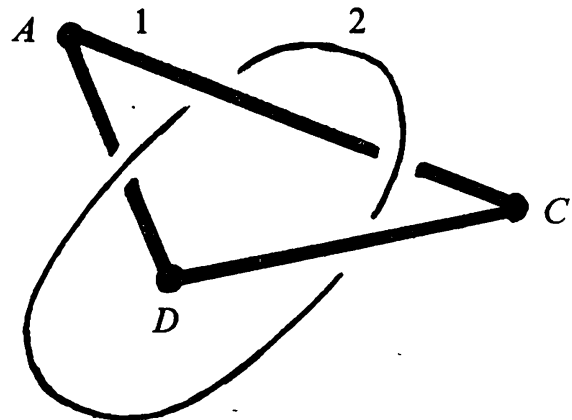


FIGURE 3.29

---

---

# 4

## A Knot Invariant

---

---

Attempts to unknot the trefoil are invariably unsuccessful. But this does not prove that this cannot be done.

A proof of this fact may be obtained, for example, by using the following strategy. Let us assign a number to each knot diagram. If this is done so that different diagrams of the same knot are assigned the same number, we say that a *knot invariant* is given. Then the value of this invariant is well defined for every knot (i.e., does not depend on the specific choice of the diagram representing the given knot). If the values of the invariant for two diagrams are different, then the diagrams represent different knots. We do not require, however, that the invariant distinguish all nonequivalent knots: for some pairs of distinct knots the values of the invariant may coincide.

For knots and links there is a very simple invariant. It may be constructed as follows. Consider all possible colorings of the knot diagram in three colors (each connected arc is painted in one color). Then at each crossing point the arcs coming together may be painted in three colors, or two colors, or one. We call a coloring *proper*, if there are no crossings where exactly two colors come together, i.e., at each crossing point either all the arcs are of the same color, or there are arcs of three different colors.

**THEOREM.** *The number of different proper colorings of a knot diagram is a knot invariant.*

**PROOF.** Consider all possible transformations of crossings that may occur in a deformation of the knot diagram (Figure 4.1). We must show that under these transformations proper colorings become well-defined proper colorings of the transformed diagram. Let us explain what this means. Suppose that a proper coloring of a diagram is given and the diagram is subjected to one of



FIGURE 4.1

the transformations shown in Figure 4.1. Let us leave the coloring of the knot as it was outside the part of the plane where the transformation took place. Then the extremities of arcs shown on the picture of the transformation are colored. We must establish that this coloring can be extended to a *proper* coloring of the part of the diagram where the changes took place. When all the extremities are painted in the same color, there is no problem: there is a unique monochromatic coloring. In each of the other (essentially distinct) cases the required extension of the coloring is shown in Figure 4.2; it is also unique. Hence the transformations do not change the number of colorings, and the theorem is proved.  $\square$

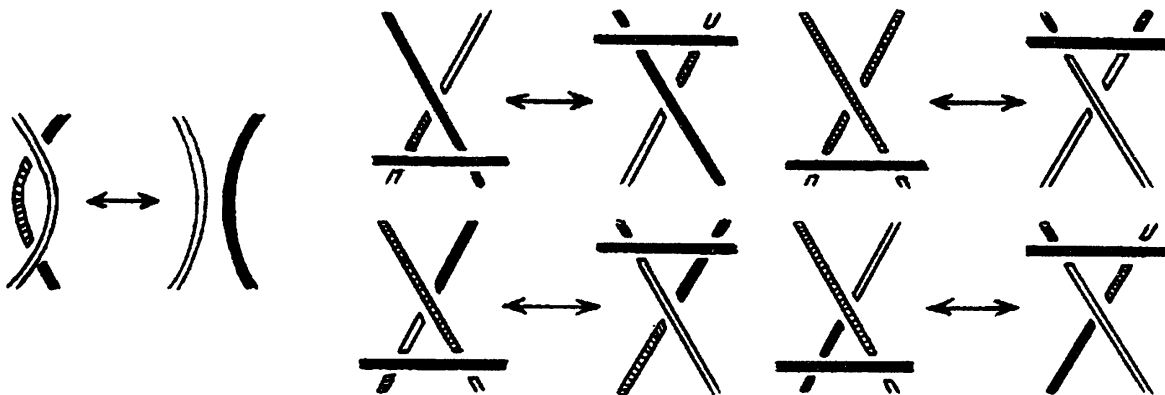


FIGURE 4.2

Now we can prove that the trefoil cannot be untied. Figure 4.3 shows a proper coloring of the trefoil that uses all three colors. The total number of proper colorings using all three colors is six. Indeed, one arc may be painted in any of the three colors, the second arc in one of the remaining two, while the coloring of the third is then uniquely determined. Besides the six colorings using all three colors, there are three monochromatic colorings. Thus there is a total of nine proper colorings of our trefoil diagram, while the unknotted circle has only three monochromatic colorings and no others. Hence there is no deformation of the trefoil into the unknot.

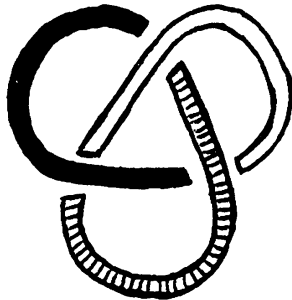


FIGURE 4.3

Unfortunately, the invariant that we have just constructed is not very powerful. For example, it does not even allow us to prove that the figure eight knot cannot be untied. Indeed, it is easy to show that each of its proper

colorings is monochromatic. Nevertheless, the invariant allows us to distinguish infinitely many knots from each other. Figure 4.4 shows two different proper colorings of the same diagram. Attaching  $n$  such diagrams into a closed chain, we get a knot that has  $3 \cdot 2^n + 3$  proper colorings. Hence for distinct  $n$  the number of colorings is different.



FIGURE 4.4

For links, the number of proper colorings of a link diagram is also an invariant. The proof of this statement does not differ from the one for knots.

Unknotted and pairwise unlinked circles may be colored independently. Therefore the number of proper colorings for  $n$  such circles is  $3^n$ . This gives us new possibilities for applying our invariant to links as compared to knots. Indeed, if a link diagram possesses only monochromatic colorings, the number of its colorings is less than that for unknotted and unlinked circles. This is the case for the links shown in Figure 4.5: they all have only monochromatic proper colorings.

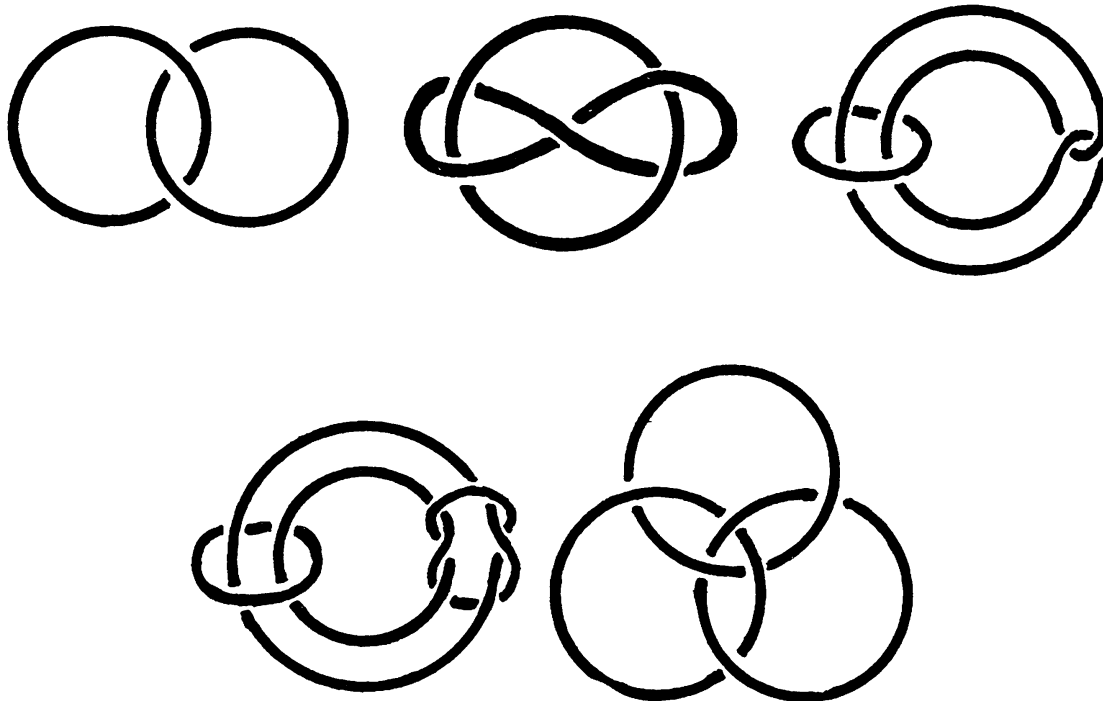


FIGURE 4.5

We have proved that the links from Figure 4.5 cannot be untied. This allows us to return to Problem 1.1 about separating hands with linked fingers. Figure 4.6 shows that if a rigid bracelet is worn on one of the hands (Figure 4.6 (a)), they can no longer be moved apart (to the position shown in Figure 4.6 (b)) by a deformation of the person's body (assumed very elastic, as the reader recalls). Indeed, if we had succeeded in moving the hands apart, then the bracelet could be taken off (Figure 4.6 (c)). But then the link in Figure 4.6 (a) could be untied.

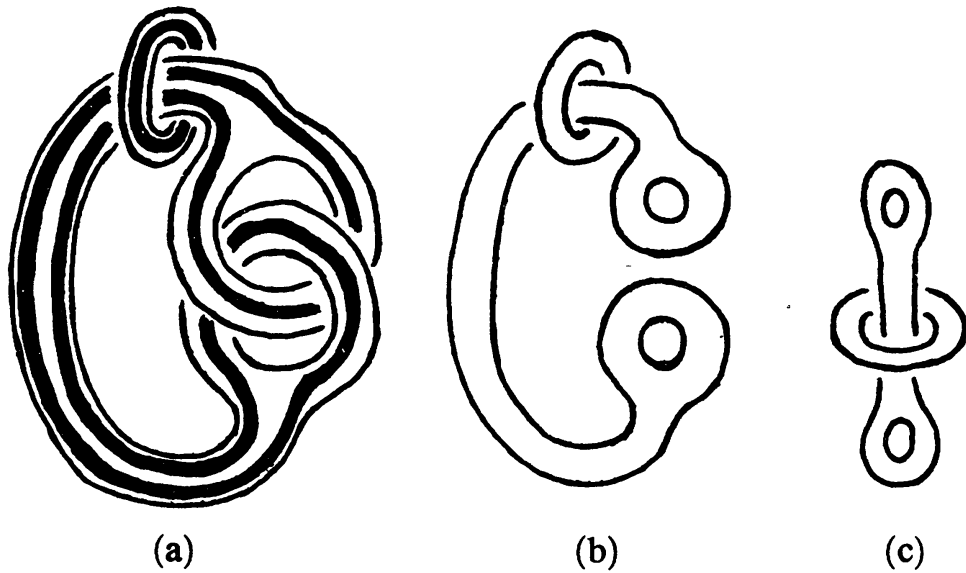


FIGURE 4.6

# 5

## Homeomorphisms

In the previous sections we have been considering objects in space “up to deformations”, i.e., we did not distinguish objects that can be deformed into each other by reshaping them. Topologists call such objects *isotopic* (in space). For example, knots or links that can be deformed into each other are called isotopic.

An even more important notion in topology is that of homeomorphism. Two geometric figures  $X$  and  $Y$  are said to be *homeomorphic*, if there exists a continuous one-to-one mapping  $f : X \rightarrow Y$  such that the inverse mapping  $f^{-1} : Y \rightarrow X$  is also continuous. Unlike isotopy, the fact that two figures are homeomorphic depends on the figures themselves and not on their disposition in space. For example, any knot is homeomorphic to the circle, but not necessarily isotopic to it.

All the surfaces that can be obtained from the rectangular strip of paper shown in Figure 5.1 (a) by gluing the arrows together are homeomorphic. Examples of such surfaces are the cylinder and the twisted cylinder (Figure 5.1 (b)). These surfaces are homeomorphic, but not isotopic. Indeed, the latter statement follows from the fact that their boundaries are nonisotopic links (Figure 5.1 (c)).

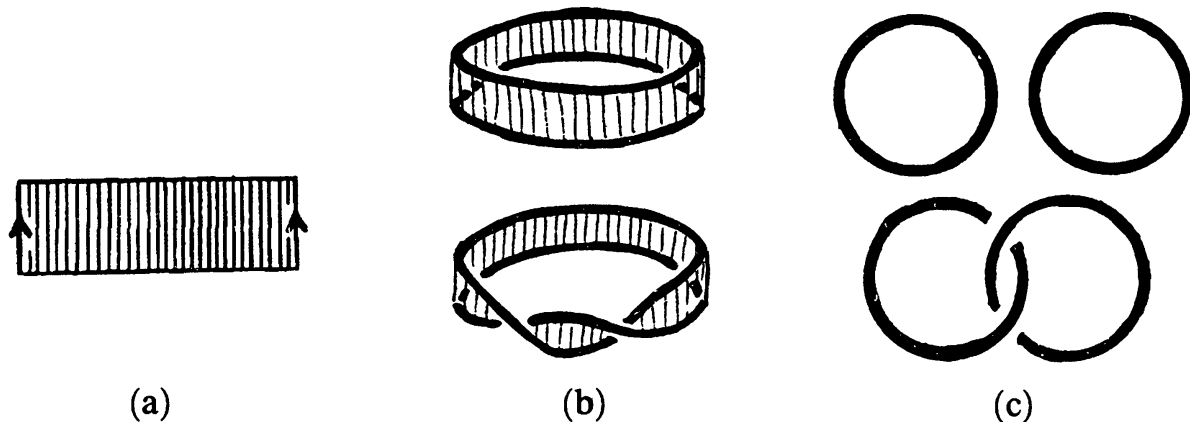


FIGURE 5.1

If the sides of the strip are glued together in the opposite way (see Figure 5.2 (a)), then surfaces homeomorphic to the Möbius band are obtained. Two of them are shown in Figure 5.2 (b). The bottom one is isotopic to the span of the trefoil knot, with which we are already familiar (Figure 5.2 (c)).

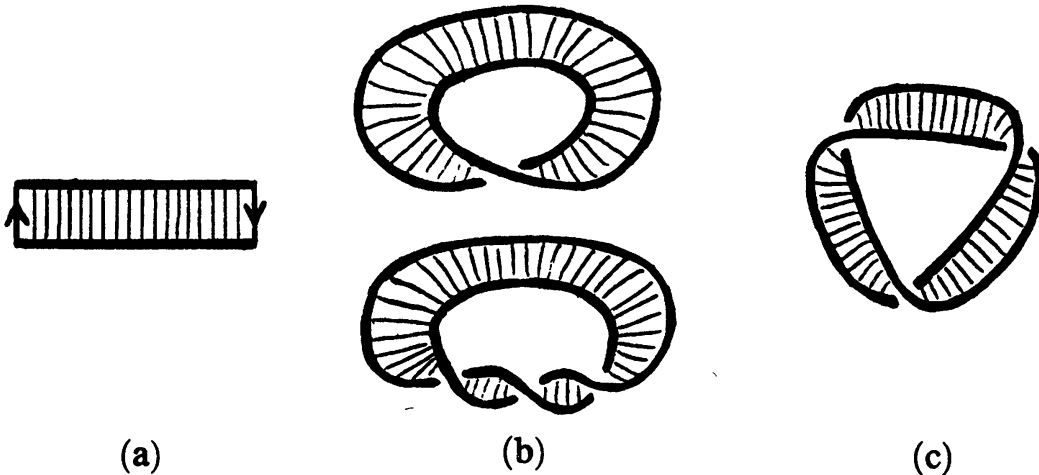


FIGURE 5.2

Let us discuss a few more examples of homeomorphic and nonhomeomorphic geometric objects.

**EXAMPLE 1.** The open interval (i.e., the segment without its endpoints) and the infinite line are homeomorphic. Indeed, it is easy to show that the open interval is homeomorphic to the semicircle (without endpoints). A homeomorphism between this semicircle and the whole line is represented in Figure 5.3.

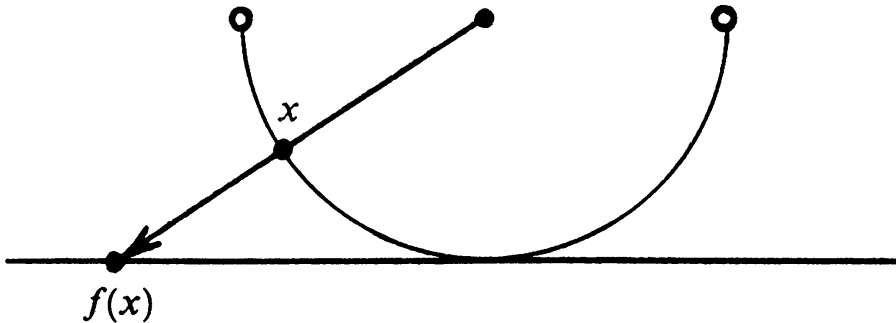


FIGURE 5.3

**EXAMPLE 2.** The punctured open disk is homeomorphic to the open annulus. By a punctured open disk we mean the set of points  $X$  such that  $0 < AX < 1$ , where  $A$  is a fixed point (the punctured center of the disk), while the open annulus is the set of points  $Y$  such that  $1 < AY < 2$ . The required homeomorphism may be defined by assigning to each point  $X$  the point  $Y$  on the ray  $AX$  such that  $AY = 1 + AX$ . Note that if the point  $A$  had not been removed from our disk, a homeomorphism of the disk on the annulus could not be constructed in this manner.

One of the simplest ways to prove that two figures are not homeomorphic is by puncturing them (removing a point).

**EXAMPLE 3.** The closed interval  $I = [0, 1]$  and the open interval  $J = (0, 1)$  are not homeomorphic. Assume the converse and let  $f : I \rightarrow J$  be a homeomorphism. The point 1 does not divide the closed interval  $I$ , i.e., after it is removed any two remaining points can be joined by a path. This property is preserved under homeomorphisms. Therefore, the point  $f(1)$  does not divide the open interval  $J$ . But any point of an open interval clearly divides it into two disjoint pieces. This contradiction shows that the homeomorphism  $f : I \rightarrow J$  cannot exist.

**Problem 5.1.** Prove that the circle and the open interval are not homeomorphic.

**Problem 5.2.** Prove that the straight line is not homeomorphic to the figure consisting of three rays with the same origin.

Another method for proving that two figures are not homeomorphic is based on the fact that the property of all loops (i.e., closed paths) being contractible to a point is preserved under homeomorphisms.

**EXAMPLE 4.** The disk and the annulus are not homeomorphic. Indeed, in the disk any loop can be contracted to a point (Figure 5.4 (a)), while the annulus has a noncontractible loop (Figure 5.4 (b)).

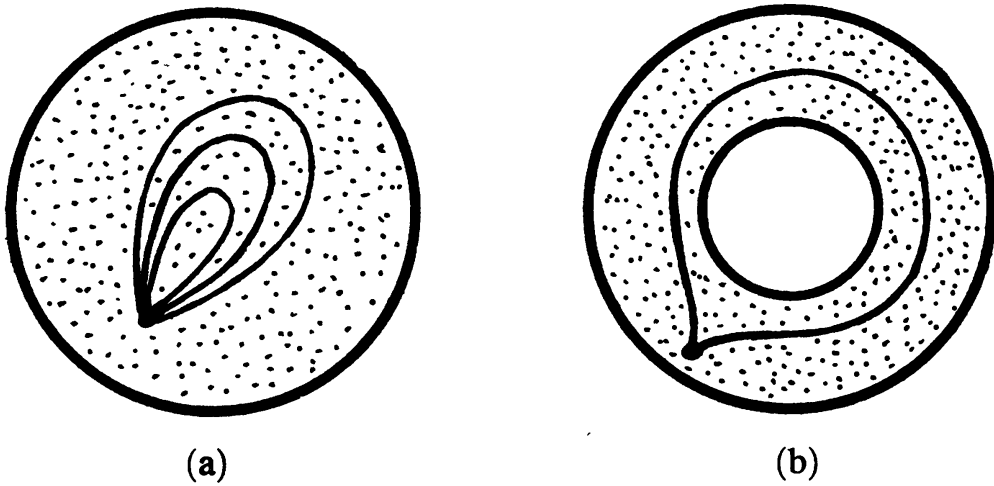


FIGURE 5.4

Now let us discuss whether the continuity condition of the mapping  $f^{-1}$  can be replaced by some weaker condition. For example, is it sufficient in the definition of homeomorphism to require only the existence of a continuous one-to-one map  $f : X \rightarrow Y$ , or the existence of two continuous one-to-one maps  $f : X \rightarrow Y$  and  $g : Y \rightarrow X$ ? The two following problems claim that this is not the case.

**Problem 5.3.** Let  $I$  be a semi-interval, i.e., a closed interval from which one of the endpoints have been removed. Show that there exists a continuous one-to-one map  $f : I \rightarrow S$ , where  $S$  is a circle.

**Problem 5.4.** Let  $F_1$  be a disk and  $F_2$  an annulus from both of which some boundary points have been removed (to solve the problem you will have

to specify these points). Prove that there exist continuous one-to-one maps  $f : F_1 \rightarrow F_2$  and  $g : F_2 \rightarrow F_1$ .

When we discussed spanning surfaces for knots, we began with two spans of the trefoil (see Figure 3.1). Later we learned that one of them is homeomorphic to the Möbius band (see Figure 5.2).

**Problem 5.5.** Show that the other spanning surface is homeomorphic (but not isotopic) to the *torus* from which a small disk has been removed (Figure 5.5).

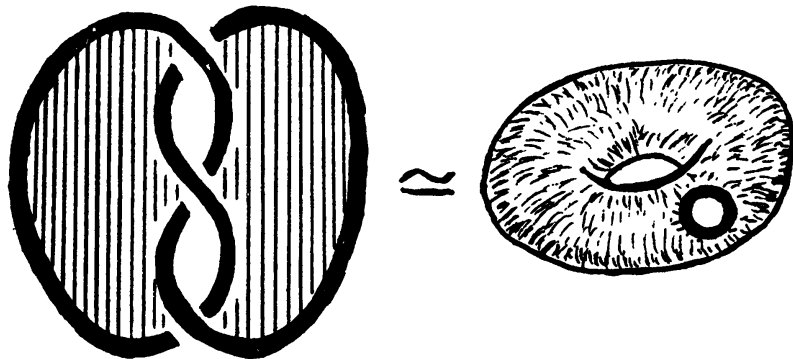


FIGURE 5.5

Now we shall study two important special types of homeomorphisms. Both will be called *twists*.

It is most convenient to describe these twists for the cylinder, although in that case twists yield nothing interesting, because for the cylinder we get a homeomorphism which is actually an isotopy. But for the torus a similar construction already yields interesting homeomorphisms.

The construction of the twisting homeomorphism for the cylinder is shown in Figure 5.6 (a). We begin by rigidly fixing the upper and lower base of the cylinder and then cut the cylinder apart along its midline. Then we also fix one of the edges of the cut and rotate the other edge until it turns by  $360^\circ$ . After that we glue the edges back together again. The result is a one-to-one map of the cylinder onto itself. It can fail to be continuous only at points of the cut. But since our rotation was by a whole turn, no points of discontinuity can appear.

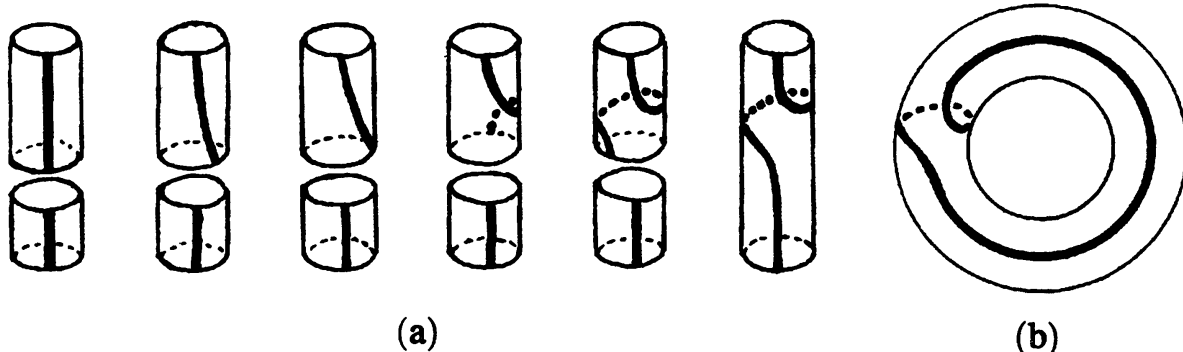


FIGURE 5.6

For the cylinder the twist is not a very interesting homeomorphism. But in a similar way one can construct an interesting homeomorphism of the torus by regarding a part of the torus as a cylinder (Figure 5.6 (b)). The twist of the torus thus obtained allows us to transform an unknotted circle on the torus into a trefoil knot (Figure 5.7). To do that, first we transform the given circle by three such twists into the curve shown in Figures 5.7 (b) and (c). The shaded annulus on the latter figure can be regarded as a cylinder. If we carry out a twist along the midline of this cylinder, we get the curve shown in Figure 5.7 (d). This curve is actually the trefoil, as can be verified by inspecting Figures 5.7 (e) and (f). Thus twists of the torus do not necessarily reduce to isotopies.

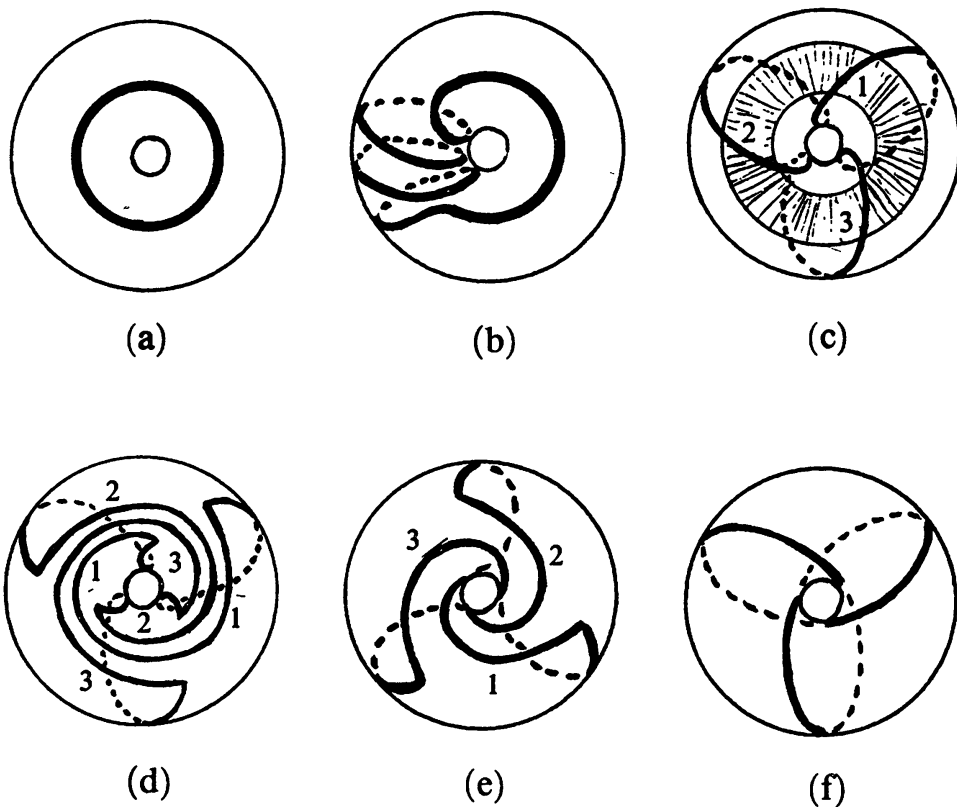


FIGURE 5.7

**Problem 5.6.** Construct a homeomorphism of the pretzel shown in Figure 5.8 (a) that transforms the unlinked circles shown in that figure into the linked curves appearing in Figure 5.8 (b).

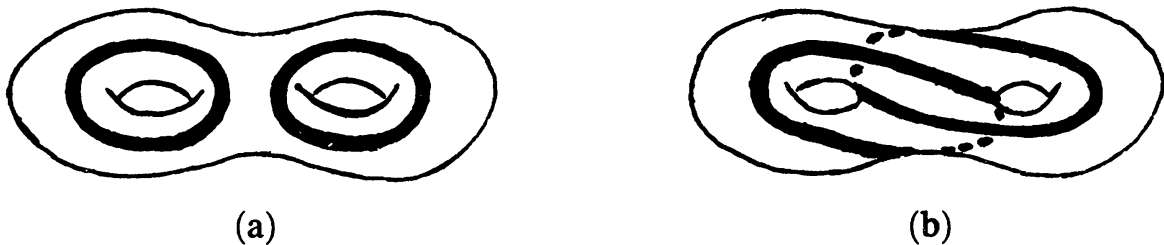


FIGURE 5.8

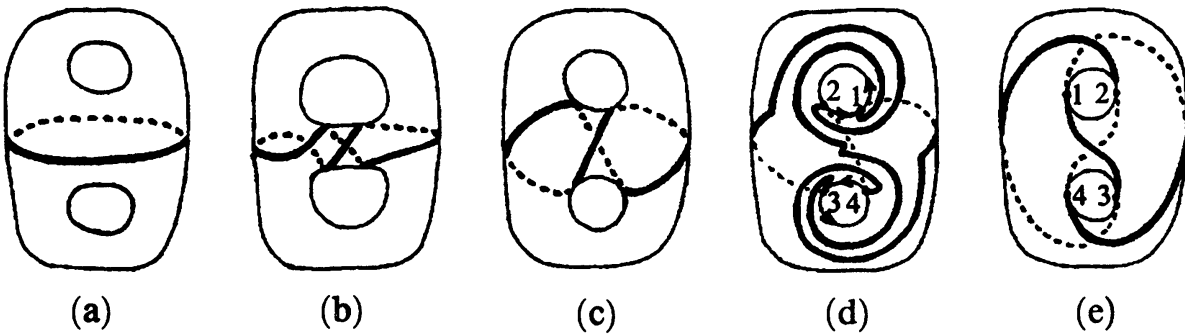


FIGURE 5.9

Figure 5.9 shows how the circle that divides the pretzel in half can be transformed into a trefoil by means of twists. The passage from (b) to (c) is done by an isotopy. The passage from (c) to (d) is similar to that from Figure 5.7 (c) to Figure 5.7 (d). Moving the points 1 and 2, 3 and 4 in Figure 5.9 (d) counterclockwise, one easily obtains Figure 5.9 (e). If we work with only one half of the pretzel (say the upper half), we get a homeomorphism between the torus with a disk removed and an oriented spanning surface of the trefoil.

The trefoil lying on the pretzel with two holes can also be obtained from a curve that does not cut the pretzel apart into two pieces (Figure 5.10). Note that a curve that does not split a surface is transformed by any homeomorphism into a curve with the same property. Hence we can conclude that the trefoil shown in Figure 5.10 (e) does not split the pretzel. Let us explain how this trefoil was obtained. We begin with two twists (Figure 5.10 (b)). An obvious isotopy takes (b) to (c). To get (d) from (c), hold the pretzel at the points  $A$  and  $B$  and rotate its upper half and its lower half by  $180^\circ$ . To get (e) from (d), one more twist is used.

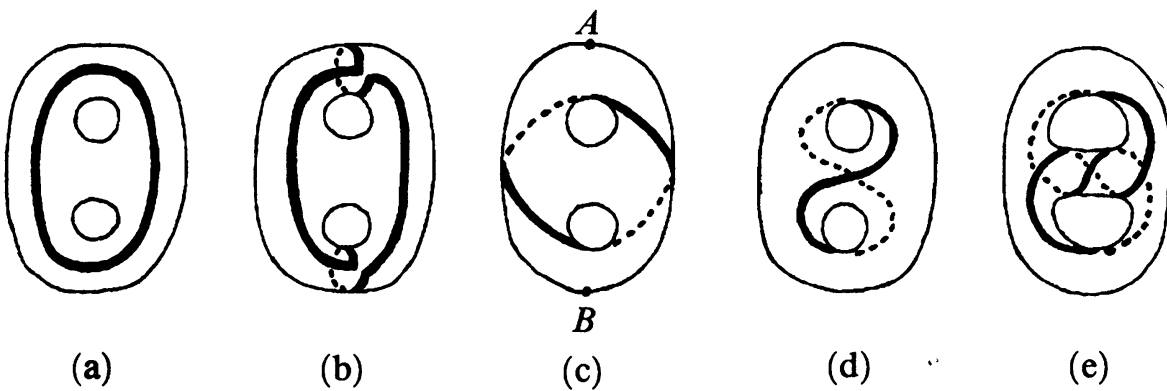


FIGURE 5.10

Now let us discuss another type of twisting homeomorphisms. Figure 5.11 shows two knot diagrams that differ only at one crossing point. The first is a trefoil, while the second is the unknot. Imagine that the entire space is filled with elastic material. Let us remove a knot  $K$  from this space. Let us denote by  $\mathbb{R}^3 - K$  the set that remains. If  $K_1$  and  $K_2$  are as above, the two sets  $\mathbb{R}^3 - K_1$  and  $\mathbb{R}^3 - K_2$  are not homeomorphic. We shall not prove this fact. We are interested in something else. Namely, it turns out that if we cut

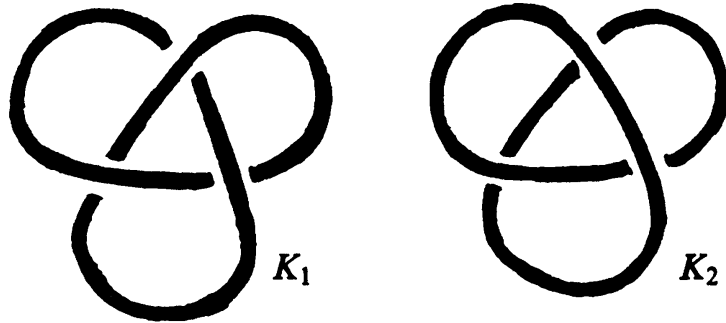


FIGURE 5.11

out, in addition to  $K_1$  and  $K_2$ , the little circles shown in Figure 5.12, we get homeomorphic sets  $\mathbb{R}^3 - L_1$  and  $\mathbb{R}^3 - L_2$ .

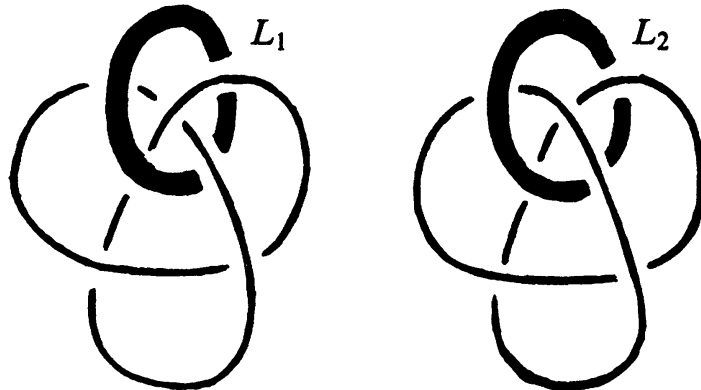


FIGURE 5.12

Before we construct a homeomorphism between  $\mathbb{R}^3 - L_1$  and  $\mathbb{R}^3 - L_2$ , let us note that instead of cutting out a curve, we can always cut out a neighborhood of this curve, i.e., remove a solid torus rather than a circle. This is related to the fact that the punctured disk is homeomorphic to the annulus (actually, to the annulus minus its inner boundary circle).

In constructing the required homeomorphism, we shall only be interested in the domain shown in Figure 5.13 (a). More precisely, the homeomorphism will only act on a cylinder surrounded by the torus: in Figure 5.13 (b) we

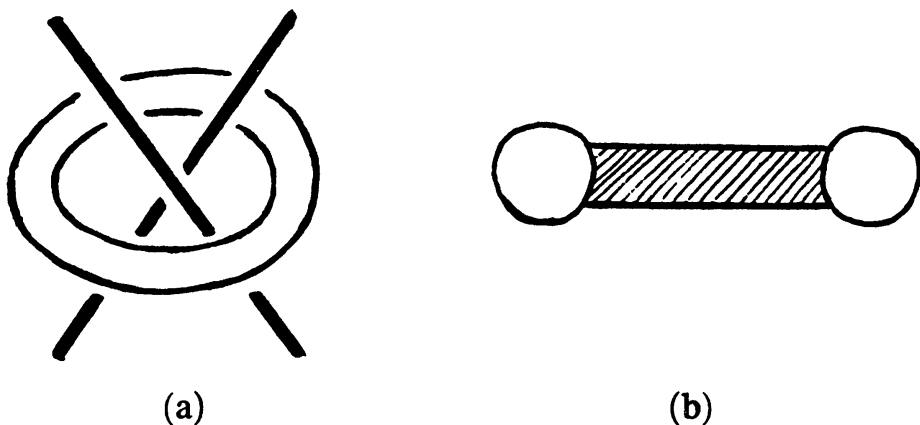


FIGURE 5.13

show the section of the cylinder as a shaded rectangle. Let us represent this cylinder separately, increasing its height for clarity (Figure 5.14 (a)). The remaining part of the set  $\mathbb{R}^3 - L_1$  touches the cylinder only along its upper and lower bases; the cylinder's lateral surface is free, i.e., it does not touch the rest of the set. Now rigidly fix the upper base of the cylinder, cut along the lower base, rotate the obtained disk through  $360^\circ$  (Figure 5.14 (b)), and glue the set back together. Once this is done, there is an obvious isotopy from (b) to (c). Comparing (a) and (c), we observe that the crossing has changed to the opposite one, so that we have transformed  $\mathbb{R}^3 - L_1$  into  $\mathbb{R}^3 - L_2$ . It remains to establish that our transformation was a homeomorphism. The lateral surface of the cylinder does not touch the rest of the set, so that discontinuity points may only appear on the lower base. But since we rotated the base by a whole turn and then glued it back, there are no discontinuity points. Thus we have constructed a homeomorphism of  $\mathbb{R}^3 - L_1$  onto  $\mathbb{R}^3 - L_2$ .

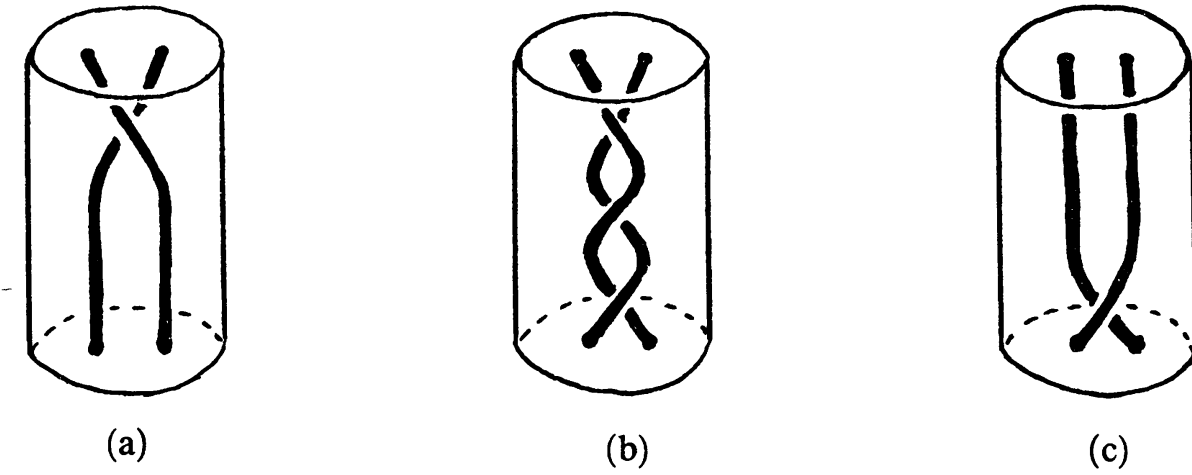


FIGURE 5.14

Let us return to the knots  $K_i$  and links  $L_i$  shown in Figures 5.11 and 5.12 respectively. Denote by  $T_1$  and  $T_2$  the two little circles that link the different crossings of the knots  $K_1$  and  $K_2$ . In other words,  $L_i$  is the union of  $K_i$  and  $T_i$ . So in fact we have not only constructed a homeomorphism  $f : \mathbb{R}^3 - L_1 \rightarrow \mathbb{R}^3 - L_2$ , but also a homeomorphism  $g : \mathbb{R}^3 - T_1 \rightarrow \mathbb{R}^3 - T_2$  that takes  $K_1$  to  $K_2$ . Thus the homeomorphism  $f$  can be extended to  $K_1$ . Having done that, the desire to extend  $f$  further to  $T_1$  is only natural. In other words, we would like to construct a homeomorphism  $h : \mathbb{R}^3 \rightarrow \mathbb{R}^3$  that takes  $L_1$  to  $L_2$  (here, as you have guessed,  $\mathbb{R}^3$  denotes three-dimensional space from which nothing has been removed). Let us see what will happen to a very small circle  $S$  linking  $T_1$  (Figure 5.15 (a)) under the homeomorphism  $f$ . Its image under  $f$  is shown in Figure 5.15 (b). This last picture demonstrates that the map  $f$  cannot be extended to  $T_1$ . Note that if a homeomorphism  $h : \mathbb{R}^3 \rightarrow \mathbb{R}^3$  taking  $L_1$  to  $L_2$  existed, we would in particular have a homeomorphism  $s : \mathbb{R}^3 - K_1 \rightarrow \mathbb{R}^3 - K_2$ , by taking for  $s$  the restriction of  $h$  to the set  $\mathbb{R}^3 - K_1$ .

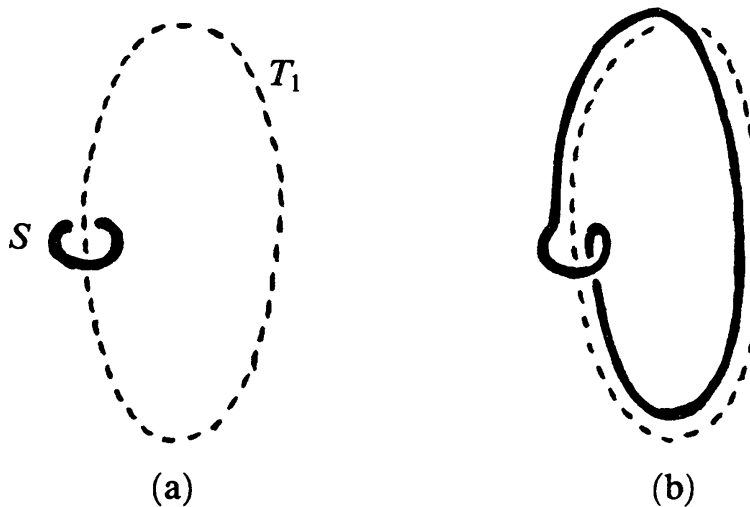


FIGURE 5.15

*Problem 5.7.* a) Show that the sets obtained from three-dimensional space by removing the links in Figure 5.16 are homeomorphic.

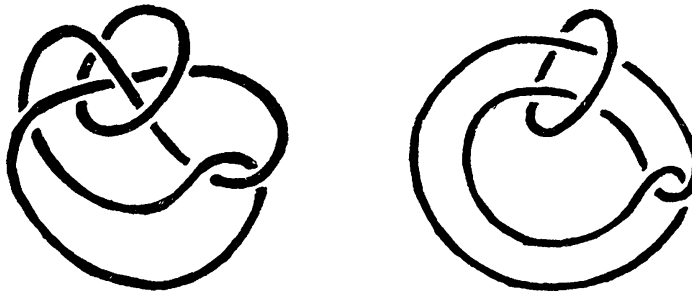


FIGURE 5.16

b) Prove a similar statement for the links in Figure 5.17.

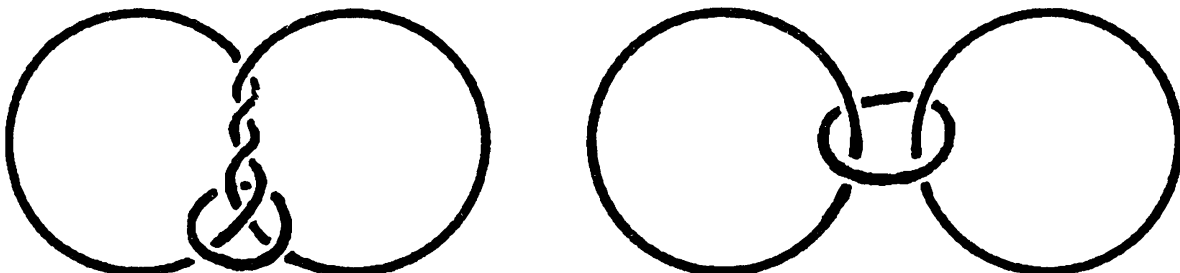


FIGURE 5.17

*Problem 5.8.* Show that any knot can be untied after appropriate crossing changes (i.e., some of its crossing points have been changed to opposite ones, the upper branch becoming the lower one and vice versa).

### Solutions.

5.1. Any point of the open interval splits it into two parts, while the circle has no such points.

5.2. The origin of the three rays splits the figure into three pieces.

5.3. The circle may be obtained from the semi-interval in a natural way (Figure 5.18).

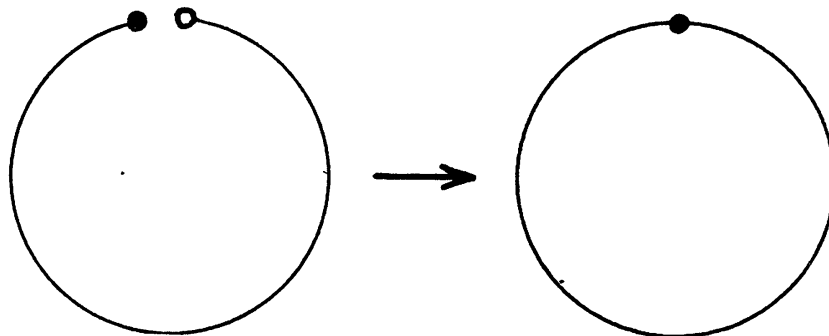


FIGURE 5.18

5.4. The solution is shown in Figure 5.19. The dotted part of the boundaries is not a part of the corresponding figures. The construction of the continuous one-to-one map of the annulus (with one point on the inner boundary) onto the disk, shown in the lower part of the figure, is similar to the construction of the homeomorphism of the annulus onto the punctured disk in Example 2.

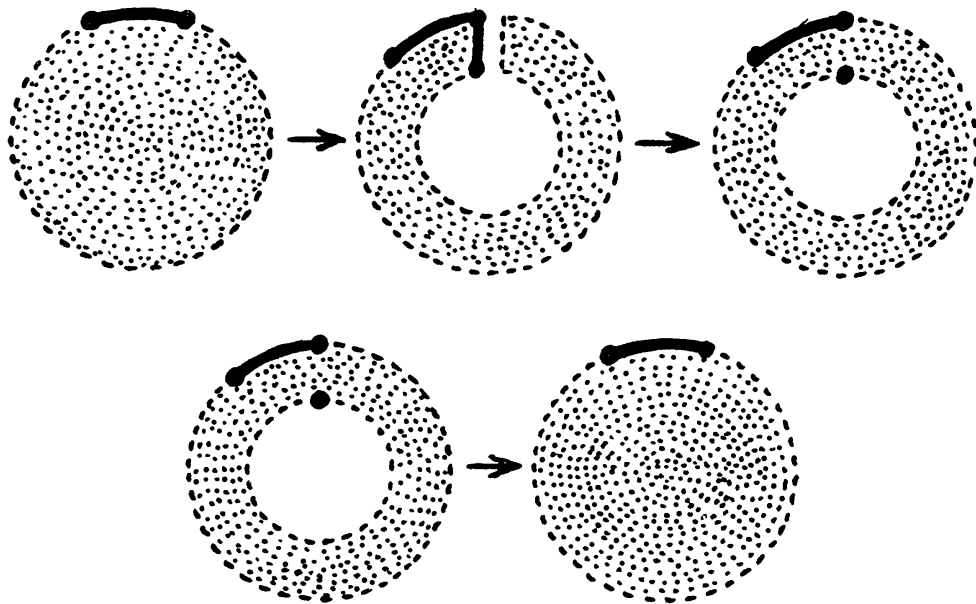


FIGURE 5.19

5.5. The required surface may be obtained by gluing the arrows of the two pieces shown in Figure 5.20 (a). Let's perform an isotopy of the shaded figure and reflect the white one with respect to a vertical line (Figure 5.20 (b)). The pairs of arrows  $a$  and  $c$  can be identified, and then one of the  $b$  arrows may be moved by means of an isotopy near the other one (Figure 5.20 (c)). If we now glue together the two  $b$  arrows, we get a surface that can be easily deformed into the torus with a disk removed. (Recall that the latter deformation was shown in Figure 1.8.)

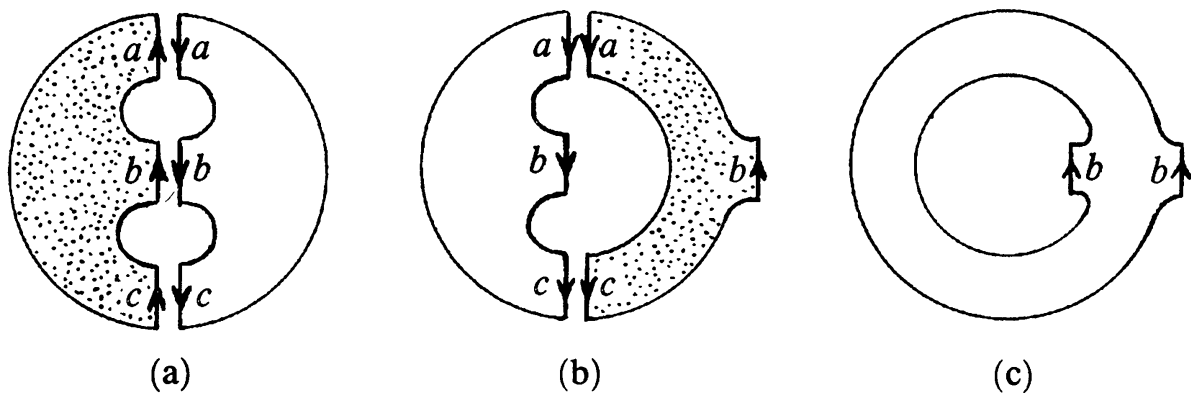


FIGURE 5.20

5.6. The required homeomorphism can be obtained by a twist (Figure 5.21) followed by an isotopy.

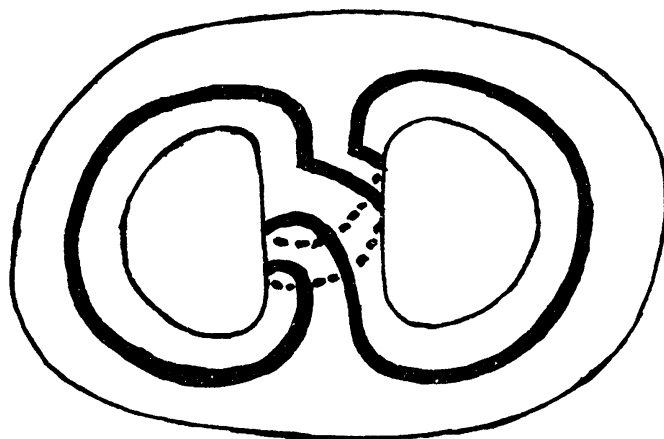


FIGURE 5.21

5.7. We shall use one of the removed curves in order to construct the required twisting homeomorphisms.

a) By means of a twist we get the configuration shown in Figure 5.22 (a); the twist here is done along the dotted line.

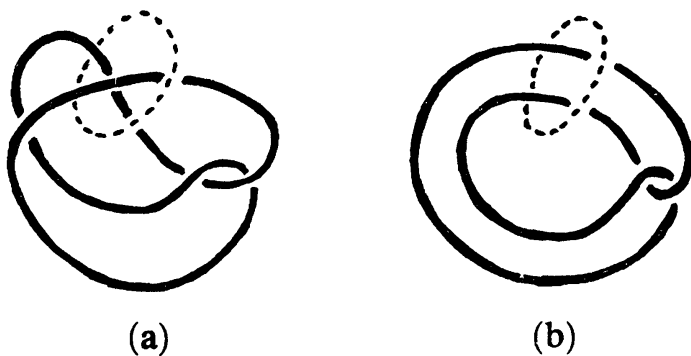


FIGURE 5.22

b) Here two twists are needed. First we get the link shown in Figure 5.23 (a). This link is isotopic to the one in (b). Another twist along the same circle yields two unlinked curves (Figure 5.23 (c)).

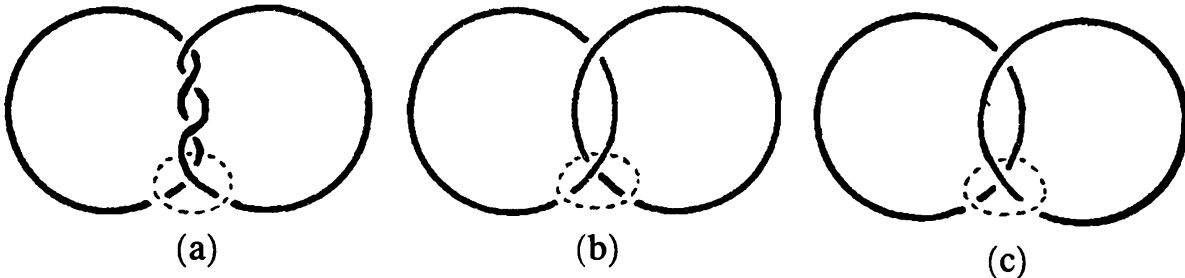


FIGURE 5.23

5.8. Consider the diagram of the knot  $K_1$ . Let  $l$  be a line in the plane of the diagram that does not intersect the knot. Let us move the line towards the knot until it touches the knot at some point  $P$  (Figure 5.24). Take a line segment  $AB$  in space that projects onto the point  $P$ . We can assume that  $A$  lies above  $B$ . Consider the trajectory of a point that moves uniformly downward from  $A$  to  $B$ , but not vertically: it circles in space above the diagram (i.e., so that its projections are points on the diagram other than  $P$ ), uniformly approaching it. This trajectory, together with the line segment, is a knot  $K_2$  in space, which can be obtained from  $K_1$  by crossing changes. It is clear that the curve  $K_2$  is unknotted. Indeed, its projection on any plane perpendicular to  $l$  has no double points.

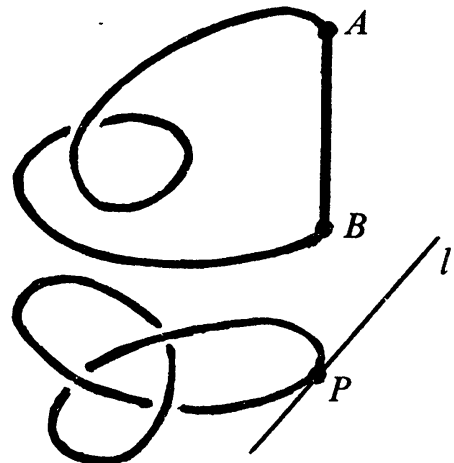


FIGURE 5.24

---

---

# 6

## Vector Fields on the Plane

---

---

Suppose that at each point of the plane (or some part of the plane) a vector is specified in such a way that the components of the vector depend continuously on the point (Figure 6.1). Then we say that a *continuous vector field* on the plane is given. Any point at which the given vector is zero is called *singular*. We shall only consider vector fields with a finite number of singular points.

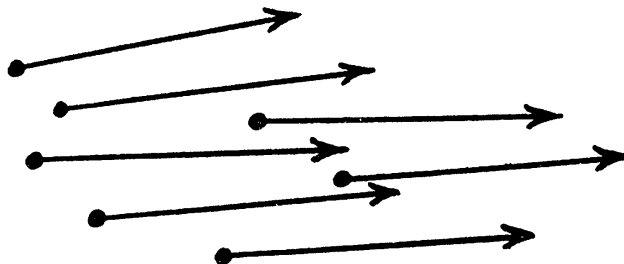


FIGURE 6.1

Let us go around a contour without self-intersections encircling exactly one singular point. For each point that we visit, consider the corresponding vector, attaching it to some fixed point. As we move, this vector rotates about the fixed point, possibly changing in length. Let us see how many complete revolutions it performs while we go around our contour. We count a full revolution with a “+” sign if it was performed in the same direction of rotation as our trip around the contour and with a “-” otherwise. The total number of “signed” revolutions (i.e., the difference between the number of positive and negative ones) is said to be the *index* of the singular point.

Clearly the index does not depend on the direction around the given contour that we choose. But does it depend on this contour? A little later we shall prove that it does not. But first some examples.

Consider the vector fields  $a$ ,  $b$ , and  $c$  (see Figure 6.2) in the plane given by

$$a(x, y) = (x, y), \quad b(x, y) = (y, -x), \quad c(x, y) = (y, x).$$

Each of these vector fields has exactly one singular point, namely the origin  $O = (0, 0)$ . Let  $\varphi$  be the angle of rotation from the  $x$ -axis to the vector  $(x, y)$ , while  $\alpha$ ,  $\beta$ , and  $\gamma$  are the angles of rotation from the  $x$ -axis to

the vectors  $a$ ,  $b$ , and  $c$  respectively. These angles depend only on  $\varphi$ . Explicitly,

$$\alpha(\varphi) = \varphi, \quad \beta(\varphi) = \varphi - 90^\circ, \quad \gamma(\varphi) = 90^\circ - \varphi.$$

When we go around the unit circle  $x^2 + y^2 = 1$ , the angles change by  $360^\circ$ . The sign of the change for the angles  $\alpha$  and  $\beta$  is the same as for  $\varphi$ , while for  $\gamma$  the sign is the opposite one. Hence the index of the origin for the vector fields  $a$  and  $b$  is equal to 1, while the index for  $c$  is equal to  $-1$ .

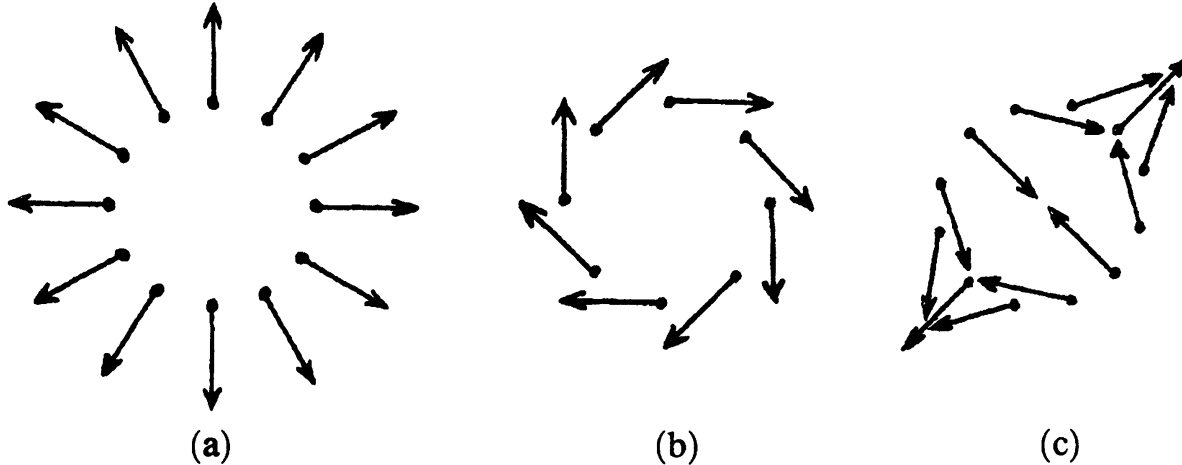


FIGURE 6.2

It is useful to regard a vector field as a velocity field describing the motion of points on the plane. In other words, each point of the plane moves along a certain trajectory, and the vector field consists of the velocity vectors of all these points. Note that here the motion is stationary, i.e., the velocity of each point depends only on its position and the velocity field does not change in time.

*Problem 6.1.* Prove that in the case of the vector fields  $a$ ,  $b$ , and  $c$ , these trajectories of all points except the origin will be rays, circles, and branches of hyperbolas respectively.

*Problem 6.2.* Find the indices of the origin for the vector fields shown in Figure 6.3.

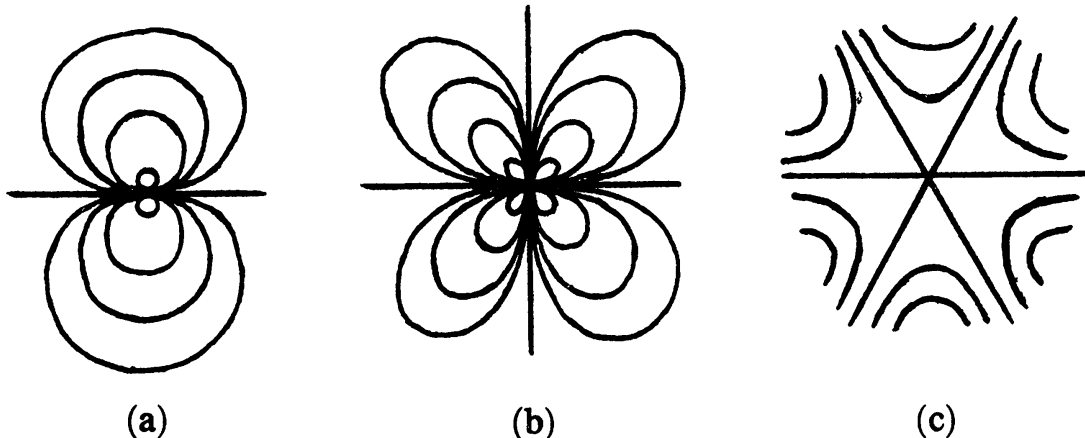


FIGURE 6.3

**Problem 6.3.** Does there exist a vector field whose trajectories are as shown in Figure 6.4?

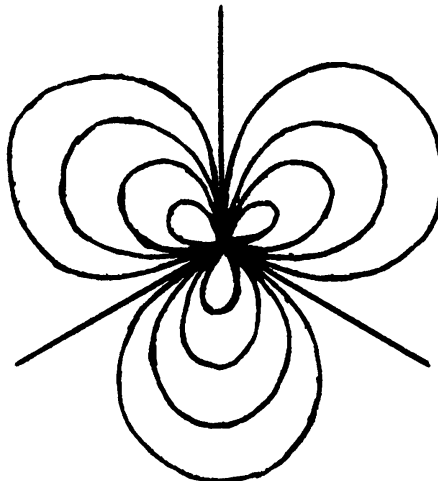


FIGURE 6.4

We shall use the term *complex plane* to designate the ordinary plane whose points have been identified with the set of complex numbers, the point  $(x, y)$  being identified with the complex number  $x + iy$ .

**Problem 6.4.** On the complex plane consider the vector field

$$v(z) = \frac{z^n}{|z|^{n-1}}, \quad z \neq 0, \quad v(0) = 0.$$

Find the indices of the singular points for these vector fields for various  $n$  and represent their trajectories graphically.

**Problem 6.5.** Let us say that a vector field  $v$  is *even* if  $v(x) = v(-x)$  and *odd* if  $v(x) = -v(-x)$ . Prove that the index of the point  $O$  for an even field is even and is odd for an odd field.

**Problem 6.6.** At each point  $X$  of a circle a vector  $v(X)$  depending continuously on  $X$  is given. The line containing this vector intersects the circle at the points  $X$  and  $Y$  (Figure 6.5). During a complete circuit about the

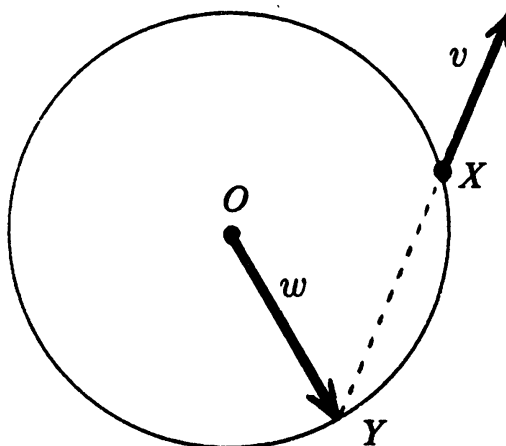


FIGURE 6.5

circle, the vector  $v$  performs  $n$  revolutions. How many revolutions will the vector  $w$  joining the center  $O$  of the circle to  $Y$  perform?

Now let us prove that the index of a singular point does not depend on the choice of the contour used to determine it. The index is an integer, and, therefore, it can change only by jumps of no less than 1: it cannot change continuously. When we continuously change the contour, a jump in the value of the index can only occur when the contour moves through a singular point. But we consider only contours that encircle exactly one point and do not pass through other singular points. Any two such contours encircling the same singular point can be deformed into each other without passing through other singular points.

*Problem 6.7.* A closed self-intersecting curve divides the plane into several regions (Figure 6.6). By choosing a point  $O$  in each region, we can assign to the region the number of revolutions performed by the vector  $\overrightarrow{OX}$  when the point  $X$  goes around the curve. Prove that if two regions have a common boundary, then the two numbers for the two regions differ by 1.

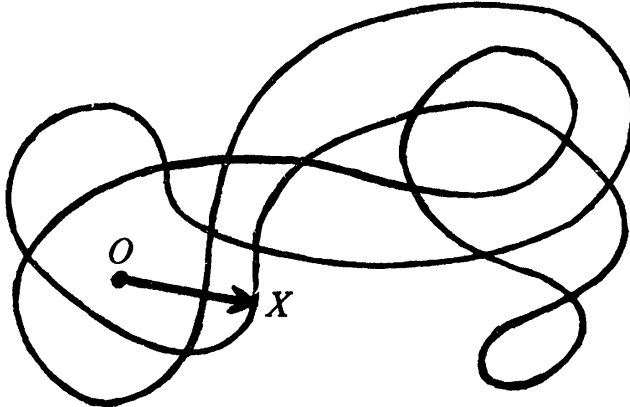


FIGURE 6.6

Suppose that a closed non-self-intersecting curve  $\gamma$  does not pass through any singular points of a vector field  $v$ . Then we can define the *index* of this curve as the number of revolutions performed by the vector  $v(X)$  when  $X$  goes once around the curve  $\gamma$ . Revolutions are counted with a “+” sign if their direction of rotation coincides with the one chosen in going around our curve.

**THEOREM 6.1.** *The index of any curve  $\gamma$  is equal to the sum of indices of the singular points that it encircles.*

**PROOF.** For the  $x$ -axis choose any line that is not perpendicular to any of the segments joining pairs of singular points encircled by the curve and join these points successively in increasing order of their  $x$ -coordinate (Figure 6.7).

The curve  $\gamma$  is isotopic to the curve  $\gamma_1$  located near the broken line that we have just constructed (in Figure 6.7 the region bounded by  $\gamma_1$  is shaded).

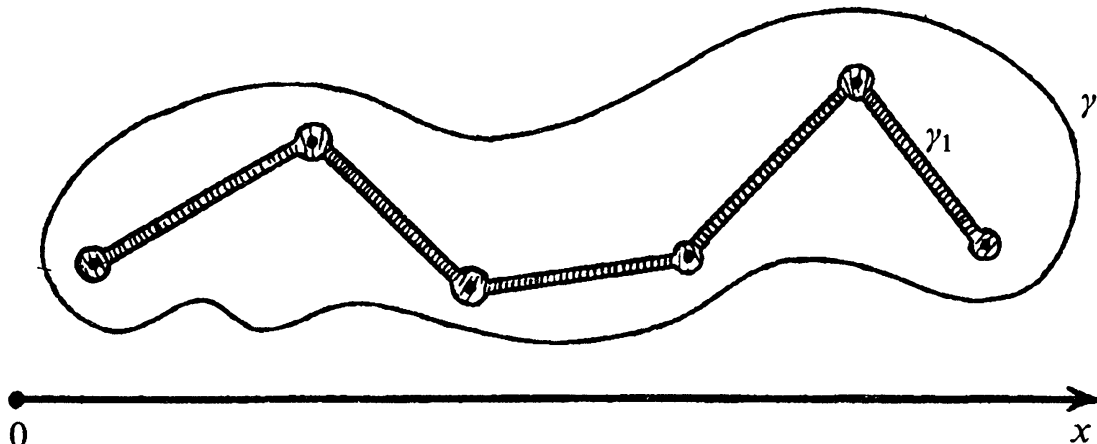


FIGURE 6.7

During the isotopy taking  $\gamma$  to  $\gamma_1$ , the curves do not pass through any singular points, hence their indices are the same. The curve  $\gamma_1$  consists of line segments located near the line segments joining the singular points and of arcs of little circles with centers at the singular points. If we move along the segment  $AB$  first from  $A$  to  $B$  and afterwards from  $B$  to  $A$ , then the absolute values of the angles of rotation will be the same, but their signs will be opposite. Hence the parts of the curve  $\gamma_1$  near the segments of the broken line give a zero contribution to the index, being traversed in opposite directions. Thus only the arcs near the singular points contribute to the index for the curve  $\gamma_1$ .

In all these arguments we assume that the curve  $\gamma_1$  is close enough to our broken line.  $\square$

**COROLLARY.** *If the index of a closed non-self-intersecting curve is not equal to zero, then it encircles at least one singular point.*

It is in fact this Corollary to Theorem 6.1 that yields the most important applications of the index of singular points. Let us present three examples of such applications (Theorems 6.2–6.4).

**THEOREM 6.2.** *Let  $f$  be a continuous map of the disk  $D^2$  into the plane such that each point of the boundary circle  $S^1$  stays in place. Then some point of the disk is mapped into its center.*

**PROOF.** On  $D^2$  consider the vector field

$$v(X) = \overrightarrow{Of(X)},$$

where  $O$  is the center of the disk (Figure 6.8; see the next page). Then on  $S^1$  we get a vector field just like the one represented in Figure 6.2 (a). Hence the index of the curve  $S^1$  is 1, and therefore there must be a singular point  $X_0$  inside  $S^1$ . The relation  $v(X_0) = 0$  is equivalent to  $f(X_0) = O$ , i.e., the point  $X_0$  is mapped to the center of the disk.  $\square$

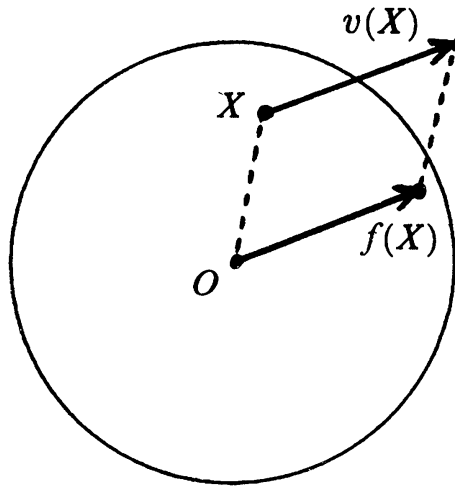


FIGURE 6.8

**THEOREM 6.3.** *Let  $f$  be a continuous map of the disk  $D^2$  into itself. Then  $f(X_0) = X_0$  for some point  $X_0$  in  $D^2$ , i.e.,  $f$  has a fixed point  $X_0$ .*

**PROOF.** On the disk  $D^2$  consider the vector field  $w(X) = \overrightarrow{Xf(X)}$ . Assume that the map  $f$  has no fixed points, i.e., the vector field  $w$  has no singular points. On the boundary circle we can also consider the vector fields  $v$  and  $v_t$ ,  $0 \leq t \leq 1$ , whose definition is clear from Figure 6.9: the point  $X'$  is diametrically opposed to the point  $X$ , while the point  $X'_t$  divides the line segment  $f(X)X'$  in the ratio

$$f(X)X'_t : X'_t X = t : (1 - t).$$

Let us agree that  $X'_0 = f(X)$  and  $X'_1 = X'$ . All the vectors  $v_t$  are nonzero, therefore we can consider the number  $n(t)$  equal to the index of the boundary circle with respect to the vector field  $v_t$ . The number  $n(t)$  is an integer and depends continuously on  $t$ . Hence  $n(0) = n(1) = 1$ . But this implies that the vector field  $w$  has a singular point. This is a contradiction.  $\square$

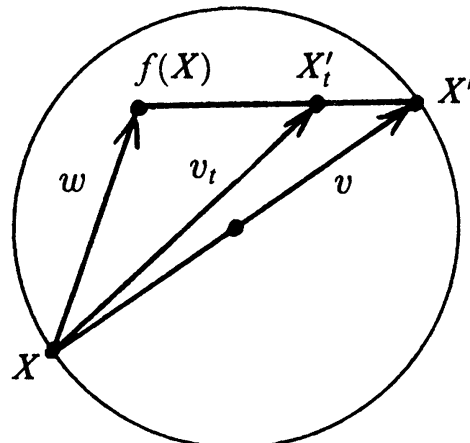


FIGURE 6.9

In the process of proving Theorem 6.3, we have in fact established the following statement, which will be used again in the sequel.

**LEMMA 6.1.** *Suppose that two vector fields  $v$  and  $w$  are given on a non-self-intersecting curve in such a way that at any point  $X$  the vectors  $v(X)$  and  $w(X)$  do not point in exactly opposite directions. Then the indices of  $\gamma$  with respect to these vector fields are equal.*

**PROOF.** Look at Figure 6.9. The vector  $v_t$  can be zero only if the vectors  $v$  and  $w$  are of opposite directions.  $\square$

**THEOREM 6.4** (The Main Theorem of Algebra). *Any polynomial*

$$P(z) = z^n + a_1 z^{n-1} + \cdots + a_{n-1} z + a_n$$

*with complex coefficients has at least one complex root.*

**PROOF.** On the complex plane consider the vector fields  $v(z) = z^n$  and  $w(z) = P(z)$ . First let us prove that for sufficiently large  $R$  and any point  $z$  of the circle  $|z| = R$  we have the inequality

$$|w(z) - v(z)| < |v(z)|.$$

Let  $a$  be the largest of the numbers  $|a_1|, \dots, |a_n|$ . Then

$$|w(z) - v(z)| = |a_1 z^{n-1} + \cdots + a_n| \leq |a_1| R^{n-1} + \cdots + |a_n| \leq n a R^{n-1}$$

whenever  $R > 1$ . Since  $|v(z)| = R^n$ , we have  $|w - v| < |v|$  whenever  $R > na + 1$ .

The inequality  $|w - v| < |v|$  implies that the vectors  $v$  and  $w$  cannot have opposite directions. Hence by Lemma 6.1 the index of the circle  $|z| = R$  with respect to the field  $w$  is equal to its index with respect to  $v$ . The latter index is equal to  $n$  (see the solution of Problem 6.4). Thus the index of the circle  $|z| = R$  with respect to the vector field  $w(z) = P(z)$  equals  $n$ . Hence inside this circle there are singular points at which  $P(z)$  vanishes.  $\square$

The basic idea underlying the proof of the last theorem may be visualized as follows. If the number  $R$  is large enough, the length of the vector  $w - v$  is much shorter than that of the vector  $v$  (Figure 6.10). The vector  $v$  performs  $n$  revolutions, therefore the vector  $w$ , which is very close to  $v$ , also performs  $n$  revolutions.

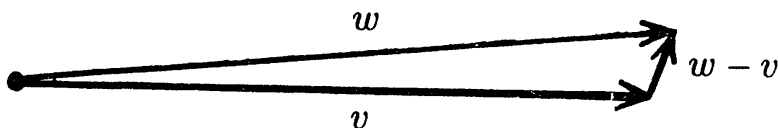


FIGURE 6.10

**Problem 6.8.** Suppose  $f$  is a continuous map of the disk  $D^2$  with center  $O$  into the plane such that whenever two points  $A$  and  $B$  are symmetric with respect to  $O$ , so are the points  $f(A)$  and  $f(B)$ . Prove that some point of the disk is mapped to the point  $O$ .

Now let us see what happens when a vector field changes inside some circle. Note first of all that the index of the circle does not change, because the vectors on the circle remain the same. Therefore, if two singular points merge into one, the index of this point will be equal to the sum of the indices of those two. For example, when two points of index 1 merge, a singular point of index 2 is obtained (Figure 6.11). The merger of three index 1 points may be visualized as follows. The horizontal “waist” of the shaded region in Figure 6.12 (a) is pinched to a point, yielding two shaded regions. When more points of index 1 are added, similar pinching processes of the added regions take place.

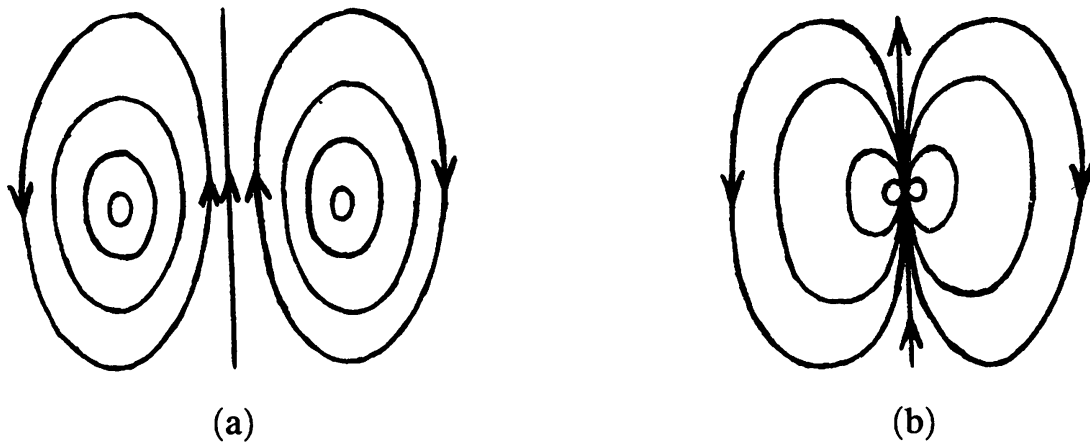


FIGURE 6.11

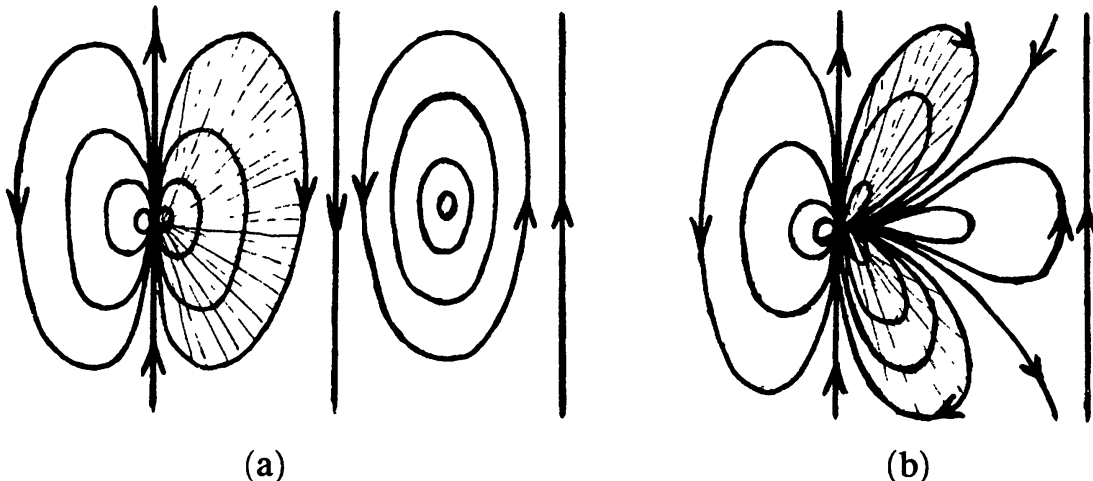
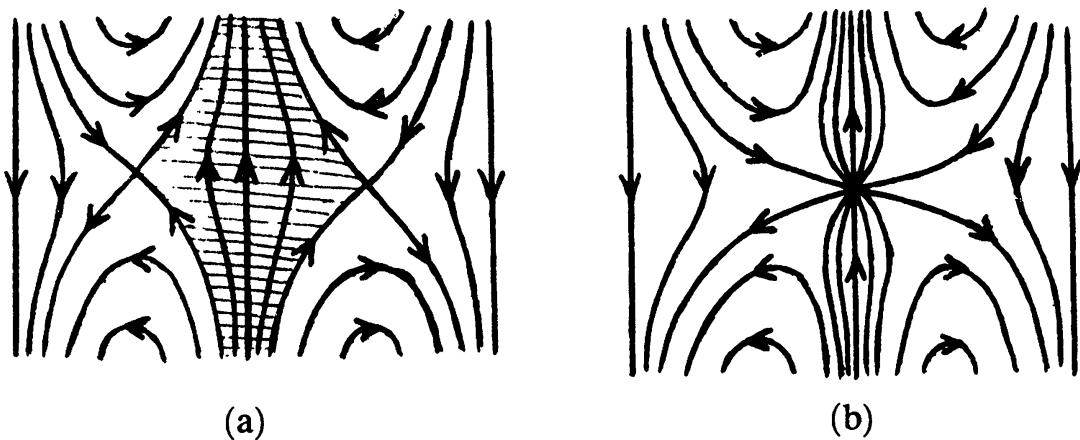
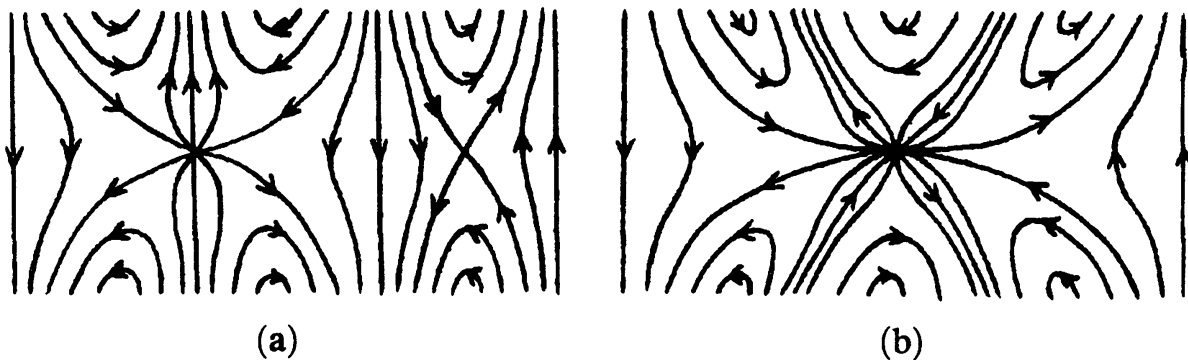


FIGURE 6.12

When two singular points of index  $-1$  merge, the pinching occurs for the region like the one shaded in Figure 6.13 (a). The result is shown in (b). If a larger number of points of index  $-1$  merge, a similar pinching process affects other regions (Figure 6.14).



**FIGURE 6.13**



**FIGURE 6.14**

When a singular point of index 1 merges with one of index  $-1$ , we get a singular point of index 0. Such a singular point can be “removed”. Problems 6.9 and 6.10 give two interpretations of this disappearance of a singular point.

**Problem 6.9.** Change the trajectories of the vector field shown in Figure 6.15 so that outside the circle  $S_2$  the trajectories remain the same, while inside the circle  $S_1$  they become parallel line segments. The result must be a vector field without singular points.

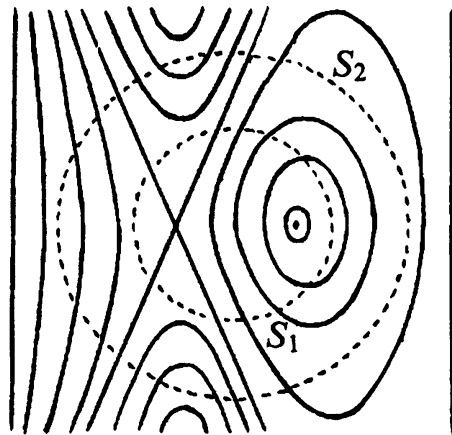


**FIGURE 6.15**

**Problem 6.10.** Change the trajectories of the same vector field so that inside the circle  $S_1$  the trajectories do not change, while outside the circle  $S_2$  they become parallel lines or rays. The result must be a vector field without singular points between the two circles.

In fact, Problems 6.9 and 6.10 deal with the construction of a vector field without singular points on an annulus when the vector field is already given on the two boundary circles. In other words, we are dealing with the extension of a vector field without singular points given on the boundary. Here is another problem of this type.

**Problem 6.11.** Extend the vector field shown in Figure 6.16 to a vector field without singular points on the entire annulus. Draw a picture of its trajectories.

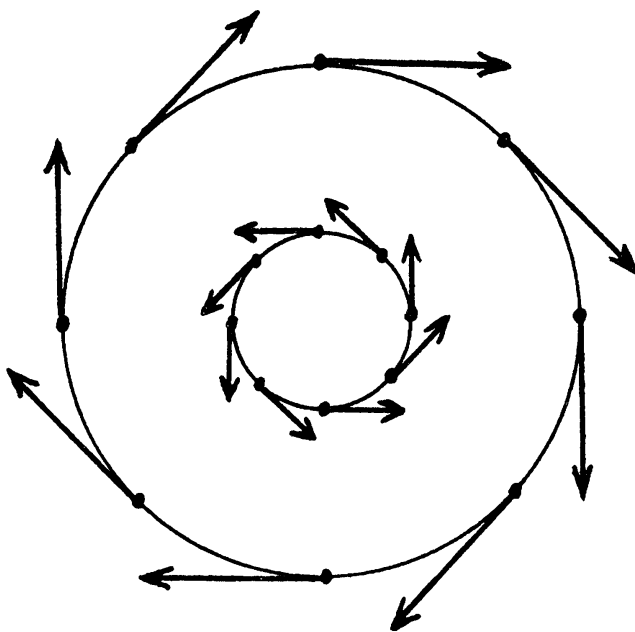


FIGURE 6.16

Problems 6.9–6.11 are particular cases of the following statement.

**THEOREM 6.5.** *A vector field given on the boundary circles of an annulus can be extended to a vector field without singular points on the entire annulus provided the indices of the two circles are equal.*

**PROOF.** First suppose that the vector field can be extended to the entire annulus without singular points. Carry out a similitude (homothety) taking the outer circle to the inner one. Since no singular points are crossed during this deformation, the indices of the outer and inner circle are equal.

Now suppose that a vector field is given on the boundary circles such that the indices of the two circles are equal. We are required to extend the vector field to the entire annulus. For an arbitrary vector field on a circle, let us construct its graph in the following way. For each angle  $\alpha$  define  $\varphi(\alpha)$  as the angle between the vectors given at the points  $X$  and  $A$  (Figure 6.17); here  $\varphi(0) = 0$ . Let us plot the graph of the function  $\varphi(\alpha)$  on the segment  $[0, 2\pi]$ .

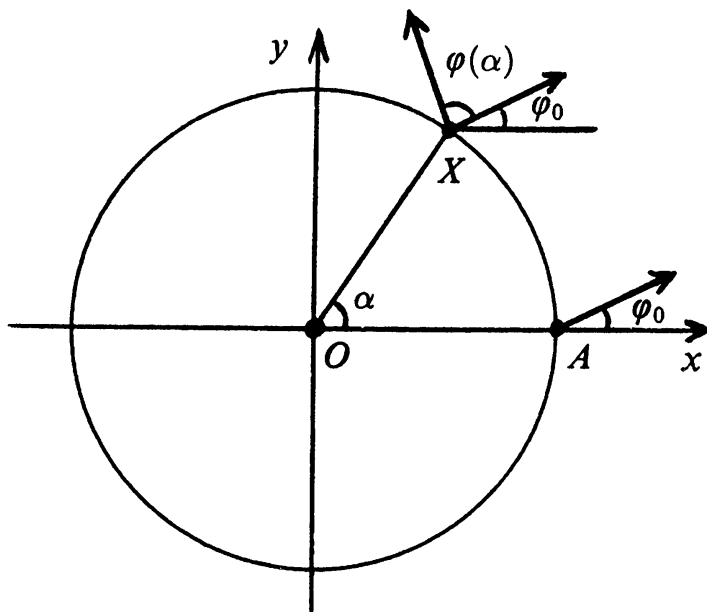


FIGURE 6.17

The graph passes through the origin and the point with coordinates  $(2\pi, 2k\pi)$ , where  $k$  is the index of the circle with respect to the given vector field.

Now, on the same figure, let us plot the two graphs corresponding to the given vector field on the two boundary circles (Figure 6.18). These graphs may be joined by a continuous family of graphs as follows. Suppose that the line parallel to the  $y$ -axis intersects the first graph at the point  $A_1$  and the second one at  $A_2$  (see Figure 6.18). Let us assume that at time  $t$  the corresponding graph divides the segment  $A_1A_2$  in the ratio  $t:(1-t)$ . Then at the moments of time  $t = 0$  and  $t = 1$  we get the first and second graph respectively, and while  $t$  changes from 0 to 1, the first continuously changes into the second. As the result, for all  $t$  and  $\alpha$ , where  $0 \leq t \leq 1$  and  $0 \leq \alpha \leq 2\pi$ , we have defined the value of  $\varphi(t, \alpha)$ . The two initial graphs correspond to  $\varphi(0, \alpha)$  and  $\varphi(1, \alpha)$ .

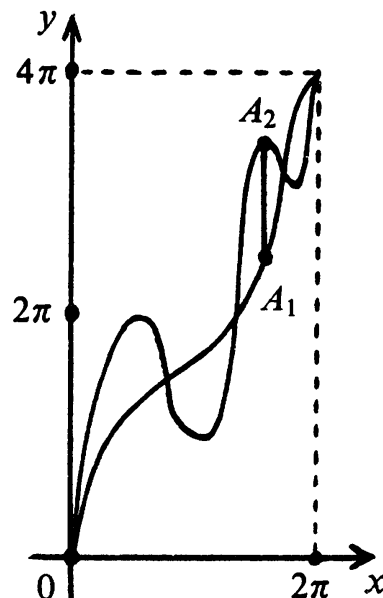


FIGURE 6.18

Now we shall construct the required vector field in the annulus by using the function  $\varphi(t, \alpha)$ . In order to define a nonzero vector, it suffices to specify its length and its angle with the  $x$ -axis. For each ray with initial point at the origin, consider its part (a line segment) contained in the annulus. We shall assume that, on each such line segment, the length of the vectors from our vector field varies uniformly from the length of the given vector on the first boundary circle to that of the one on the second circle. Using Figure 6.17, define the angle that our vector makes with the  $x$ -axis as the sum of angles  $\varphi(t, \alpha)$  and  $\varphi_{0,t}$ , where the angle  $\varphi_{0,t}$  corresponds to the angle  $\varphi_0$  in Figure 6.17 and uniformly varies from  $\varphi_{0,0}$  to  $\varphi_{0,1}$ . The vector field thus constructed possesses all the required properties.  $\square$

Along with vector fields, one can consider line element fields. Suppose that at each point of the plane (or part of the plane) a straight line is chosen so that the directions of the lines vary continuously with the point, i.e., the angle between the lines chosen at two points that are sufficiently close is small. Then we say that a *continuous line element field* is given.

In the case of line element fields, it is also possible to consider *trajectories*, i.e., curves which are tangent at each point to the line from the line element field at this point.

To any vector field without singular points it is possible to assign a line element field simply by replacing each vector by the line that contains it. The converse operation cannot always be performed. Indeed, remove the point  $O$  from the plane and on this punctured plane consider the line element field shown in Figure 6.19 (it is assumed that, at all points of each ray emanating from the origin, the lines of the line element field are parallel). As can be seen from the same figure (observe the arrows!), our attempt to get a vector field from this line element field was not successful.

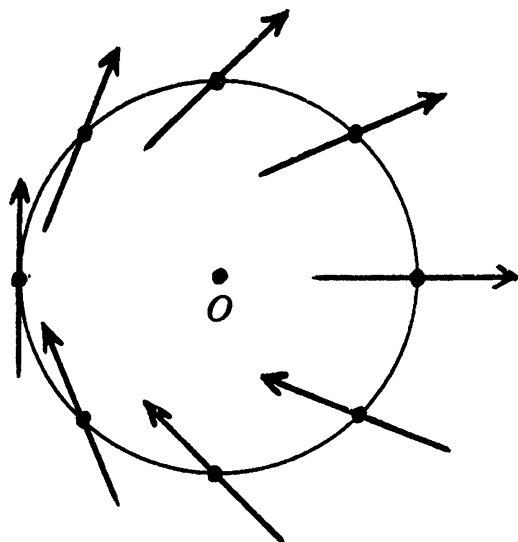


FIGURE 6.19

*Problem 6.12.* Prove that from any continuous line element field defined on the entire plane it is possible to construct a continuous vector field.

*Problem 6.13.* In three-dimensional space with one point removed does there exist a continuous line element field from which no vector field can be constructed?

### Solutions.

6.1. If  $(x(t), y(t))$  is a trajectory of the vector field  $a$ , then

$$\frac{dx(t)}{dt} = x(t), \quad \frac{dy(t)}{dt} = y(t).$$

Therefore, as can easily be verified,  $x(t) = pe^t$ ,  $y(t) = qe^t$ , which implies that  $qx = py$  and each trajectory lies entirely inside one of the quadrants. Thus the trajectories are rays emanating from the origin. The origin itself is a separate trajectory.

For the trajectories of the vector field  $b$ , we get the equations

$$\frac{dx}{dt} = y, \quad \frac{dy}{dt} = -x.$$

In polar coordinates  $x = r \cos \varphi$ ,  $y = r \sin \varphi$  these equations will acquire the form

$$\frac{dr}{dt} \cos \varphi - r \sin \varphi \frac{d\varphi}{dt} = r \sin \varphi,$$

$$\frac{dr}{dt} \sin \varphi - r \cos \varphi \frac{d\varphi}{dt} = r \cos \varphi.$$

Solving this system of linear equations with respect to  $dr/dt$ ,  $d\varphi/dt$ , we get

$$\frac{dr}{dt} = 0 \quad \text{and} \quad \frac{d\varphi}{dt} = 1.$$

Therefore,  $x = R \cos(t + t_0)$ ,  $y = R \sin(t + t_0)$ , where  $R$ ,  $t_0$  are constants.

For the trajectories of the vector field  $c$ , we get the equations

$$\frac{dx}{dt} = y, \quad \frac{dy}{dt} = x.$$

Now we use the change of variables  $u = x + y$ ,  $v = x - y$ , obtaining

$$\frac{du}{dt} = \frac{dx}{dt} + \frac{dy}{dt} = y + x = u,$$

$$\frac{dv}{dt} = \frac{dx}{dt} - \frac{dy}{dt} = y - x = -v.$$

Therefore,  $u = pe^t$ ,  $v = qe^t$ , so that  $u = pq/v$ . In the coordinates  $Ouv$ ,

the trajectories are branches of the hyperbolas  $u = c/v$  (Figure 6.20) or rays originating at  $O$  and lying on the coordinate axes.

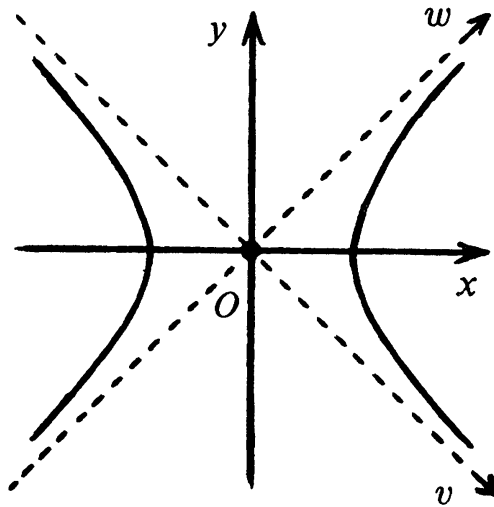


FIGURE 6.20

6.2. Answer: (a) 2; (b) 3; (c) -2.

6.3. If we attempt to choose directions on the trajectories shown in Figure 6.4, we come to a contradiction (Figure 6.21).

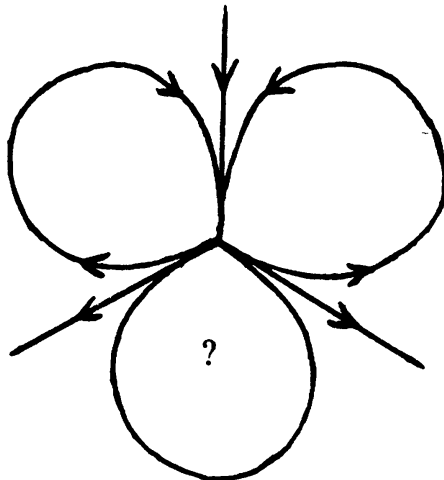


FIGURE 6.21

6.4. Let  $z = Re^{i\varphi}$ . Then  $v(z) = Re^{in\varphi}$ . When  $\varphi$  varies from 0 to  $2\pi$ , the number  $n\varphi$  varies from 0 to  $2n\pi$ , i.e., the vector  $v(z)$  performs  $n$  revolutions. Hence the index of the vector field  $v$  is  $n$ .

Figure 6.3 will help you draw the trajectories of the vector field.

6.5. When we go half way around the circle, the vector  $v$  rotates by  $2k\pi$  in the case of an even vector field, and by  $(2k+1)\pi$  in the case of an odd one.

6.6. Look at Figure 6.22. Suppose  $\alpha$  and  $\varphi(\alpha)$  are the angles between the  $x$ -axis and the vectors  $\overrightarrow{OX}$  and  $v$  respectively. Then

$$\angle ZOY = 2\angle ZXY = 2\varphi(\alpha), \quad \angle IOY = 2\varphi(\alpha) - \alpha.$$

Therefore, when the vector  $v$  performs  $n$  revolutions, the vector  $w$  performs  $2n - 1$  revolutions.

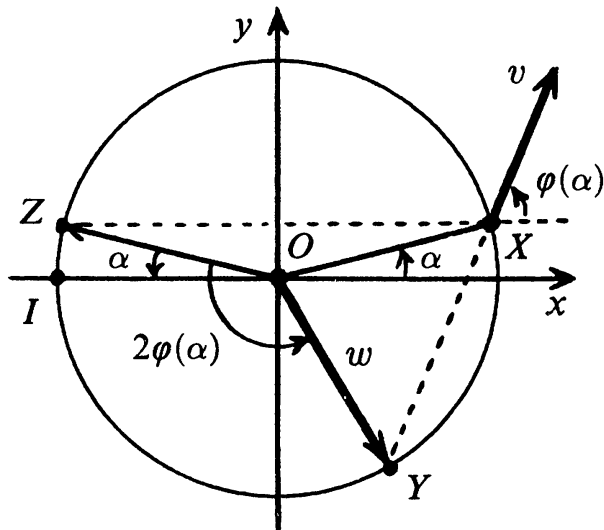


FIGURE 6.22

6.7. Note first of all that inside each region the number of revolutions varies continuously with the point, so this number must be constant within the region.

The number of revolutions performed by the vector  $\overrightarrow{OX}$  as we go around the curve may be calculated as follows. From the point  $O$  construct a ray which is not tangent to the curve. At the intersection points with the curve, write the numbers  $\pm 1$  in accordance with the direction (right to left, left to right) of the intersecting part of the curve (Figure 6.23). Then the number of revolutions (with sign taken into account) is equal to the sum of these

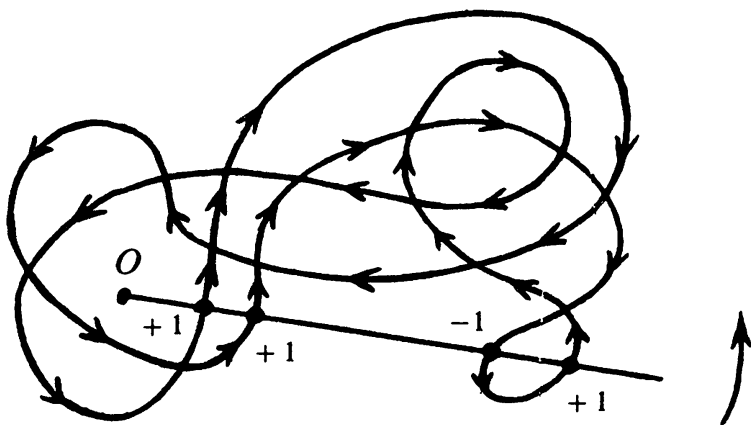


FIGURE 6.23

numbers. In other words, if you are standing in place and your dog is running around you, in order to find out how many revolutions about you the dog has performed, you need not keep track of it all the time. All you need to do is look in a fixed direction and count the number of times the dog runs past from left to right and from right to left.

The points  $A$  and  $B$  inside neighboring regions may be chosen so that the segment  $AB$  intersects the boundary at exactly one point. For the ray  $AB$  and the ray with origin at  $B$  having the same direction, the sums described in the previous paragraph differ only by the number written near this intersection point.

6.8. We shall assume that the center of the circle is the origin of coordinates on the plane. To each point  $X$  of the disk  $D^2$  let us associate the vector  $\overrightarrow{Of(X)}$ . Assume that all these vectors are nonzero. Then the index of the boundary circle of the disk is defined and is an odd number, because the vector field that we have obtained is odd (see Problem 6.5). Hence inside the disk there is a singular point  $X$  for which  $\overrightarrow{Of(X)} = 0$ . This is a contradiction. Therefore, inside the disk or on its boundary, there is a singular point for which  $\overrightarrow{Of(X)} = 0$ , i.e.,  $f(X) = O$ .

6.9. See Figure 6.24.

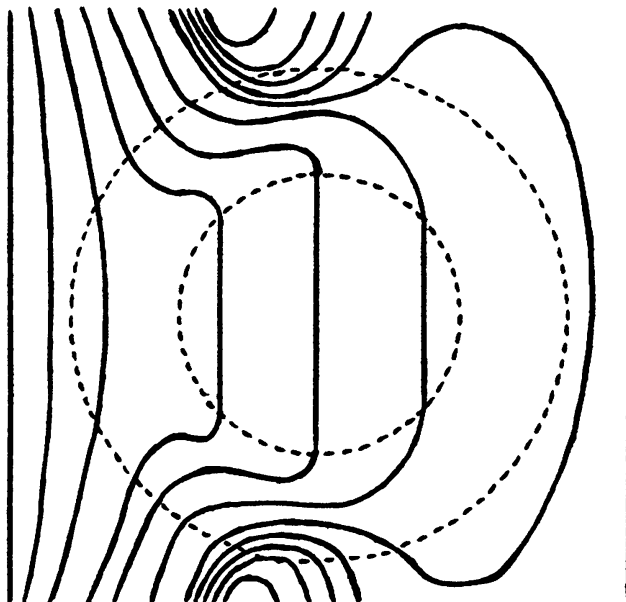


FIGURE 6.24

6.10. See Figure 6.25.

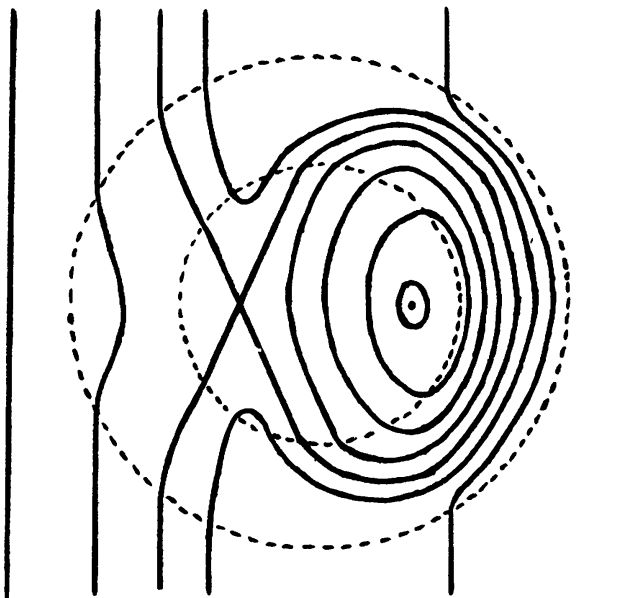


FIGURE 6.25

6.11. The trajectories of the required vector field are shown in Figure 6.26. The vector field itself is obtained by rotating the vectors as we move along the segments of the radii between the two boundary circles. As we go from one endpoint of this segment to the other, the vector turns by  $180^\circ$ .

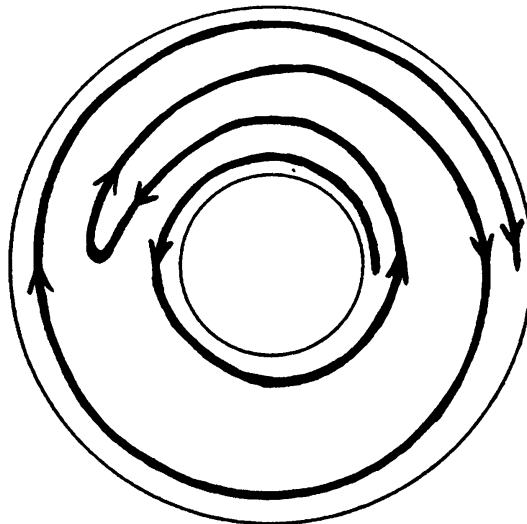


FIGURE 6.26

6.12. In the plane choose a fixed point  $O$ . Two unit vectors correspond to the line of the line element field at this point; choose one. Then at any point  $A$  choose a unit vector on the line at this point in the following way: moving along the segment  $OA$  from  $O$  to  $A$  choose one of the two unit vectors on the line at each of the intermediate points  $X$  on  $OA$  so that these vectors vary continuously.

For the punctured plane this construction does not work, because the line segment  $OA$  may happen to pass through the deleted point.

6.13. Answer: no, it doesn't exist.

The vector field in space can be constructed almost as in Problem 6.12. The only difference is that it is not always possible to transport the vector field along  $OA$  because this line segment may happen to pass through the deleted point. In that case we can transport the vectors along some other path joining  $O$  and  $A$  and avoiding the deleted point. But then the question of the dependence of the result on the choice of the path arises. This is by no means an idle question: Figure 6.19 shows that in the case of the punctured plane the results of transport along different paths may be different.

But in three-dimensional space with one point deleted any closed path may be pulled to a point without touching the deleted point. It is precisely this property that implies the coincidence of the result of transports along different paths. Indeed, if the transport of a vector along two different paths yields different results, then when we go around the closed path constituted by the two given paths, the vector will be transformed into its opposite. This property is preserved in the process of pulling our closed path to a point. On the other hand, it cannot be true of the path pulled to a single point.

---

---

# 7

## Vector Fields on Two-Dimensional Surfaces

---

In a way similar to the case of plane vector fields, one may define vector fields on the sphere. Of course to each point of the sphere we can assign a vector in space. For vector fields in the plane we did not have to worry about the trajectories staying in the plane, this is automatic. But for vector fields on the sphere, this will not happen automatically, we must require the vectors to be tangent to the sphere. Let us say that a *continuous vector field on the sphere* is defined if a vector tangent to the sphere is given at each of its points, and these vectors continuously depend on the point. In the sequel we shall only consider vector fields with a finite number of singular points.

Let us give two examples of vector fields on spheres.

**EXAMPLE 1.** Consider the rotation of the sphere with some constant angular velocity about an axis passing through the center of the sphere. Then the vector field of the velocities of all the points arises on the sphere (Figure 7.1). This vector field has two singular points, namely the intersection points of the axis of rotation with the sphere. The indices of both singular points are equal to 1.

**EXAMPLE 2.** It is possible to construct a vector field with only one singular point on the sphere. Such is the vector field whose trajectories are the sections of the sphere by planes passing through some tangent to the sphere (Figure 7.2). The index of the singular point is equal to 2.

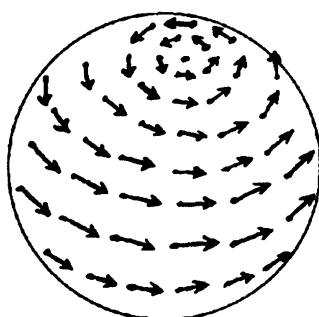


FIGURE 7.1

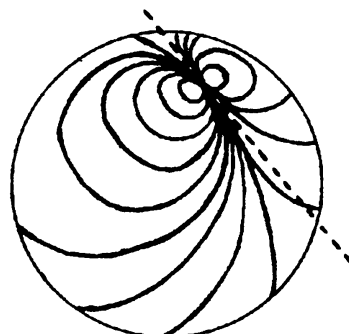


FIGURE 7.2

In both examples the sum of indices of singular points is equal to 2. This is not a coincidence.

**THEOREM 7.1.** *Suppose that a continuous vector field on the sphere has a finite number of singular points. Then the sum of their indices is equal to 2.*

**FIRST PROOF.** The sphere may be divided into two parts by a curve not containing any singular points. For our aims, any closed curve not containing singular points will do. But we shall prove a stronger statement, namely that if the number of singular points is finite, then there exists a great circle (i.e., the section of the sphere by a plane containing the sphere's center) that avoids all the singular points. Consider the correspondence  $\{A, A^*\} \leftrightarrow a$ , where  $A$  and  $A^*$  are diametrically opposed points of the sphere, and  $a$  is the section of the sphere by the plane passing through the center of the sphere perpendicularly to the line  $AA^*$ . It is easy to verify that the point  $A$  belongs to the plane  $b$  (where  $b \leftrightarrow \{B, B^*\}$ ) if and only if the point  $B$  belongs to the plane  $a$ . Suppose  $A_1, \dots, A_n$  are the given (singular) points. Let  $a_1, \dots, a_n$  be the corresponding great circles. There exists a point  $M$  which does not belong to any of these circles. Then none of the given points lies on the circle  $m$  corresponding to  $M$ .

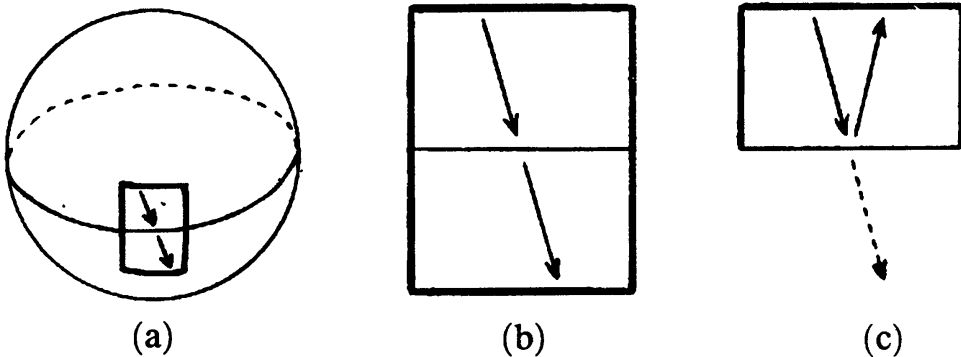


FIGURE 7.3

Now imagine the sphere as a rubber balloon. If we let the air out, we can flatten the balloon so that the two parts into which the circle  $m$  divides the sphere coincide with each other, forming a (double) disk. Let us choose some neighborhood of a point of the great circle and see what happens to it. Figure 7.3 shows that on the boundary circle the vectors of the two fields are symmetric with respect to the tangent. It remains to prove the following simple fact, which we state in the form of a problem.

**Problem 7.1.** Suppose the vector fields  $v$  and  $w$  have no singular points on the circle  $S$  and, at each point  $X$  of  $S$ , the vectors  $v(X)$  and  $w(X)$  are symmetric with respect to the tangent. Prove that the sum of indices of the singular points for the fields  $v$  and  $w$  lying within the circle is equal to 2.  $\square$

**SECOND PROOF.** Take an arbitrary nonsingular point of the given vector field on the sphere and choose a neighborhood of this point so small that

all the vectors in it are almost the same (Figure 7.4 (a)). The neighborhood contains no singular points, so we can consider the remaining part of the sphere. This part can be deformed into a disk (Figure 7.4 (b)). We obtain a vector field, which is directed inward on the arcs  $BC$  and  $CD$  and outward on the arcs  $DA$  and  $AB$ . The index of the circle with respect to the vector field thus obtained is 2. Indeed, when we move through each of the arcs  $AB$ ,  $BC$ ,  $CD$ ,  $DA$  the vector turns by  $180^\circ$ , the direction of rotation coinciding with that chosen to go around the circle.  $\square$

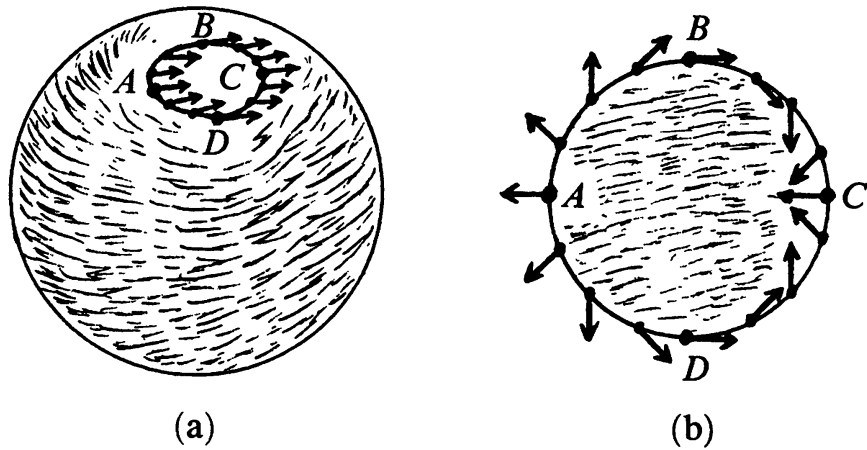


FIGURE 7.4

As an example of the application of Theorem 7.1, let us prove the following *Descartes-Euler Theorem* on convex polyhedra.

**THEOREM 7.2.** *Let  $V$  be the number of vertices of a convex polyhedron,  $E$  the number of edges, and  $F$  the number of faces. Then  $V - E + F = 2$ .*

**PROOF.** Place the polyhedron inside the sphere so that it contains the sphere's center. Project the edges of the polyhedron on the sphere from this center, forming a curvilinear network on its surface. Inside each curvilinear face choose a point and join pairs of such points when they are in neighboring faces by a path passing through the center of their common edge. In Figure 7.5 (a) the new network thus obtained is represented by dotted lines.

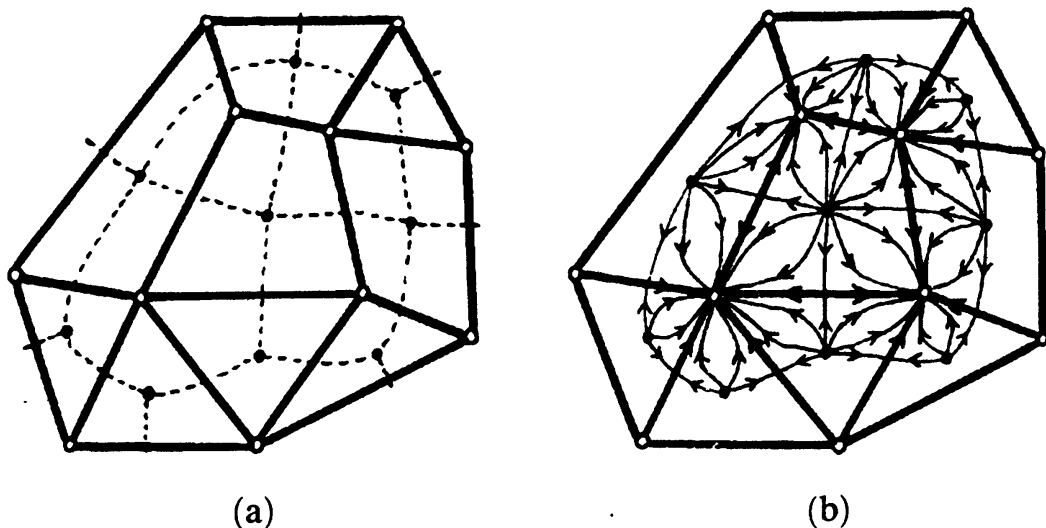


FIGURE 7.5

On the sphere consider the network consisting of both the old and the new networks and draw arrows on its edges, directing them away from the chosen points on the faces and towards the vertices. This network can be included in the system of trajectories of a vector field (Figure 7.5 (b)). The appearance of this vector field at a vertex, at a chosen point of a face, and at the midpoint of an edge is shown in Figure 7.6 (a), (b), and (c) respectively. Our vector field has no other singular points, hence the sum of indices of its singular points equals  $V - E + F$ . By Theorem 7.1 this number is equal to 2.  $\square$

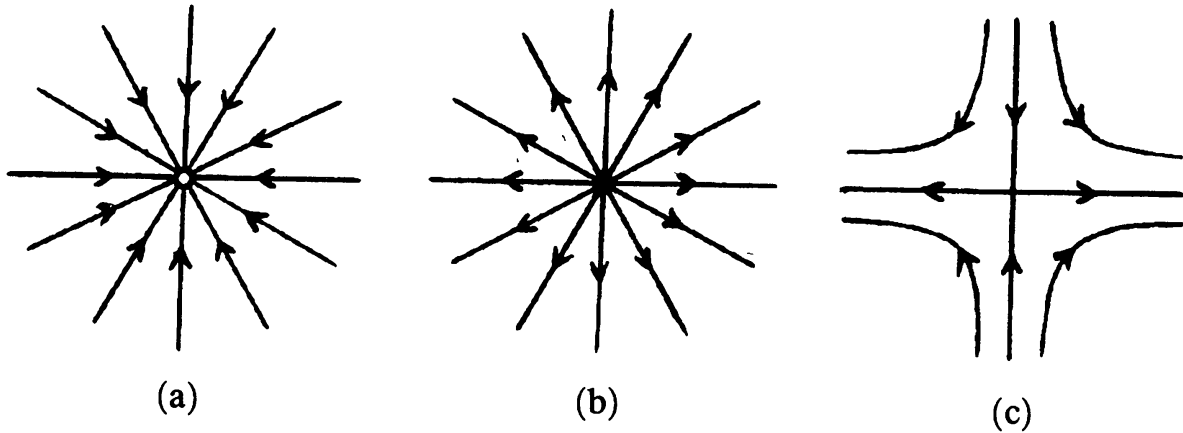


FIGURE 7.6

*Problem 7.2.* To each point  $X$  of the sphere a nonzero vector  $v(X)$  in space is assigned. The vector depends continuously on the point of the sphere, but is not necessarily tangent to it. Prove that at least one of the vectors  $v(X)$  is perpendicular to the tangent plane to the sphere at the point  $X$ .

Vector fields can also be considered on two-dimensional surfaces other than the sphere. One such surface is represented in Figure 7.7 in different ways. It is called the *sphere with three handles*; the origin of such a name should be clear from Figure 7.7 (b). In a similar way one defines a *sphere with  $g$  handles*. On the sphere with  $g$  handles, we shall also consider vector fields consisting only of tangent vectors.

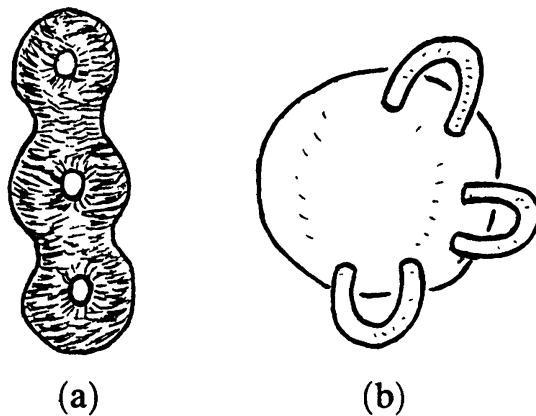


FIGURE 7.7

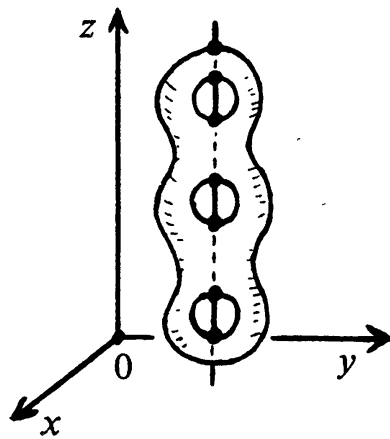


FIGURE 7.8

We can always assume that the sphere with  $g$  handles has an axis of symmetry parallel to the  $z$ -axis (Figure 7.8). On this surface consider a vector field whose trajectories lie in horizontal planes  $z = c$ . The singular points of this vector field are the intersection points of the surface with its symmetry axis. The highest and lowest of these points (i.e., those with greatest and least  $z$ -coordinate) are of index 1, because the trajectories near these points are like concentric circles. The other singular points all have index  $-1$ , because the trajectories near these points look like families of hyperbolas and their asymptotes. The vector field under consideration has 2 singular points of index 1 and  $2g$  singular points of index  $-1$ , therefore the sum of indices of its singular points equals  $2 - 2g$ .

**THEOREM 7.3.** *The sum of the indices of all singular points of any continuous vector field on the sphere with  $g$  handles equals  $2 - 2g$ .*

**FIRST PROOF.** The sphere with three handles may be cut into two pieces, each of which may be flattened into the plane region  $F$  shown in Figure 7.9.

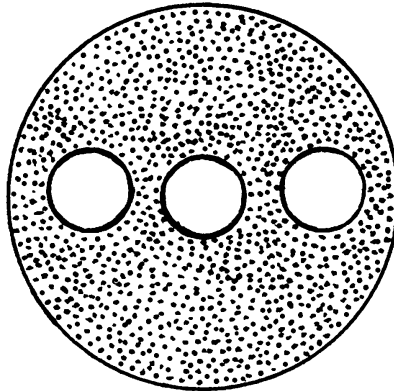


FIGURE 7.9

The sphere with  $g$  handles may be cut in a similar way. If the curve along which we cut happens to pass through a singular point, we can always modify it a little bit so as to avoid it. Hence we can (and will) assume that the curve does not contain any singular points. The sphere with  $g$  handles, just like the ordinary sphere, can be flattened so that its two halves coincide with  $F$ . From the sphere with  $g$  handles we therefore get two vector fields  $v$  and  $w$  on  $F$  such that at each point  $X$  of any of the boundary circles the vectors  $v(X)$  and  $w(X)$  are symmetric with respect to the tangent to the circle at  $X$ . We must prove that the sum of indices of these vector fields equals  $2 - 2g$ .

To this end let us apply the result of Problem 7.1. Suppose  $a$  and  $b$  are the indices of the outer circle with respect to the vector fields  $v$  and  $w$ , while  $a_1, \dots, a_g$  and  $b_1, \dots, b_g$  are the indices of the inner circles with respect to these vector fields. Then we have

$$a + b = 2, \quad a_1 + b_1 = 2, \quad \dots, \quad a_g + b_g = 2$$

according to Problem 7.1. Let us extend the vector fields  $v$  and  $w$  to the plane disks bounded by the inner circles. This can be done by means of homotheties with centers at the centers of the inner circles. The sum of

indices of all the singular points for the extended vector field  $v$  will equal  $a$ . On the other hand, it is equal to  $a_1 + \dots + a_g + A$ , where  $A$  is the sum of indices of all the singular points of the given field  $v$ , i.e., of those points that belong to  $F$ . Therefore  $a = a_1 + \dots + a_g + A$ . Similarly,  $b = b_1 + \dots + b_g + B$ . Adding the last two relations, we get

$$a + b = (a_1 + b_1) + \dots + (a_g + b_g) + (A + B),$$

i.e.,  $A + B = 2 - 2g$ , as required.  $\square$

**SECOND PROOF.** Figure 7.10 shows how one can get a sphere with  $g - 1$  handles from a sphere with  $g$  handles. To do that we cut one of the handles (Figure 7.10 (a)) and then attach a little hemisphere to each of the two cuts (Figure 7.10 (b)).

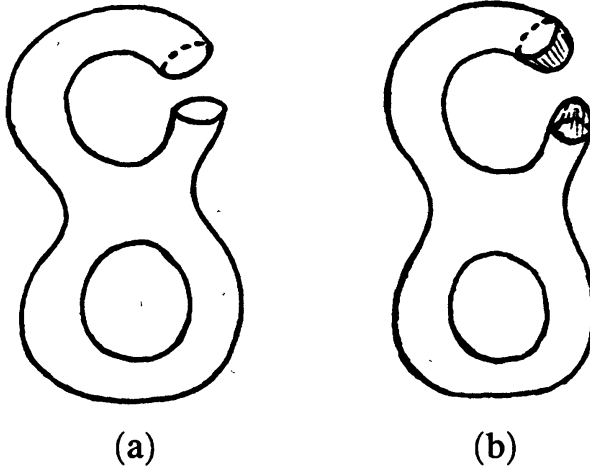


FIGURE 7.10

For  $g = 0$ , i.e., for the ordinary sphere, Theorem 7.3 has already been proved (see Theorem 7.1). Suppose that the assertion of Theorem 7.3 has been proved for any continuous vector field on the sphere with  $g - 1$  handles. We must prove it for a sphere with  $g$  handles. Let us pass to the sphere with  $g - 1$  handles as indicated in Figure 7.10. Now the vector field is not defined on the two hemispheres. But we can extend it continuously by flattening the hemispheres to disks and then considering the homothety with center at the disk's center. By slightly modifying the cut, we can assume that it does not contain any singular points. The vector fields on the curves of the cut come from the same vector field on the sphere with  $g$  handles. Hence we can glue the two hemispheres together, obtaining an ordinary sphere with a continuous vector field on it. Therefore (by Theorem 7.1 again), the sum of indices of the singular points on the two hemispheres is 2. Thus to find the sum of indices of all the singular points of the remaining part of the sphere with  $g - 1$  handles we must subtract 2 from the same sum for the entire sphere with  $g - 1$  handles. So we get

$$2 - 2(g - 1) - 2 = 2 - 2g,$$

as required.  $\square$

**COROLLARY.** If  $g \neq 1$ , then any vector field on the sphere with  $g$  handles has at least one singular point.

The sphere with one handle is the torus. A vector field without singular points can be constructed on it. For example, imagine the torus as a uniformly rotating wheel and take the corresponding velocity field.

On the sphere with  $g$  handles it is possible to construct a vector field with exactly one singular point of index  $2 - 2g$ . To do that take an arbitrary continuous vector field with a finite set of singular points. Let us join two singular points by a path and merge them into one by pulling the path to a point. As a result, the number of singular points will decrease by 1. Repeating this procedure an appropriate number of times, we get a vector field with exactly one singular point. However, it is not easy to picture it on the curved surface of the sphere with  $g$  handles. To obtain a clear picture of a vector field with one singular point on the sphere with  $g$  handles, we shall use a different approach. Cut the sphere with  $g$  handles in half and flatten out the halves so as to obtain the set shown in Figure 7.9. (It will be easier to draw plane pictures.) On one of the halves, let us take a vector field  $v$  of parallel vectors. For the sphere with two handles its trajectories are shown in Figure 7.11 (a). On the boundary circles on the other half, we obtain a vector field  $w$  for which each vector  $w(X)$  is symmetric to  $v(X)$  with respect to the tangent to the circle at the point  $X$ . The vector field  $w$  on the boundary circles (for the sphere with two handles) is represented in Figure 7.11 (b).

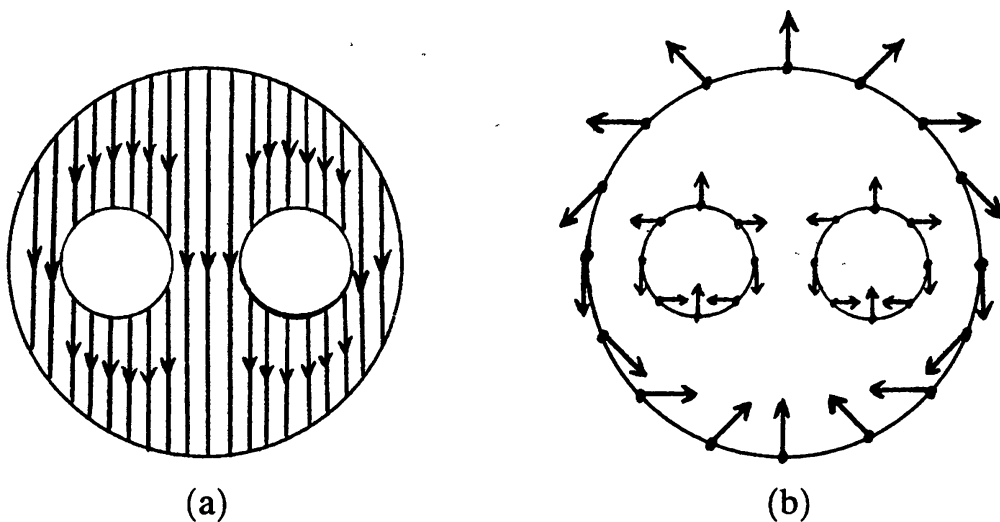


FIGURE 7.11

**Problem 7.3.** Extend the vector field shown in Figure 7.11 (b) to the entire plane region with two holes.

### Solutions.

7.1. Let us use the notation from Figure 7.12. Since the vectors  $v$  and  $w$  are symmetric with respect to the tangent, we have  $\varphi_1 + \varphi_2 = 2(90^\circ + \alpha)$ . Therefore  $\varphi_2 = 180^\circ + 2\alpha - \varphi_1$ . Suppose that the point  $X$  performs a

complete revolution around the circle, i.e., the angle  $\alpha$  varies from  $0^\circ$  to  $360^\circ$ . If at the same time the angle  $\varphi_1$  changes by  $n \cdot 360^\circ$ , then the angle  $\varphi_2$  changes by  $2 \cdot 360^\circ - n \cdot 360^\circ$ . This means that if the vector  $v$  performs  $n$  revolutions as we go around the circle, then the vector  $w$  performs  $2 - n$  revolutions. According to Theorem 6.1, the sum of indices of singular points of the vector fields  $v$  and  $w$  is equal to  $n$  and  $2 - n$  respectively. Thus the sum of indices of singular points for the fields  $v$  and  $w$  is equal to  $n + (2 - n) = 2$ .

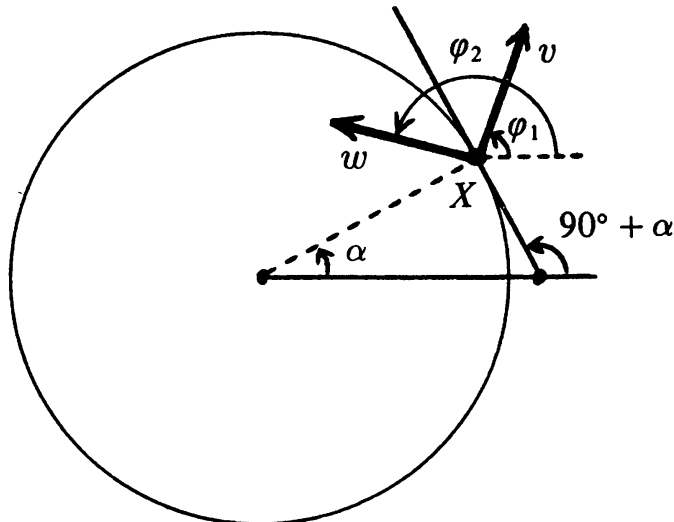


FIGURE 7.12

7.2. To each point  $X$  of the sphere assign the projection of the vector  $v(X)$  on the tangent plane to the sphere at the point  $X$ . The result will be a continuous vector field on the sphere. According to Theorem 7.1, this vector field has a singular point  $X_0$ , i.e., the projection of the vector  $v(X_0)$  on the tangent plane is zero. But this means that the vector  $v(X_0)$  is perpendicular to the tangent plane.

7.3. See Figure 7.13.

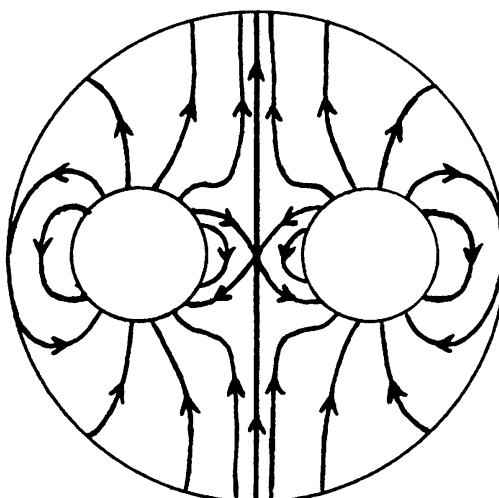


FIGURE 7.13

---

---

# 8

## Fixed Point Free and Periodic Homeomorphisms

---

According to Theorem 6.3, any continuous map of the disk  $D^2$  into itself has a fixed point. But if we remove several smaller disks from  $D^2$ , then a continuous map of this disk with holes into itself without fixed points can be constructed. This is not difficult.

*Problem 8.1.* Construct a continuous map without fixed points of the disk with  $n$  holes into itself.

Problem 8.1 may be made more difficult by requiring that the map without fixed points be a homeomorphism. Such a map is very easy to construct for the annulus (i.e., the disk with one hole). One can simply take the rotation by any nonzero angle. If the number of holes  $n$  is greater than 2, the required map is also easy to find: we can assume that one of the holes is located in the very middle of the disk and that the rotation by the angle  $2\pi/(n - 1)$  about the center of the central hole maps our set into itself (Figure 8.1).

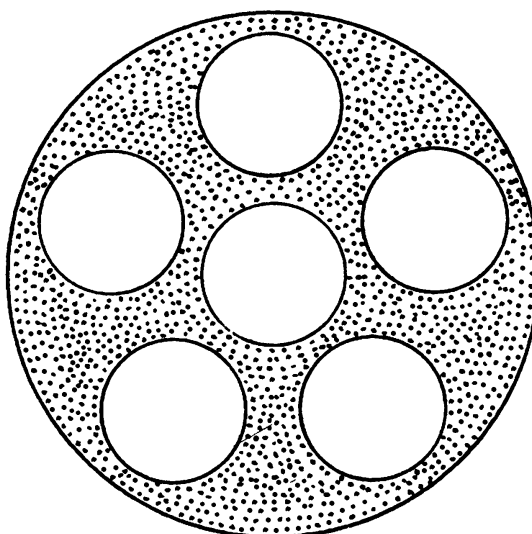


FIGURE 8.1

*Problem 8.2.* Does there exist a homeomorphism without fixed points of the disk with two holes?

Let  $f : M \rightarrow M$  be a map of some set  $M$  into itself and  $m$  be an element of  $M$ . Put

$$f^2(m) = f(f(m)) \quad \text{and} \quad f^k(m) = f(f^{k-1}(m)) \quad \text{for } k \geq 3.$$

The map  $f$  is called *periodic* if for some  $p \geq 2$  we have  $f^p(m) = m$  for any element  $m$  of the set  $M$ . The smallest such number is said to be the *period* of the map  $f$ .

*Warning.* The notion of periodicity for maps has nothing to do with the notion of periodicity for functions. Recall that the period of a function  $f$  is a number  $T$  such that  $f(x + T) = f(x)$  for all numbers  $x$ .

An example of a periodic map is the rotation of a set by an angle whose product by an integer equals  $\pi$ .

The notion of period is perfectly meaningful not only for continuous maps, but, as before, we shall restrict ourselves to continuous periodic maps.

*Problem 8.3.* Give an example of a continuous periodic map  $f$  of period 4 such that for part of the points it has period 2, i.e., for these points  $f(f(m)) = m$  and  $f(m) \neq m$ .

Maps of period 2 play a special role in the theory of periodic maps. They even have a special name: a map of period 2 is said to be an *involution*. In other words, an involution is a nonidentical map  $f : M \rightarrow M$  such that  $f(f(m)) = m$ .

Examples of involutions are provided by symmetries with respect to a point, a plane, or a line.

Let  $f$  be an involution of the set  $M$ . To each element  $m$  of this set assign the pair  $\{m, f(m)\}$ . Note that the same pair will be assigned to  $f(m)$ , since  $f(f(m)) = m$ . In some cases the elements  $m$  and  $f(m)$  coincide, i.e.,  $m = f(m)$ . Recall that such elements are called *fixed points*.

Thus, given the involution  $f$ , we can partition the set  $M$  into pairs of elements  $\{m, f(m)\}$  and singletons (i.e., one-point sets) which are fixed points. It is also clear that the converse statement is also true: from a partition of the set  $M$  into pairs of elements and singletons an involution may be constructed. This is the map that leaves the singletons in place and interchanges the two points of each pair.

An example of an involution of the circle may be obtained as follows. Choose a point  $A$  not on the circle. Let  $X$  be an arbitrary point on the circle. Let us map this point to the point  $f(X)$  at which the line  $AX$  intersects the circle for the second time (if  $AX$  is tangent to the circle, put  $f(X) = X$ ). If the point  $A$  is inside the circle, we get an involution without fixed points (Figure 8.2 (a)), whereas if  $A$  is outside the circle, we get an involution with two fixed points (Figure 8.2 (b)). This is because it is impossible to draw a tangent to the circle from a point inside it, whereas there are exactly two

tangents to the circle from a point outside it. It turns out that there are no other involutions of the circle, i.e., no involutions whose number of fixed points differs from 0 and 2.

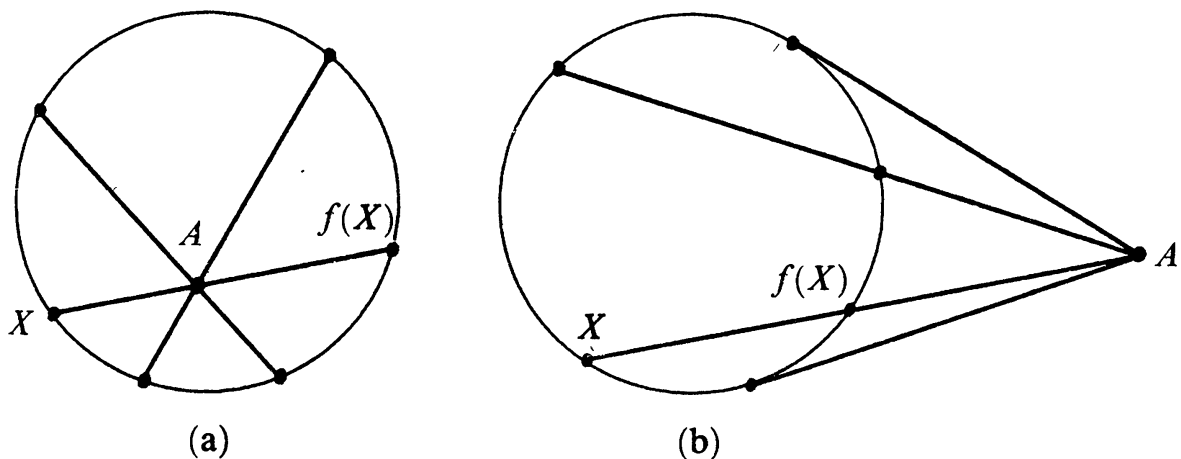


FIGURE 8.2

*Problem 8.4.* Prove that the number of fixed points of any continuous involution of the circle is either 0 or 2.

- Problem 8.5.* a) Construct an involution of the torus without fixed points.  
b) Construct an involution of the torus with four fixed points.  
c) Construct an involution of the torus whose set of fixed points is a circle.

*Problem 8.6.* Construct a map of the torus into itself of period 3 with three fixed points.

Let us consider two examples of involutions of spheres with  $g$  handles.

**EXAMPLE 1.** We can assume that the sphere with  $g$  handles has a center of symmetry  $O$  (Figure 8.3). The symmetry with respect to  $O$  is an involution of the sphere with  $g$  handles, and it has no fixed points. This is because the only fixed point of a symmetry with respect to a point is the point itself. In our case, the point  $O$  is either inside or outside the sphere with  $g$  handles (depending on the parity of  $g$ ), never on its surface.

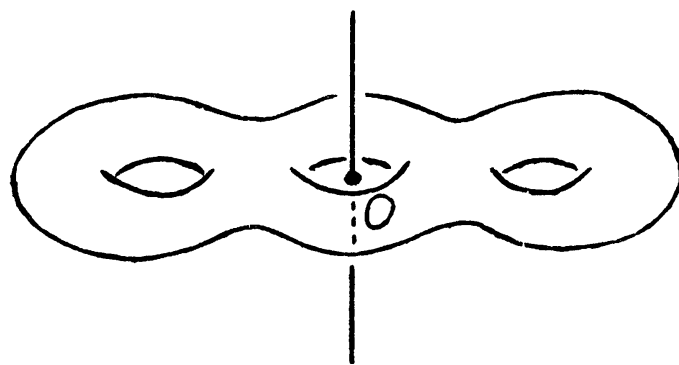


FIGURE 8.3

**EXAMPLE 2.** We can assume that the sphere with  $g$  handles has an axis of symmetry (see the same Figure 8.3). The symmetry with respect to this axis is an involution of the sphere with  $g$  handles. But this involution is not free of fixed points for all  $g$ . This is because for even  $g$  the axis of symmetry intersects the sphere with  $g$  handles at two points. On the other hand, for odd  $g$ , we do get an involution without fixed points.

There is an essential difference between the involutions of Examples 1 and 2. The involution from Example 1 changes the orientation of the sphere with handles, while the one from Example 2 does not. By this we mean the following. Consider a frame (i.e., an ordered pair of noncollinear vectors) tangent at some point to the sphere with handles. The direction of rotation from the first vector to the second one determines the orientation of the sphere with handles. The involution takes the frame to another frame. In the case of a symmetry with respect to a point, the new frame determines the opposite orientation of the sphere with handles, whereas for a symmetry with respect to a line it yields the same orientation.

If an involution  $f$  is given on the set  $M$ , we can identify each point  $m$  with the point  $f(m)$ ; then  $f(m)$  will be identified with  $m$ , because  $f(f(m)) = m$ . This operation will be called *gluing along the involution*.

Let's see what happens to our sphere with handles when we glue it along the involutions from Examples 1 and 2. We begin with the simplest case of the involution from Example 2 when the number of handles is odd. Such involutions preserve orientation and have no fixed points.

Consider a sphere with  $g$  handles, symmetric with respect to an axis (Figure 8.3). Such a surface may be cut by a plane containing the axis of symmetry into two halves, one of which is shown in Figure 8.4. Points of one of them may be identified with those of the other, therefore it suffices to consider only one of the halves. But on the boundary of this half there are points that are symmetric to each other with respect to the given axis of symmetry. They must be identified. Figure 8.4 shows the arrows that must be glued together. For the sphere with three handles, we shall then get a sphere with two handles. In the general case, the sphere with  $2g + 1$  handles becomes one with  $g + 1$  handles.

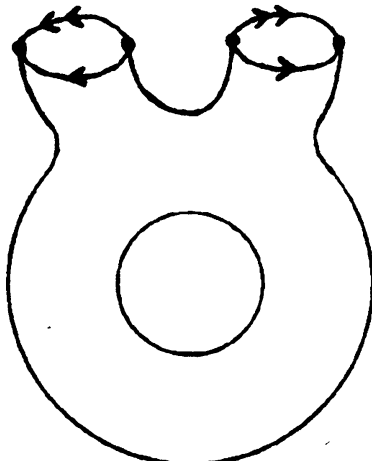


FIGURE 8.4

Now let us consider the gluings corresponding to the involutions from Example 1. Recall that they reverse orientation and have no fixed points. We will have to consider the cases of an odd and an even number of handles separately. Figure 8.5 shows what gluings must be performed for spheres with two and three handles. Note that the arrows in Figure 8.5 (b) are not the same as those in Figure 8.4.

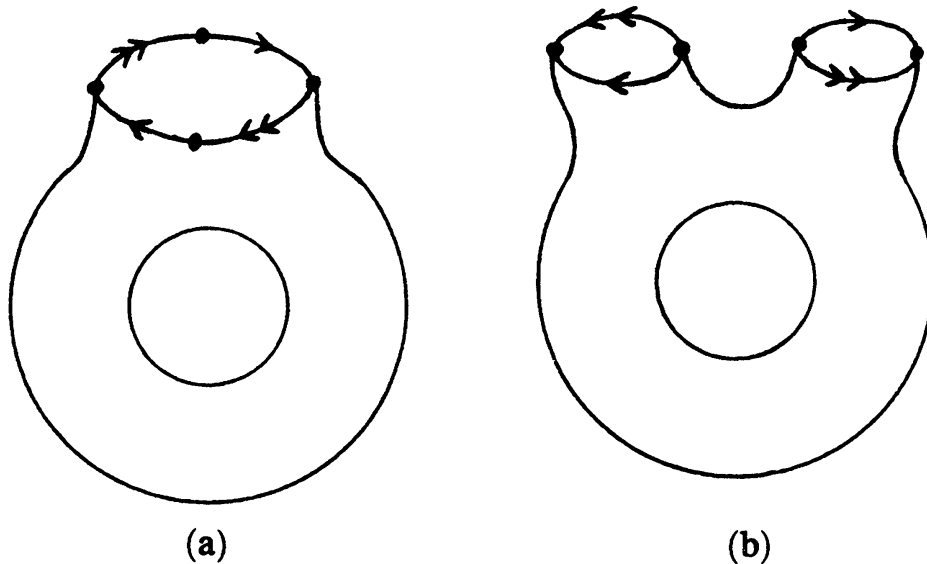


FIGURE 8.5

When we try to perform the identifications shown in Figure 8.5, certain difficulties arise. The trouble is that these identifications cannot be performed in three-dimensional space. More precisely, this can be done only if self-intersections of the surfaces are allowed. The result of such a gluing is shown in Figure 8.6.

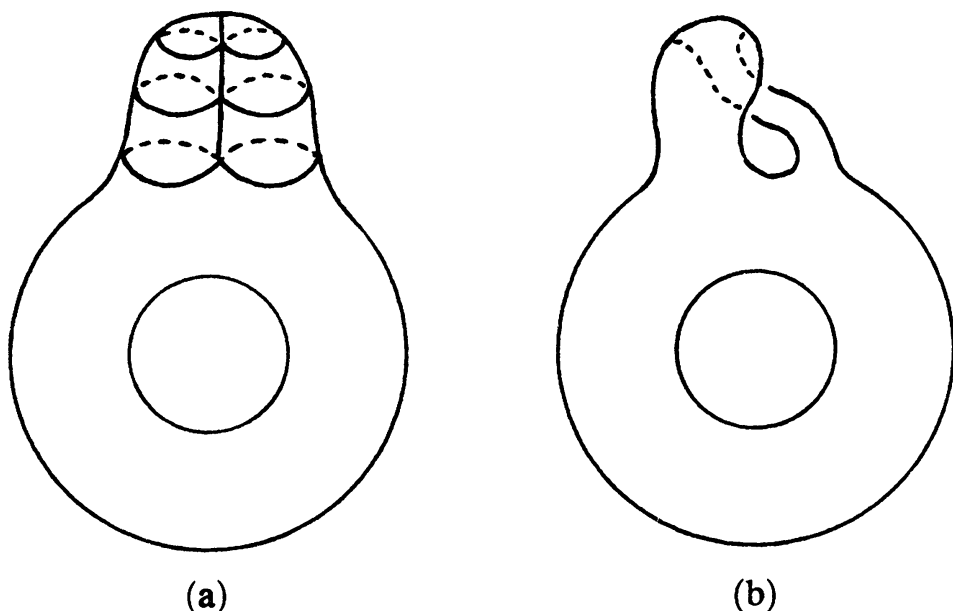


FIGURE 8.6

But if we are interested in a surface only up to homeomorphism, there is no need to place it in 3-space. It is only important to know the structure of the neighborhoods of its points (and how these neighborhoods fit together). Each point of a sphere with  $g$  handles has a neighborhood homeomorphic to the disk. Each point of the surface obtained from the sphere with  $g$  handles by gluing along the involution described in Example 1 also has such a neighborhood. This can be easily understood from Figure 8.5.

So far we have only studied gluings along involutions without fixed points. For such involutions the image of some neighborhood  $U$  of the point  $x$  is a neighborhood  $V$  of the point  $f(x)$ . After gluing together the neighborhoods  $U$  and  $V$ , we get a neighborhood  $W$  which is homeomorphic both to  $U$  and to  $V$ .

In the case when the involution does have a fixed point  $x$ , then, instead of gluing together points from two different neighborhoods  $U$  and  $V$ , we must glue together points from one and the same neighborhood  $U$  of  $x$ . This may lead to several difficulties, only one of which we shall discuss.

Suppose  $A$  is a sphere with handles,  $f$  is an involution on it, and  $B$  is the set obtained from  $A$  by gluing along the involution  $f$ . Consider the map  $p : A \rightarrow B$  that takes a point  $a$  to the point  $b$  obtained when  $a$  and  $f(a)$  are glued together. If  $f$  is an involution without fixed points, then each sufficiently small neighborhood  $W$  of  $b$  is obtained as the result of identifying two nonintersecting neighborhoods  $U$  and  $V$ . This means that the inverse image of  $W$  under the map  $p$  consists of two nonintersecting sets  $U$  and  $V$ , while the inverse image of the point  $b$  consists of the points  $a$  and  $f(a)$  lying in  $U$  and  $V$  respectively. Now if  $f$  has a fixed point  $x$ , the situation is drastically different. The point  $x = a$  is identified with  $f(x)$ , i.e., with itself. Therefore, the inverse image of the point  $b$  obtained by this identification consists of a single point instead of two.

If the set  $B$  is obtained from the sphere with  $g$  handles  $A$  by gluing along an involution without fixed points, then each point  $b$  of the surface  $B$  has a neighborhood homeomorphic to the disk. Hence we can consider vector fields on  $B$  as well.

**THEOREM 8.1.** *The sum of indices of all the singular points of any continuous vector field on  $B$  equals  $1 - g$ .*

**PROOF.** Given a vector field  $w$  on  $B$ , one can construct a vector field on  $A$  (called the *pullback* of  $w$ ), which is taken to  $w$  under the projection

$$p : A \rightarrow B$$

(Figure 8.7). To each singular point of the vector field on  $B$  correspond two singular points of the same index in its pullback on  $A$ . Hence the sum of indices of all the singular points of the vector field on  $A$  is twice that for the vector field on  $B$ . On the other hand, Theorem 7.3 implies that the sum of indices of all singular points of any continuous vector field on the sphere with  $g$  handles  $A$  equals  $2 - 2g$ .  $\square$

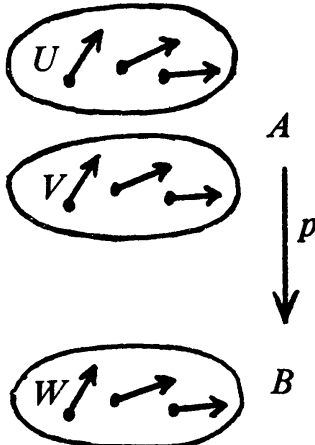


FIGURE 8.7

*Problem 8.7.* Introduce the coordinates  $(\varphi, \psi)$  on the torus as shown in Figure 8.8. Consider the involution of the torus that takes the point with coordinates  $(\varphi, \psi)$  to the point  $(\psi, \varphi)$ . Prove that the result of gluing the torus along this involution is the Möbius band.

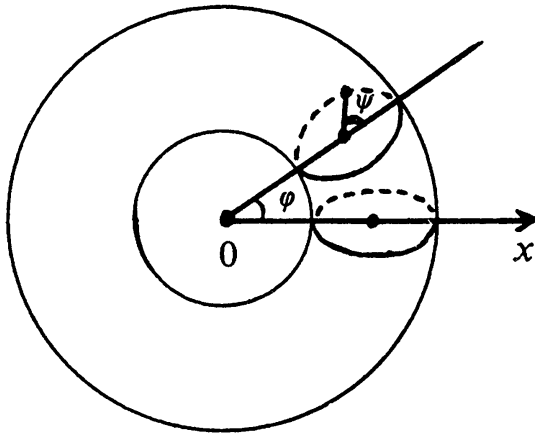


FIGURE 8.8

### Solutions.

8.1. Inside one of the holes choose the point  $O$ . First map each point  $X$  of the disk with holes to the point where the ray  $OX$  intersects the boundary circle of the disk. Under this map only the points of this circle will be fixed. Now turn the circle by a nonzero angle. The result will be a map without fixed points.

8.2. Answer: yes, it exists.

The disk with two holes can be deformed into the sphere with three holes (Figure 8.9). Moreover, we may assume that the obtained surface is symmetric with respect to the plane  $\Pi$  and is mapped onto itself when rotated by  $120^\circ$  about the line  $l$  perpendicular to the plane  $\Pi$ . It is clear that the plane  $\Pi$  and the line  $l$  pass through the center of the sphere. The required

homeomorphism is the composition of the symmetry with respect to the plane  $\Pi$  and the rotation by  $120^\circ$  about the line  $l$ :

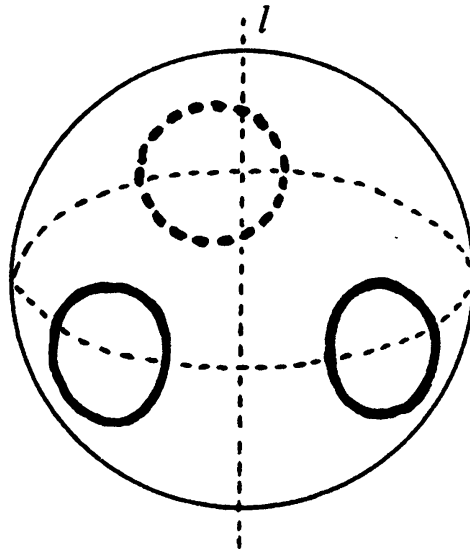


FIGURE 8.9

8.3. Let us construct the required map for the Möbius band. To do that glue the Möbius band from a long rectangular strip. Draw a family of lines parallel to the longer side of the rectangle. Move each point along such a line by a distance equal to half the length of the strip (Figure 8.10). If the point  $A$  is not on the midline of the strip (i.e., is not equidistant from the long sides of the rectangle), then  $f^4(A) = A$ , and the four points  $A$ ,  $f(A)$ ,  $f^2(A)$ ,  $f^3(A)$  are all distinct. If the point  $B$  is on the midline, then  $f^2(B) = B$ .

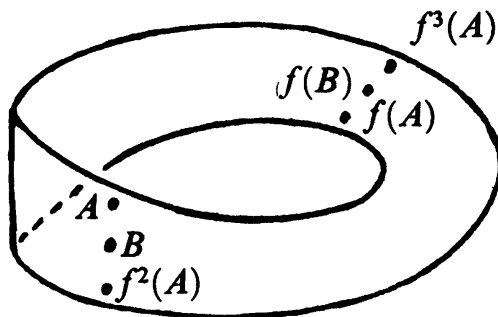


FIGURE 8.10

8.4. It suffices to consider the case when the involution  $f$  of the circle has a fixed point  $A$ . We must prove that the involution  $f$  has exactly one fixed point other than  $A$ .

Suppose that  $B$  is a point of the circle such that  $f(B) = C \neq B$ . The involution  $f$  is a homeomorphism since  $f^{-1} = f$ . Therefore,  $f$  homeomorphically maps the arc  $AB$  onto one of the two arcs of our circle determined by the points  $A$  and  $C$ . Denote this arc by  $AC$ . For the two arcs  $AB$  and

$AC$  two configurations are possible:

- 1) the arcs  $AB$  and  $AC$  have no common interior points;
- 2) one of the arcs contains the other.

Let us prove that in our case the second configuration is not possible. To be definite, suppose that the arc  $AB$  is contained in the arc  $AC = f(AB)$ . Then the arc  $f(AB) = AC$  is contained in the arc  $f(AC) = f(f(AB)) = AB$ . Therefore the arcs  $AB$  and  $AC$  coincide; but this contradicts the condition  $C \neq B$ .

Thus the arcs  $AB$  and  $AC$  do not have any common points other than  $A$ . Moreover, if the arc  $AB$  is contained in the arc  $AB_1$ , then the arc  $AC$  is contained in the arc  $AC_1$ , where  $C_1 = f(B_1)$ . This means that if the point  $B$  moves along the circle so that the length of the arc  $AB$  increases, then the length of the arc  $AC$  also increases. Hence at some moment the points  $B$  and  $C$  will meet. The point at which they meet is obviously a fixed point of the involution  $f$  and  $f$  has no fixed points other than this point and the point  $A$ .

8.5. Suppose that  $O$  is the center of symmetry of the torus,  $l$  is its axis of symmetry, and  $l$  intersects the torus at four points (Figure 8.11). The symmetry of the torus with respect to  $O$  has no fixed points, while the symmetry with respect to  $l$  has four of them.

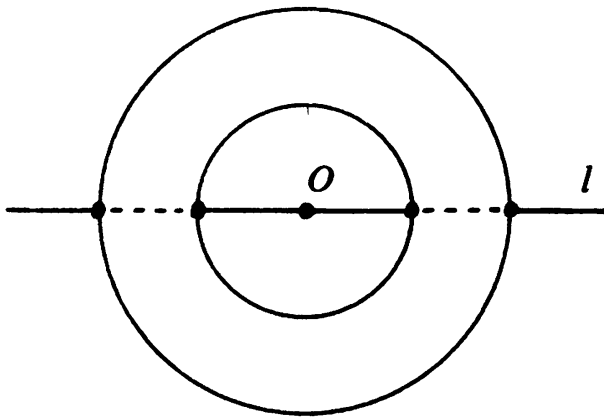


FIGURE 8.11

An example of the involution of the torus for which the fixed point set is the circle was in fact described in Problem 8.7. Indeed, the set of points for which  $\varphi = \psi$  is a circle.

8.6. Let us use the coordinates  $(\varphi, \psi)$  introduced in Problem 8.7. Consider the map of the torus that takes the point with coordinates  $(\varphi, \psi)$  to the point with coordinates  $(\psi, -\varphi - \psi)$ . Under this map the point  $(\varphi, \psi)$  is taken successively to the points  $(\psi, -\varphi - \psi)$ ,  $(-\varphi - \psi, -\varphi)$ , and  $(\varphi, \psi)$ . The fixed points will be those for which

$$\varphi = \psi + 2m\pi \quad \text{and} \quad \psi = -\varphi - \psi + 2n\pi,$$

where  $m$  and  $n$  are integers. Substituting the first of the displayed relations

into the second, we get  $3\psi = 2(n-m)\pi$ , i.e.,  $\psi = (2(n-m)\pi)/3$ . Since the point of the torus with coordinates  $(\psi + 2k\pi, \psi + 2l\pi)$  coincides with the point  $(\varphi, \psi)$ , we get three fixed points on the torus, namely

$$\varphi = \psi = 0, \quad \varphi = \psi = 2\pi/3, \quad \varphi = \psi = 4\pi/3.$$

8.7. In the plane  $O\varphi\psi$  consider the square  $OB\bar{C}D$  given by the inequalities  $0 \leq \varphi, \psi \leq 2\pi$ . Gluing together the opposite sides of this square (Figure 8.12 (a)), we get the torus. The map of the square that takes the point  $(\varphi, \psi)$  to the point  $(\psi, \varphi)$  is a symmetry with respect to the diagonal  $OC$ . Let us identify points symmetric with respect to this diagonal. In this process, the arrows drawn on the sides  $OD$  and  $OB$  are glued together. Therefore, when we glue the torus along the involution under consideration, we get the same result as when we identify the two arrows drawn on the two sides of the right triangle (Figure 8.12 (b)). Now cut this triangle along the arrow  $b$  (Figure 8.13 (a)) and then identify the  $a$  arrows (Figure 8.13 (b)). Now it is clear that after we glue together the  $b$  arrows, we get the Möbius band.

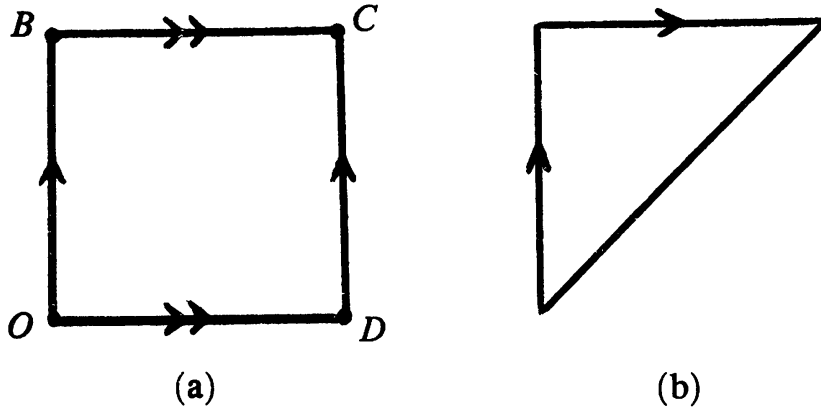


FIGURE 8.12

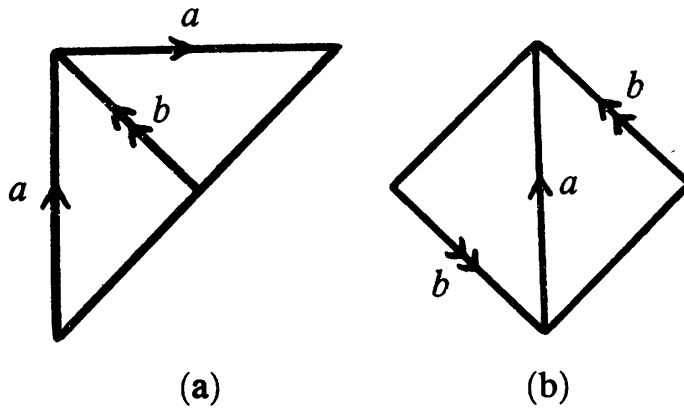


FIGURE 8.13

---

---

# 9

## Two-Dimensional Surfaces

---

In this section we shall look at certain properties of two-dimensional surfaces in more detail.

The trefoil knot can be drawn on the torus (Figure 9.1). It will then be a curve that winds around the direction of the meridian of the torus three times and around the direction of the parallel twice.

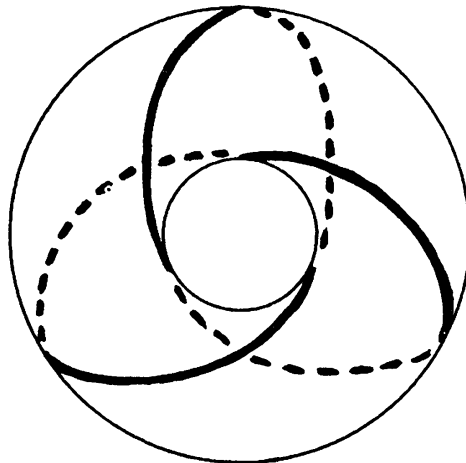


FIGURE 9.1

*Problem 9.1.* Let  $p$  and  $q$  be relatively prime positive integers. Show that on the torus there exists a closed curve without self-intersections that winds  $p$  times around the direction of its meridian and  $q$  times around the direction of its parallel.

For the meridian we have  $p = 1$  and  $q = 0$ , while for the parallel  $p = 0$  and  $q = 1$ . It turns out that these values for  $(p, q)$ , together with those indicated in Problem 9.1, are the only possible values for  $(p, q)$ . One of the simplest proofs of this fact uses the result of the next problem.

*Problem 9.2. a)* On the plane consider an arbitrary curve joining the points  $A$  and  $B$ . Prove that if  $n$  is a natural number, then there exists a line segment  $PQ$  of length  $AB/n$  whose endpoints lie on the given curve and which is parallel to the line  $AB$ .

b) Prove that if the positive number  $d$  is not an integer, there exists a curve joining the points  $A$  and  $B$  for which the assertion of a) is false, i.e., if the points  $P$  and  $Q$  belong to the curve and the line segment  $PQ$  is parallel to  $AB$ , then the length of the segment  $PQ$  is not equal to  $AB/d$ .

*Problem 9.3.* Prove that if a closed curve without self-intersections on the torus winds  $p$  times around the direction of the meridian and  $q$  times around the direction of the parallel, then either  $p$  and  $q$  are relatively prime, or one of them is equal to 1 and the other to 0.

The sphere may be described by the polynomial equation

$$P(x, y, z) = x^2 + y^2 + z^2 - 1 = 0.$$

Can the sphere with  $g$  handles also be described by a polynomial equation? It turns out that it can.

*Problem 9.4.* Indicate a polynomial  $P(x, y, z)$  for which the equation  $P(x, y, z) = 0$  determines the sphere with  $g$  handles.

Now let us study in more detail two surfaces encountered in Chapter 8, namely, the surfaces obtained by identifying diametrically opposed points of the sphere and by gluing together points on the torus symmetric with respect to its center of symmetry. Recall that they can be obtained by gluing together the arrows shown in Figure 9.2 (a) and (b).

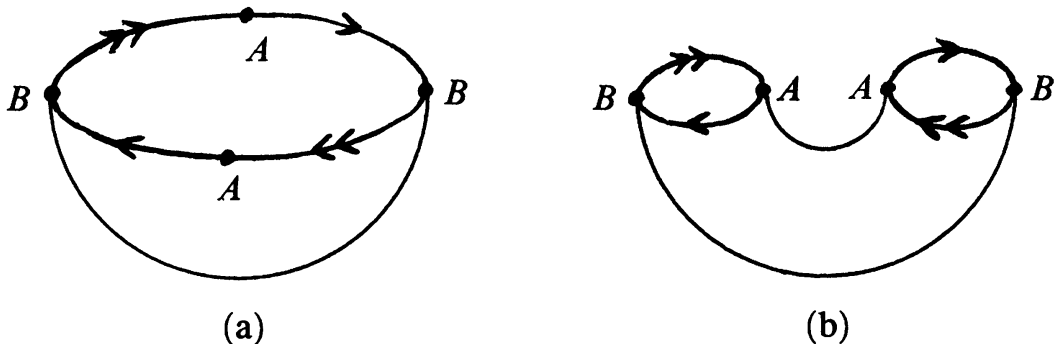


FIGURE 9.2

As we already mentioned, the involution constructed in Example 1 of Chapter 8 reverses the orientation of the sphere with handles. This implies that the surface obtained by gluing along this involution is nonorientable. Indeed, on the sphere with handles, let us join a point  $A$  to the symmetric point  $A'$  by some curve. As the result of gluing along our involution, the curve will become a closed curve, since the points  $A$  and  $A'$  are identified. A trip around this curve reverses orientation, and so the surface obtained is nonorientable.

First let us consider the surface obtained by identifying diametrically opposite points of the sphere. This surface is known as the *projective plane*. In order to explain the origin of this term, let us give another definition of the projective plane. This definition is longer, but it is related to certain important notions of projective geometry.

Parallel lines, e.g. rails of a railroad track, seem to intersect at the horizon. This motivates the desire to extend the plane by new points at which parallel lines intersect. How should one go about that? Take a point  $O$  not lying in the plane  $\Pi$ . To each point  $A$  in the plane  $\Pi$  assign the line  $OA$  (Figure 9.3). To a line in  $\Pi$  a plane will then be assigned, namely the plane containing the given line and the point  $O$ , or, more precisely, this plane except for the line passing through  $O$  parallel to the given line. If the lines  $l_1$  and  $l_2$  intersect at the point  $A$ , then the corresponding planes intersect along the line  $OA$ . But now if the lines  $l_1$  and  $l_2$  are parallel, the corresponding planes intersect along a line  $m$ , which is parallel to the lines  $l_1$  and  $l_2$ . The line  $m$  does not intersect the plane  $\Pi$ , hence it does not correspond to any point of this plane.

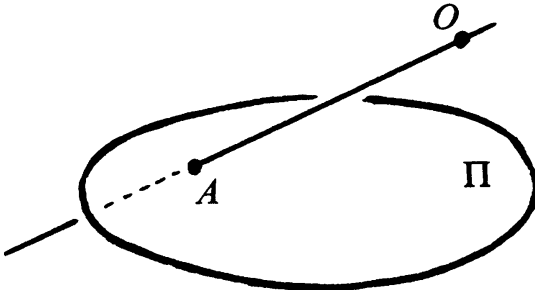


FIGURE 9.3

Now we can give the following definitions. Let us call *points of the projective plane* all the straight lines passing through the point  $O$ , and call all the planes passing through the point  $O$  *projective lines*. Further the lines passing through  $O$  parallel to the plane  $\Pi$  will be called *points at infinity*. Two projective lines always intersect in exactly one point. In particular, projective lines corresponding to parallel (ordinary) lines of the plane  $\Pi$  intersect in a point at infinity.

Note that the plane  $\Pi$  does not participate in the definition of points of the projective plane or in the definition of a projective line. So we could have entirely avoided mentioning the plane  $\Pi$ . Then there is no reason to distinguish points at infinity from other points.

Now let us show that the set of all points of the projective plane defined above is homeomorphic to the surface obtained by identifying diametrically opposed points of the sphere. To this end consider a sphere of center  $O$ . To each point of the projective plane there correspond two points of the sphere, namely, the points at which the line  $AO$  intersects the sphere. These points are diametrically opposed. Thus by identifying diametrically opposed points of the sphere, we get a surface homeomorphic to the projective plane (regarded as the set of points of the projective plane).

*Problem 9.5.* Prove that if a disk is cut out of the projective plane, then what remains is homeomorphic to the Möbius band.

*Problem 9.6.* On the projective plane choose two projective lines and delete a disk that does not intersect these lines. The set obtained is homeomorphic to the Möbius band. Draw the chosen lines on it.

*Problem 9.7.* Consider the set whose points correspond to straight lines in the plane, two points being regarded as near each other if they correspond to lines that are near each other, i.e., either they intersect, forming a small angle, or they are parallel and their distance is small. Prove that this set is homeomorphic to the Möbius band.

Now we pass to the study of the surface obtained by identifying pairs of points of the torus symmetric with respect to its center of symmetry. This surface is known as the *Klein bottle*. As we have already mentioned, it can be obtained by gluing together the arrows shown in Figure 9.2 (b). If self-intersections are allowed, this surface may be represented as shown in Figure 9.4.

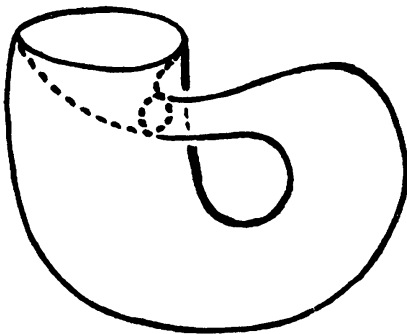


FIGURE 9.4

The Klein bottle may be obtained by gluing together the sides of the square in a specific way. To obtain such a representation of the Klein bottle, let us cut the surface shown in Figure 9.2 (b) along the arc joining the symmetric points  $A$  and  $A$  (these two points are denoted by the same letter because after our identification they are glued together, becoming the same point). The result is a square whose sides are identified as shown in Figure 9.5 (a). The two short arrows can be replaced by one. Slightly changing the notation, we get Figure 9.5 (b).

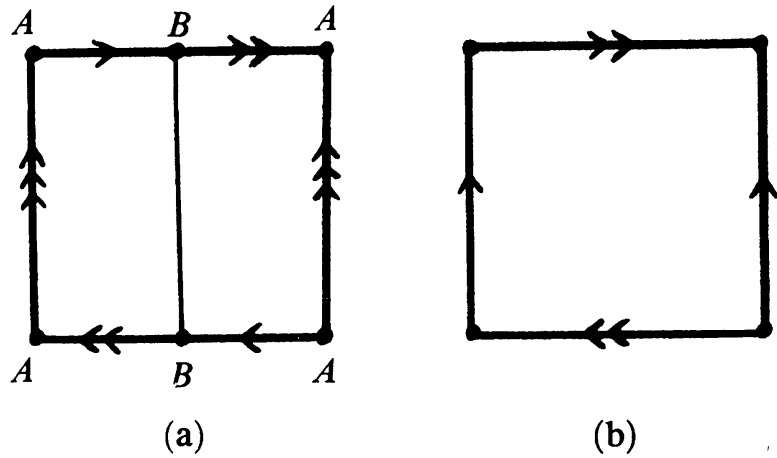


FIGURE 9.5

One more representation of the Klein bottle may be obtained by cutting the square along its diagonal (Figure 9.6 (a)). Gluing together one pair of arrows, we come to the picture in Figure 9.6 (b). The triangle may be replaced by the square (Figure 9.6 (c)).

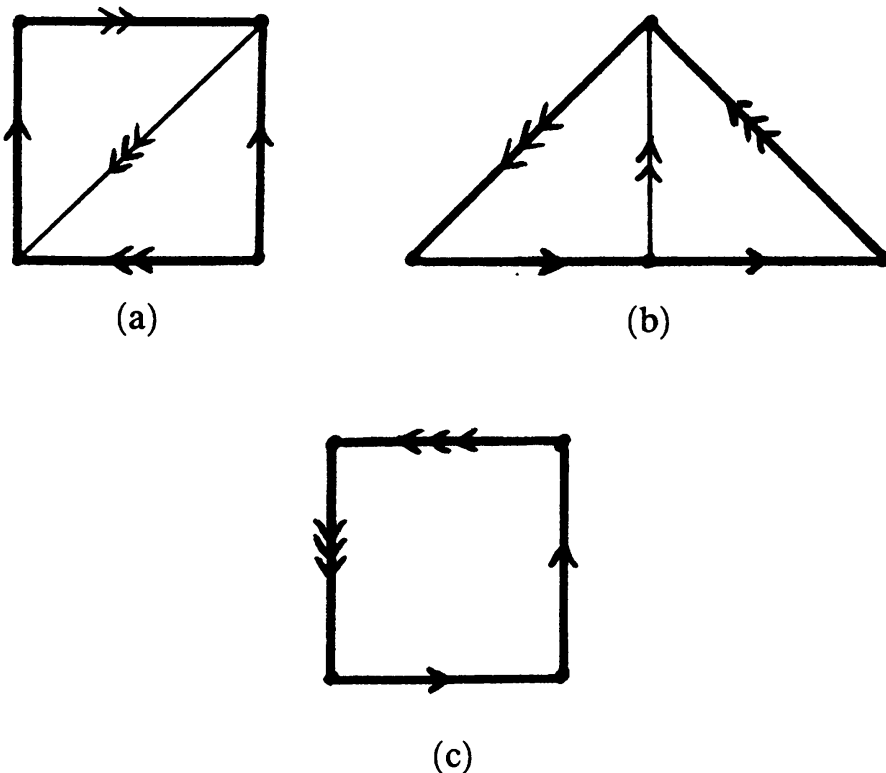


FIGURE 9.6

*Problem 9.8.* Prove that the Klein bottle may be cut apart into two Möbius bands.

*Problem 9.9.* Consider the set  $F$  whose points correspond to pairs of points  $\{x, y\}$ , where  $x$  is a point of the closed interval  $[0, 1]$  and  $y$  is a point of the Möbius band. Here we suppose that points  $\{x_1, y_1\}$  and  $\{x_2, y_2\}$  are near each other if the points  $x_1$  and  $x_2$  of  $[0, 1]$  are close to each other, as well as the points  $y_1$  and  $y_2$  of the Möbius band. Prove that the boundary of this set is homeomorphic to the Klein bottle.

*Problem 9.10.* Construct an involution without fixed points on the Klein bottle.

If we cut out a disk from the projective plane, we get a Möbius band (Problem 9.5). This means that the projective plane may be obtained by cutting out a disk from the sphere and attaching a Möbius band to the boundary of the obtained surface. The reader will recall that the boundary of the Möbius band is a circle; we shall identify this circle with the one constituting the boundary of the hole in the sphere.

The Klein bottle may be cut apart into two Möbius bands. This means that the Klein bottle may be obtained by cutting out two disks from the sphere and attaching a Möbius band to each of the boundary circles.

Besides the operation of attaching a Möbius band, one can consider the operation of attaching a handle (Figure 9.7).

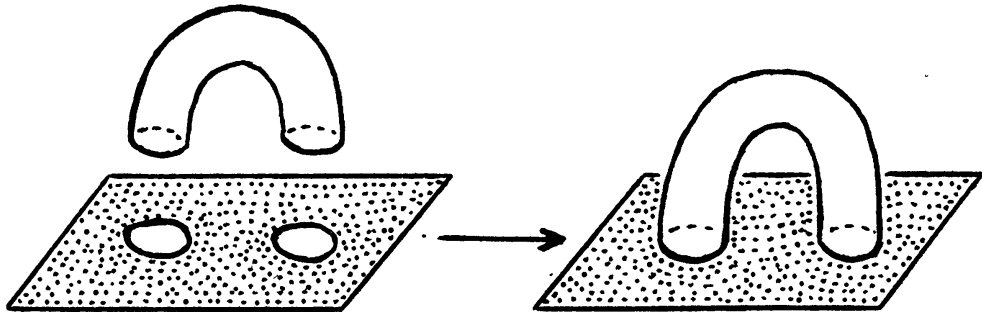


FIGURE 9.7

*Problem 9.11.* Prove that the sphere with three Möbius bands attached is homeomorphic to the sphere with one handle and one Möbius band attached.

### Solutions.

9.1. The torus may be obtained by identifying points of the plane with coordinates  $(x, y)$  and  $(x + n, y + m)$ , where  $m$  and  $n$  are integers. Indeed, the result of such a gluing is a square with identified sides as shown in Figure 9.8; the arrows on the picture indicate what further identifications must be made to get the torus.

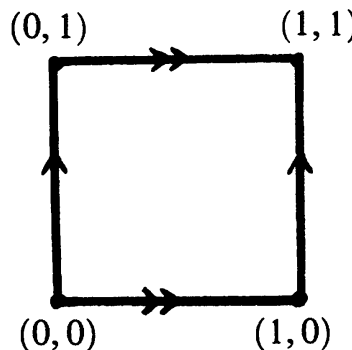


FIGURE 9.8

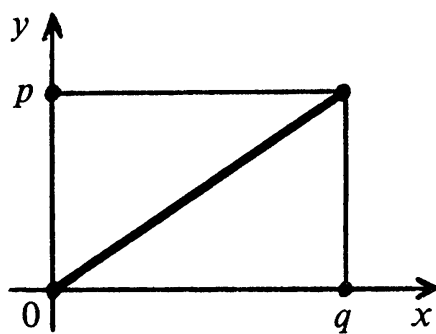


FIGURE 9.9

To obtain the torus in this way, there is no need to consider the whole plane. One may take any part of it containing the square shown in Figure 9.8. For example, one can take the rectangle with vertices

$$(0, 0), \quad (0, p), \quad (q, 0), \quad (q, p)$$

(see Figure 9.9). The diagonal of this rectangle will become a closed curve on the torus as the result of our identifications. This curve winds around the torus  $p$  times around the direction of the meridian and  $q$  times around the parallel (or vice-versa: this depends on the order in which we glue the arrows together to get the torus).

It remains to verify that our curve on the torus has no self-intersections. The coordinates of the points on the diagonal of the rectangle satisfy the equation  $px = qy$ . Assume that the points  $(x_1, y_1)$  and  $(x_2, y_2)$  lying on the diagonal were glued together in our identifications, i.e.,  $x_1 = x_2 + m$  and  $y_1 = y_2 + n$ , where  $m$  and  $n$  are integers. Since  $px_1 = qy_1$  and  $px_2 = qy_2$ , we get  $p(x_2 + m) = q(y_2 + n)$  and  $pm = qn$ . Since  $p$  and  $q$  are relatively prime, we get  $m = kq$  and  $n = kp$ . Therefore, only the endpoints (and no other points) of the diagonal are identified: our curve has no self-intersections.

9.2. a) We shall say that the distance  $d$  is *implemented* on the curve joining the points  $A$  and  $B$  if there exists a line segment of length  $d$  parallel to  $AB$  with endpoints on the curve. We must prove that the distance  $AB/n$  is implemented on any curve joining  $A$  and  $B$ . First let us prove that if  $0 < \alpha < 1$ , then, for any curve joining  $A$  and  $B$  at least one of the distances  $\alpha AB$  or  $(1 - \alpha)AB$  is implemented. We can assume that the segment  $AB$  is located on the  $x$ -axis and joins the points with abscissas 0 and 1. Suppose that both distances  $\alpha$  and  $1 - \alpha$  are not implemented on some curve  $\gamma_0$  joining the points  $a$  and  $b$ . Then if we shift the curve along the  $x$ -axis by the distances  $\alpha$  and  $1 - \alpha$ , we get curves that have no common points with the given curve. Suppose that  $\gamma_\alpha$  and  $\gamma_1$  are the curves obtained from  $\gamma_0$  by shifting in the positive direction along the  $x$ -axis by the distance of  $\alpha$  and 1 respectively. Then the curve  $\gamma_\alpha$  does not intersect either  $\gamma_0$  or  $\gamma_1$ . Construct the curve  $L$  in the following way. On the curve  $\gamma_\alpha$  choose a point with the largest  $y$ -coordinate and draw a ray from it parallel to the  $y$ -axis in the positive direction, and from a point of  $\gamma_\alpha$  with the smallest  $y$ -coordinate draw a ray in the opposite direction (Figure 9.10). The curve  $L$  consists of these two rays and of the part of the curve  $\gamma_\alpha$  between their extremities. The curves  $\gamma_0$  and  $\gamma_1$  do not intersect either the curve  $\gamma_\alpha$  or the two rays.

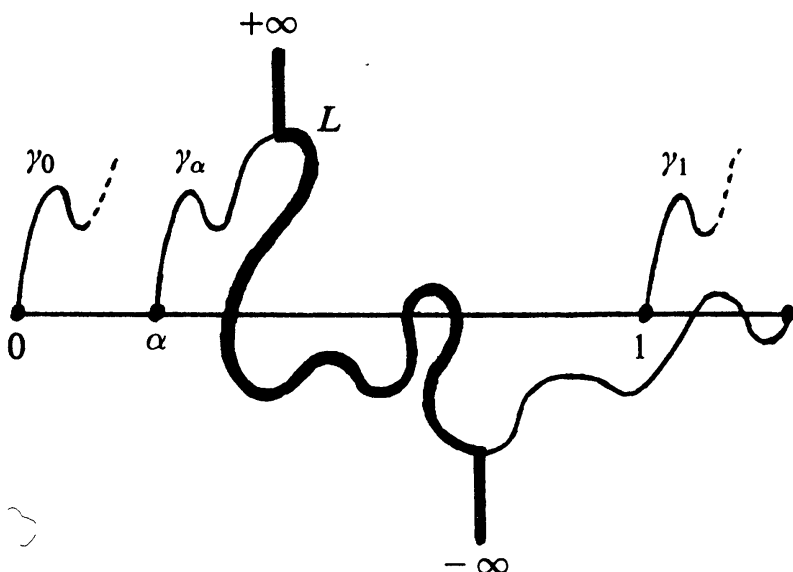


FIGURE 9.10

Therefore, they do not intersect  $L$ . But since  $L$  splits the plane into two parts, and the points with maximal  $y$ -coordinates of the curves  $\gamma_0$  and  $\gamma_1$  lie in different parts, it follows that so do the curves  $\gamma_0$  and  $\gamma_1$  themselves. On the other hand, the curves  $\gamma_0$  and  $\gamma_1$  have a common point, namely  $(1, 0)$ . This contradiction means that at least one of the distances  $\alpha$  and  $1 - \alpha$  is implemented.

Now let us prove by induction on  $n$  that the distance  $AB/n$  can be implemented on any curve. For  $n = 1$  the statement is obvious. The induction step is carried out as follows. Let  $\alpha = 1/n$ . Then

$$1 - \alpha = \frac{n-1}{n},$$

so that one of the distances  $AB/n$  or  $(n-1)AB/n$  is implemented. If the first distance is implemented, then our statement is proved. Now if the distance  $(n-1)AB/n$  is implemented, then for any curve joining the endpoints of a line segment of length  $(n-1)AB/n$ , according to the assumption of induction, the distance

$$\frac{1}{n-1} \cdot \frac{(n-1)AB}{n} = \frac{AB}{n}$$

can be implemented.

b) Let  $n$  be the integer part of the number  $d$ . Divide the segment  $[n, d]$  into  $n$  equal parts. Figure 9.11 shows the curve  $\gamma$  joining the endpoints of the segment  $AB$  of length  $d$ . The dotted curve  $\gamma'$  is obtained from the curve  $\gamma$  by a shift along  $AB$  of distance 1. Since the curves  $\gamma$  and  $\gamma'$  do not intersect, the distance  $AB/d = 1$  is not implemented on the curve  $\gamma$ .

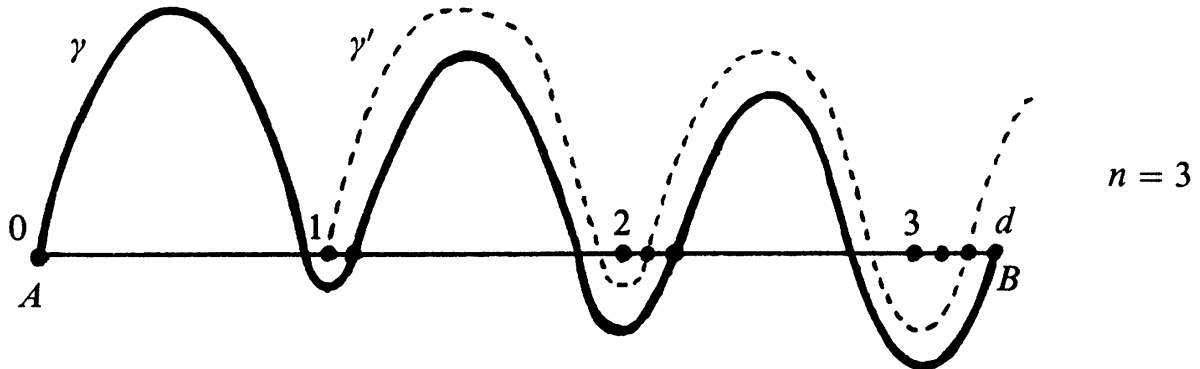


FIGURE 9.11

9.3. Suppose the closed curve  $\gamma$  winds  $p$  times around the direction of the meridian of the torus and winds  $q$  times around the direction of the parallel. Identify the points of the plane with coordinates  $(x, y)$  and  $(x + m, y + n)$ , where  $n$  and  $m$  are integers. As the result, we get the torus. For this identification, the curve  $\gamma$  can be obtained from the curve  $\Gamma$  joining the points

$$A = (0, 0) \text{ and } B = (p, q).$$

Assume that the integers  $p$  and  $q$  are either both nonzero and have a common divisor  $d \neq 1$ , or one of them is zero, while the other is  $d \neq 1$ . According to Problem 9.2 a), the curve  $\Gamma$  implements the distance  $AB/n$ . This means that we can choose points  $P$  and  $Q$  on  $\Gamma$  so that

$$PQ = (1/d)AB.$$

The vector  $\overrightarrow{PQ}$  has integer coordinates  $(p/d, q/d)$ , hence the points  $P$  and  $Q$  are identified, i.e., they correspond to the same point on the torus. This means that the curve  $\gamma$  is self-intersecting.

9.4. First let us note that if  $Q(x, y)$  is the product of  $g$  factors of the form  $(x - 2k + 1)^2 + y^2 - 1$ , where  $k = 1, \dots, g$ , then the equation  $Q(x, y) = 0$  describes a set in the plane consisting of  $g$  circles (Figure 9.12). Hence the equation

$$Q(x, y) + z^2 - \varepsilon = 0,$$

where  $\varepsilon$  is a sufficiently small positive number, describes the sphere with  $g$  handles.

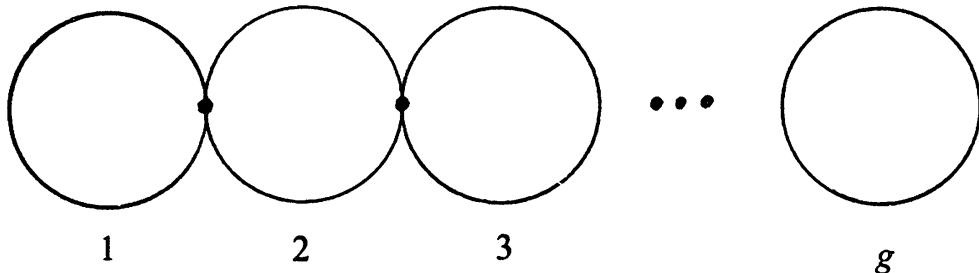


FIGURE 9.12

9.5. Figure 9.13 (a) shows how the projective plane with a disk removed may be represented. Let us perform the cuts  $b$  and  $c$  shown in Figure 9.13 (b). Now glue together the arrows  $a$  (Figure 9.13 (c)). The result is the Möbius band.

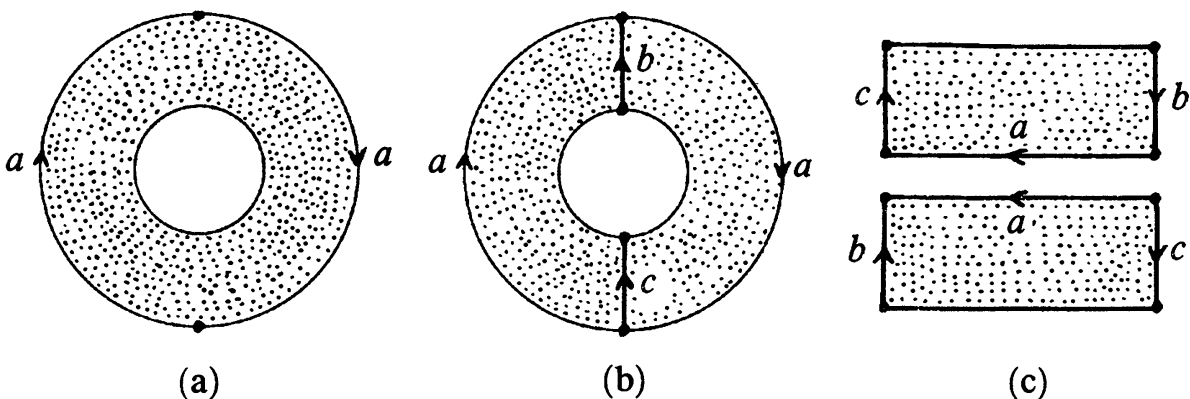


FIGURE 9.13

9.6. On the Möbius band the two projective lines appear as shown in Figure 9.14.

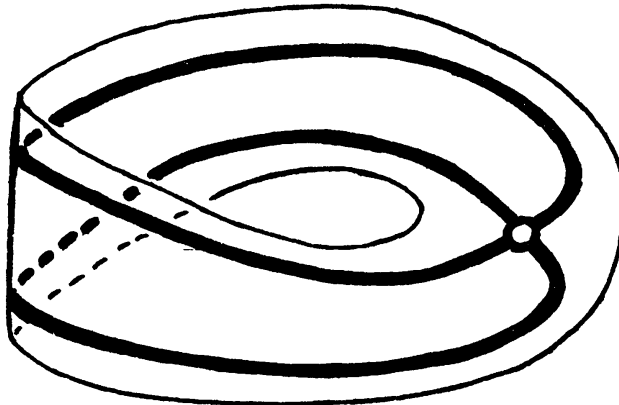


FIGURE 9.14

9.7. A line on the plane is given by an equation of the form

$$ax + by + c = 0,$$

where the numbers  $a$  and  $b$  do not vanish simultaneously. Hence to such a line we may assign the triple of numbers  $(a, b, c)$ . The triples  $(a, b, c)$  and  $(\lambda a, \lambda b, \lambda c)$ , where  $\lambda \neq 0$ , determine the same line. Hence the set of lines in the plane is homeomorphic to the projective plane from which the point corresponding to the triple  $(0, 0, 1)$  has been deleted.

The projective plane with a point removed is homeomorphic to the open Möbius band (i.e., the Möbius band without its boundary).

9.8. Recall that the two ways of gluing the Klein bottle from a square are shown in Figures 9.5 (b) and 9.6 (c). Figure 9.15 shows the required cuts for each of the two cases as dotted lines.

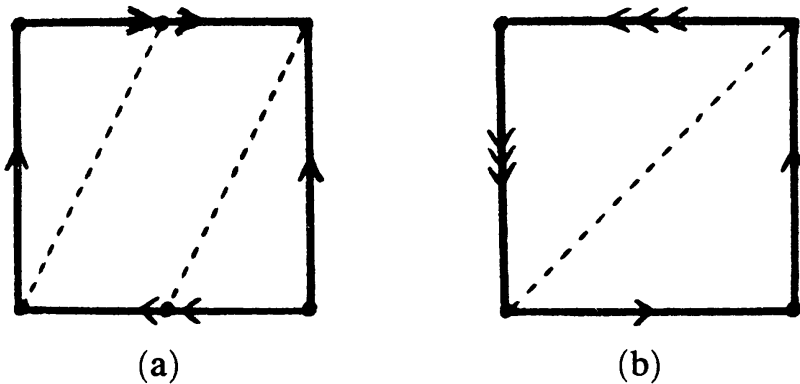


FIGURE 9.15

9.9. Represent the Möbius band as the projective plane with disk removed, i.e., as the annulus on whose inner boundary diametrically opposed points are identified (Figure 9.16 (a)). Then the set under consideration may be represented as a cylinder from which a smaller cylinder has been removed,

the boundary points of the deleted cylinder being identified as shown in Figure 9.16 (b). After the identification of the boundary points of the smaller cylinder, all of them, except those on its lower and upper base, cease being boundary points. Therefore the boundary of the obtained set is a sphere from which two disks have been removed and Möbius bands have been attached in their place. Such a surface is homeomorphic to the Klein bottle.

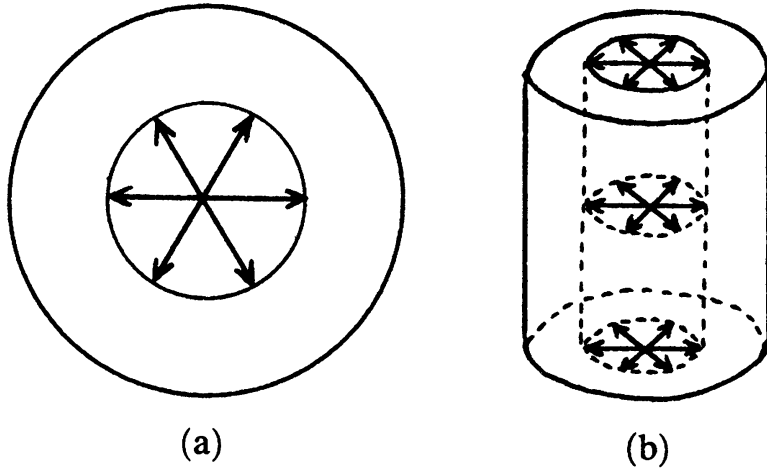


FIGURE 9.16

9.10. Consider the lateral surface of the cylinder. Its boundary is a pair of circles. By identifying points on them symmetric with respect to the center of symmetry of the cylinder, we get a Klein bottle. The required involution  $f$  of this Klein bottle is the symmetry with respect to the axis of the cylinder (Figure 9.17).

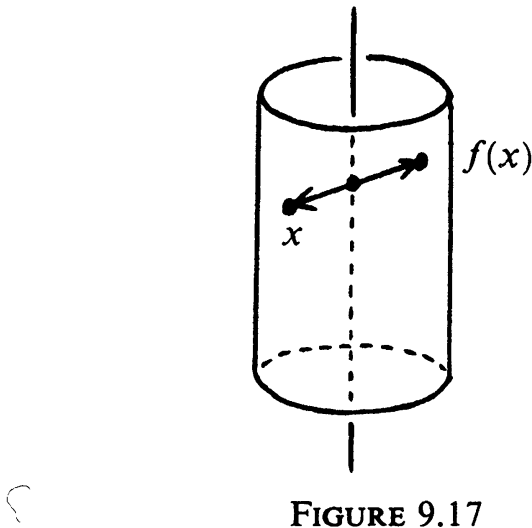


FIGURE 9.17

9.11. The sphere to which two Möbius bands are attached is homeomorphic to the Klein bottle. Hence the sphere to which three Möbius bands are attached is homeomorphic to the Klein bottle to which one Möbius band is attached. Such a surface is shown in Figure 9.18 (a). Cut this surface along

$c$  and then identify the  $b$  arrows (Figure 9.18 (b)). The result is a sphere to which the handle  $a$  and the Möbius band  $c$  have been attached.

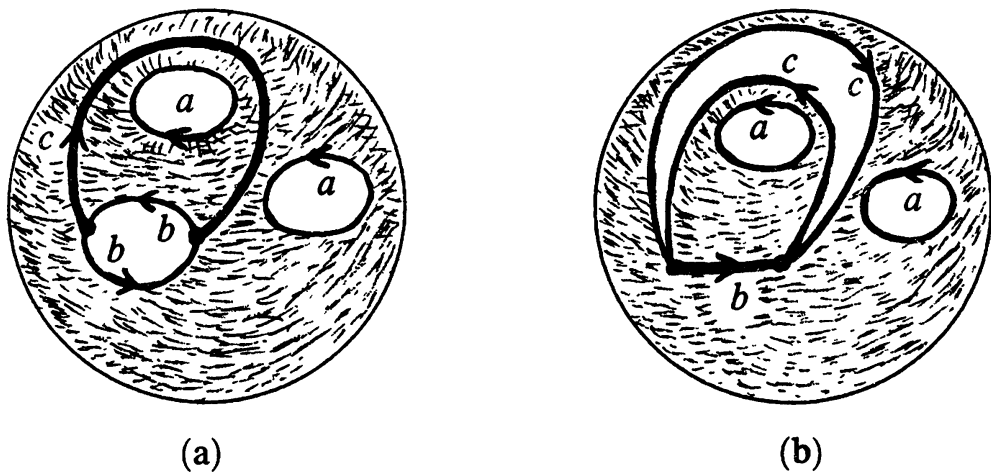


FIGURE 9.18

---

---

## References

---

1. Richard H. Crowell and Ralph H. Fox, *Introduction to knot theory*, Ginn, Boston, New York, and Chicago, 1963.
2. William S. Massey, *Algebraic topology: An introduction*, Hardcourt, Brace & World, New York, Chicago, San Francisco, and Atlanta, 1967.
3. D. Rolphsen, *Knots and links*, Publish or Perish, Berkeley, CA, 1976.
4. John Stallings, *Group theory and three-dimensional manifolds*, Yale Univ. Press, New Haven and London, 1971.
5. O. Viro, *Colored knots*, Kvant 3 (1981). (Russian)
6. *Topology of 3-manifolds and related topics*, Proceedings of the University of Georgia Institute, 1961, Prentice-Hall, Englewood Cliffs, NJ, 1962.



---

---

# Index

---

---

- Borromean ring, 10  
complex plane, 47  
component of a link, 9  
connected surface, 22  
continuous line element field, 56  
continuous vector field, 45  
continuous vector field on the sphere, 63  
deformation, 1  
Descartes–Euler Theorem, 65  
even vector field, 47  
figure eight knot, 8  
fixed point, 50  
gluing along an involution, 74  
homeomorphic figures, 33  
Hopf link, 9  
implemented distance, 87  
index of a curve, 48  
index of a singular point, 45  
involution, 72  
isotopic objects (figures), 33  
Klein bottle, 16, 84  
knot, 7  
knot invariant, 29  
left trefoil, 7  
line element field, 56  
link, 9  
Main Theorem of Algebra, 51  
Möbius band, 16  
nonorientable span, 16  
odd vector field, 47  
orientable span, 16  
orientation, 20  
oriented surface, 20  
period (of a periodic map), 72  
periodic map, 72  
point at infinity (of the projective plane), 83  
point of the projective plane, 83  
projective line, 83  
projective plane, 82  
proper coloring, 29  
pullback (of a vector field), 76  
right trefoil, 7  
Seifert algorithm, 17  
Seifert circle, 17  
Seifert surface, 17  
singular point (of a vector field), 45  
span of a knot, 15  
spanning film of a knot, 15  
spanning surface of a knot, 15  
sphere with  $g$  handles, 66  
sphere with three handles, 66  
torus, 36  
trajectory of a line element field, 56  
trajectory of a vector field, 46  
trefoil knot, 7  
twist, 36  
vector field, 45  
vector field on the sphere, 63  
Whitehead link, 9